The synthesis and characterisation of novel organotin biocides.

Purcell, T. G.

Award date:
1985

Awarding institution:
University of Bath

THE SYNTHESIS AND CHARACTERISATION OF NOVEL ORGANOTIN BIOCIDES.

submitted by T.G. Purcell

for the degree of Ph.D

of the University of Bath

1985

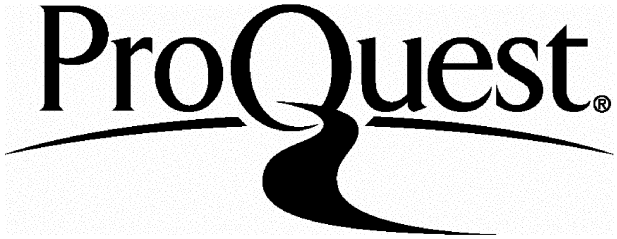

CONTENTS

Abbreviations

Me	:	methyl
Et	:	ethyl
Pr	:	propyl
Bu	:	butyl
Oct	:	octyl
Ph	:	phenyl
Bz	:	benzyl
Cy	:	cyclohexyl
IAAH	:	3-Indolyl Acetic Acid
N-Me,IAAH	:	N-Methyl,3-Indolyl Acetic Acid
mbtH	:	2-Mercaptobenzothiazole
mboH	:	2-Mercaptobenzoxazole
mbiH	:	2-Mercaptobenzimidazole
pipdtc	:	Piperazine bis(dithiocarbamate)
TEPA	:	N,N,N',N' Tetraethylphosphorodiamidic Acid
DPPA	:	N,N' Diphenylphosphorodiamidic Acid
$Pq^{2+}2Cl^{-}$	:	Paraquat dichloride
$Dq^{2+}2Br^{-}$	:	Diquat dibromide

Abstract

A series of novel organotin derivatives of various biologically active ligands have been synthesised and characterised by several spectroscopic techniques and in two cases by X-ray crystallography. Five of these compounds were tested for biocidal activity and were found to exhibit varying degrees of fungicidal, bactericidal and herbicidal activity.

Tributyltin and trimethyltin derivatives of 3-Indolyl acetate and its N-methyl analogue were considered, from spectroscopic (i.r., ^{1}H n.m.r., Mössbauer) evidence, to adopt five coordinate polymeric structures, with bridging ligand moieties. Tricyclohexyltin (3-indolyl acetate) was found by X-ray studies to adopt a distorted tetrahedral geometry arising from rehybridisation to increase percentage p-orbital contribution to the bond to electronegative oxygen. The lattice structure of this compound was found to contain H-bonds linking the N-H group of the Indole ring to the carbonyl group of a neighbouring atom. A similar molecular (though not lattice structure) is proposed for tricyclohexyltin (N-methyl, 3-indolyl acetate) on the basis of analogous spectroscopic behaviour.

Tricyclohexyltin (2-mercaptobenzothiazole) was similarly found to adopt a distorted tetrahedral geometry but no intermolecular bonding was observed. Other triorganotin derivatives of this ligand were considered to adopt the same geometry with varying degrees of distortion towards cis-R_3SnNS caused by a close approach of the ring nitrogen. Derivatives

of 2-mercaptobenzoxazole are also considered to be four coordinate with the exception of $Bu_3Sn(mbo)$ which seems to form a five coordinate structure at low temperature, based upon 77K Mössbauer spectroscopic evidence. The tricyclohexyltin derivative of 2-mercaptobenzimidazole is thought to form a polymeric H-bonded lattice with pendant four coordinate Cy_3Sn-.

Spectroscopic studies on tri- and diorganotin derivatives of piperazine bis-di-thiocarbamate indicate bonding by the ligand in an anisobidentate fashion. The triorganotin derivatives form ditin complexes (supported by Mass Spectrometry) while the diorganotins form covalently bonded polymers.

Triorganotin derivatives of N,N' diphenylphosphorodiamidic acid and N,N,N',N', tetraethylphosphorodiamidic acid were all considered to contain tin in a five coordinate <u>trans</u>-R_3SnO_2 configuration. For triphenyltin derivatives of these ligands a long chain polymeric structure is proposed but for the other derivatives, in particular the trimethyltin derivatives, evidence for cyclic structures is found.

Inorganic and organometallic tin salts of paraquat and diquat were synthesised in which, with the exception of the tin(II) derivative, tin was in a six coordinate octahedral configuration. Voltammetric studies on aqueous solutions of paraquat in the presence of $SnCl_4$ indicated that the first reduction step becomes more difficult and the second reduction step less difficult with increasing concentration of $SnCl_4$.

This was taken as evidence for a fall in activity of these herbicides on forming such complexes.

ACKNOWLEDGEMENTS

I would like to extend particular thanks to Dr. K.C. Molloy for his continued advice and help during the course of this work. I would also like to thank Dr. E. Hahn and Dr. D. Cunningham for carrying out the crystallographic work reported here, Dr. S. Blunden for collecting ^{119}Sn n.m.r. data, and Mr. C. Cryer for collecting Mass Spectra.

Thanks are also due to the technical support staff of the National Institute for Higher Education (Ireland) and the University of Bath and to the Department of Education (Ireland) and University of Bath for financial assistance. Finally I would like to thank Mrs. V. Edwards for her meticulous typing of this thesis.

Introduction

The challenge facing the synthetic chemist in the development of new biocidal compounds is to obtain a finer "tuning" of biocidal formulation with desired activity. Desired qualities in new formulations are increased species selectively, reduced environmental strain and an ability to overcome any acquired resistance to existing formulations.

Approaches to the development of new biocidal compounds is on three general levels of understanding; (1) Trying to totally understand the biochemical process which one wishes to selectively target and building up the reactive chemical template from knowledge of the active site. (2) Studying structure-activity relationships wherein compounds of known activity are modified slightly and then tested to see which modifications produce the greatest activity. (3) the "hit and miss" approach of randomly testing any available chemical. While the first two approaches appear to have the monopoly on scientific logic, in practice all three have lead to the development of new formulations in the past.

In this work organotin templates of known biocidal activity are modified by attaching to the tin atom ligands which are also biologically active, the logic being that the activity of the novel formulation may be greater than the sum of the activities of the individual components. This greater activity may arise from, among other factors, a reciprocal masking of one component by the other towards existing resistance.

The different solid and solution phase structures adopted by organotins are known to have varying degrees of biocidal activity and in this work physical techniques, in particular various forms of spectroscopy, are employed to determine the structures of novel compounds synthesised with a view to extending further, knowledge on structure-activity relationships for these compounds.

CHAPTER ONE

Synthesis, Structure, and Biocidial Activity of Organotin Compounds.

1.1 Introduction

Organotin compounds are compounds which contain at least one carbon-tin bond. Tin is a group IV element, and is situated between germanium and lead in the periodic table. It has a valence electron configuration of $5s^2 5p^2$, and like lighter members of the group, has a dominant oxidation state of IV. Tin compounds with a valency of II do exist but are considerably less stable than the higher oxidation state. Tin forms sigma bonds to carbon, which give rise to metal-alkyls and metal aryls of high stability.

This high stability has allowed organotins extensive industrial usuage, with annual production now in the region of 35,000 tonnes (1). One of the growth areas of organotin chemistry is their application as selective biocides. This thesis describes the synthesis of novel organotin biocides, which contain other known biocides as ligands. As background to this work, the synthetic, structural and biocidal aspects of organotin chemistry is herein reviewed.

Organotin chemistry has received extensive general literature coverage and there are several comprehensive reviews (1,2,3), monographs (4,5) and books (6,7) available.

1.2. Synthesis of Organotin Compounds

The starting material for the preparation of nearly all organotin compounds is stannic chloride. Organic groups are introduced onto the tin atom using other organometallic reagents. Three of the main industrial methods are listed here (8).

$$4RMgX + SnCl_4 \rightarrow R_4Sn + 4MgXCl \quad \text{(Grignard)} \qquad \text{(a)}$$

$$8Na + 4RCl + SnCl_4 \rightarrow R_4Sn + 8NaCl \quad \text{(Wurtz)} \qquad \text{(b)}$$

$$4R_3Al + 3SnCl_4 + 4R_2O \rightarrow 3R_4Sn + 4AlCl_3.R_2O \quad \text{(Aluminium/alkyl)} \qquad \text{(c)}$$

The appropriate tetraorganotin is synthesised first and then the mono-, di-, and triorganotins are made by the Kocheshkov comproportionation reaction (1), in which appropriate ratios of R_4Sn and $SnCl_4$ are mixed at high temperatures. The resulting organotin halides, are starting materials for a large variety of other organotin compounds as illustrated in Scheme 1. The main reaction pathways employed in this work are the nucleophilic displacement of chloride by X^-, and the dehydration reaction of organotin oxides, and hydroxides with the acid form of a ligand.

1.3. The Structure of Organotin Compounds

The amount of organotin x-ray structures successfully solved continues to increase, and several reviews are now available (2,3,9). It was generally believed that all organotin compounds were four coordinate, until 1963, when Hulme (10) demonstrated that trimethyltin chloride monopyridine was in fact five coordinate (Fig. 1.1). In the twenty years since then, organotin compounds have been found which exhibit four, five, six and seven coordination.

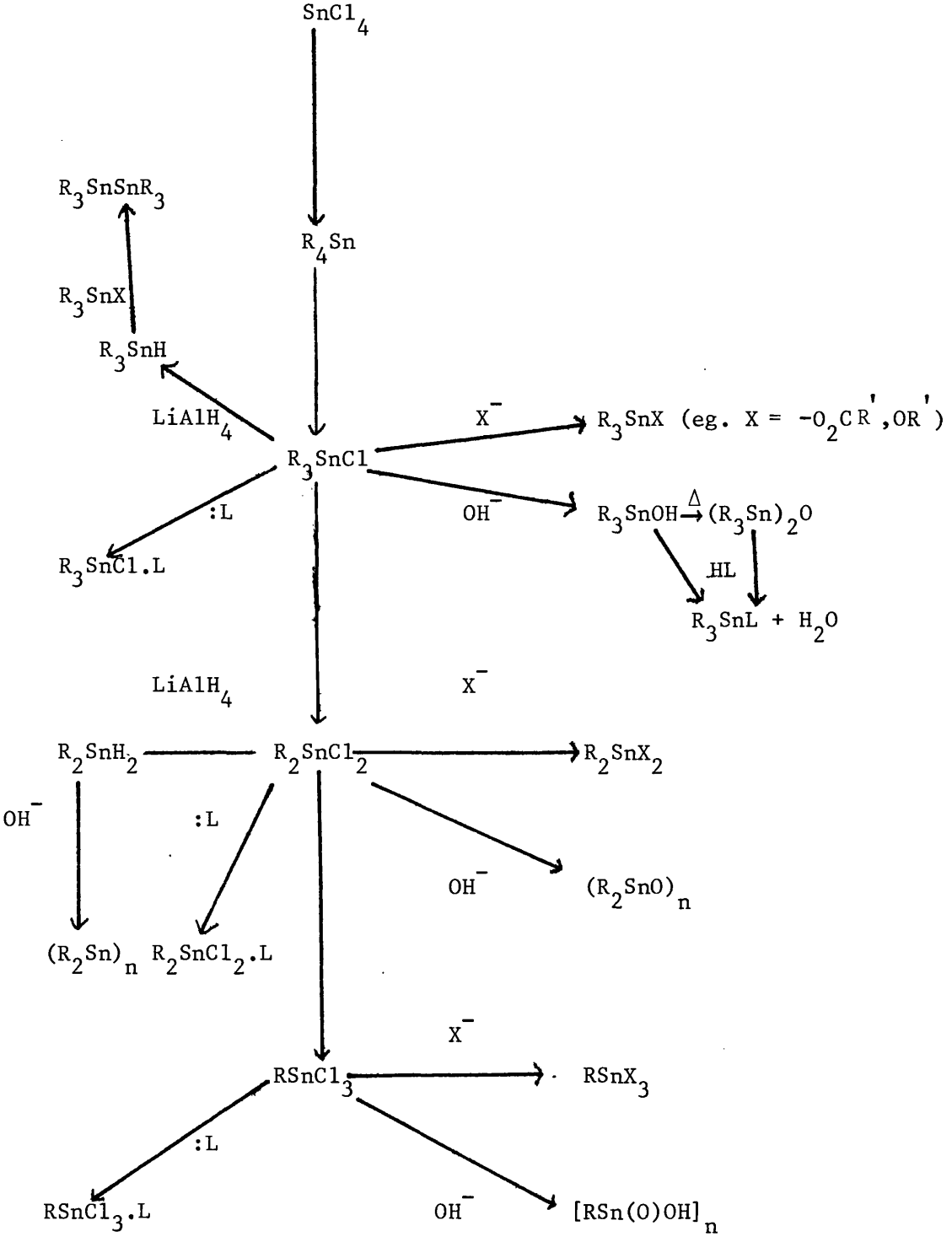
SnCl4
R4Sn
R3SnSnR3
R3SnX
R3SnH
LiAlH4
X⁻
R3SnX (eg. X = -O2CR',OR')
R3SnCl
:L
R3SnCl.L
OH⁻
R3SnOH → (R3Sn)2O
HL
R3SnL + H2O
LiAlH4
X⁻
R2SnH2
R2SnCl2
R2SnX2
OH⁻
:L
OH⁻
(R2SnO)n
(R2Sn)n
R2SnCl2.L
X⁻
RSnCl3
RSnX3
:L
RSnCl3.L
OH⁻
[RSn(O)OH]n

Scheme 1.

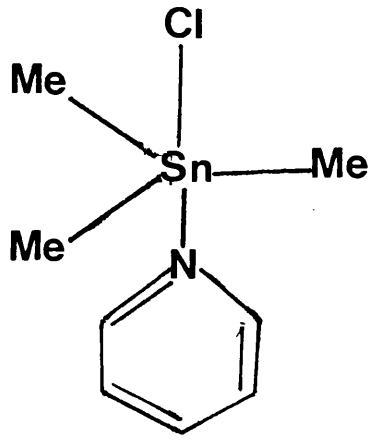

Fig. 1.1 Trimethyltinchloride monopyridine

1.3.1 Four Coordinate Organotins

Tetraorganotin compounds whose structures have been determined, such as Ph_4Sn (11), have all been found to be four coordinate. Tetraorganotins do not expand their coordination number because they are weak Lewis acids and therefore poor electron acceptors. If the organic R groups in the generalized formula R_nSnX_{4-n}, are progressively replaced by the more electronegative X group, then the Lewis acidity of the molecule increases and it is more likely to expand its coordination sphere. An example of this are the compounds shown in Fig. 1.2. The tetraorganotin (1.2(a)) has a Sn---Br interaction of 4.35Å (12), which is greater than the sum of the Van der Waals radii, and the molecule is essentially tetrahedral. In the triorganotin bromide (1.2(b)), the same Sn---Br interaction has shortened to 3.77Å (13), which is within the sum of the Van der Waals radii. A Br-Sn-Br angle of 149.5° also suggests that the geometry is altering towards trigonal bipyramidal.

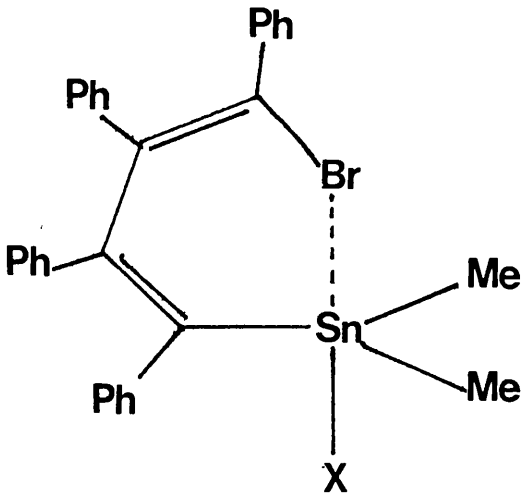

Fig. 1.2 (a) X = Ph; (b) X = Br

Four coordination may still be preserved even if R groups are replaced by electronegative X groups. Cyclic systems such as the $(t\text{-}Bu_2SnO)_3$ trimer still have a tetrahedral geometry about tin (14). Four coordination may also be preserved if there are bulky groups attached to the ligand e.g. $Ph_3SnSC_6H_2Me_3$ - 2,4,6 (15). Bulky R groups on the tin as found in $[(Me_3Si)_2CH]_3SnCl$ (16) will also help maintain four coordination.

1.3.2. Five Coordinate Organotins

Because of their greater Lewis acidity triorganotins readily accept an electron pair from another donor atom to give a five coordinate R_3SnX_2 structure. Either a square pyramidal or trigonal bipyramidal (tbp) geometry is possible for a R_3SnX_2 system, but only the latter are found. A tbp geometry gives rise to three configurations illustrated in Fig. 1.3.

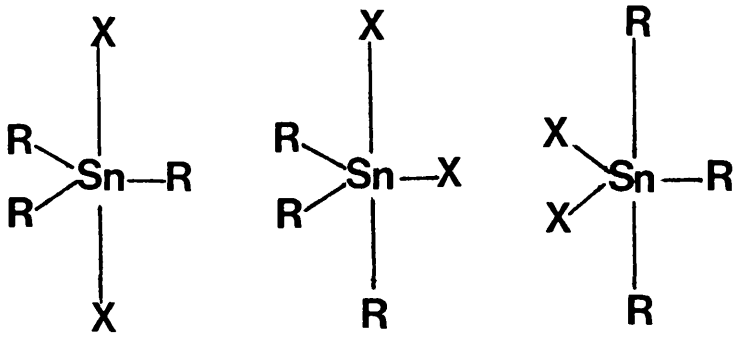

Fig. 1.3. (a) (b) (c)

The trans-configuration (a) is the commonest, while the mer-form (c) has yet to be demonstrated crystallographically. The cis-configuration (b) invariably arises from chelation, while the trans-structure is principally the result of a bridging interaction, and hence many compounds adopting the trans-structure are polymers. Monomeric forms of the trans-structure do exist however, for example the anions $R_3SnX_2^-$, and adducts R_3SnXL where L is a monodentate Lewis base. Trimethyltinchloride monopyridine is an example of the latter (10).

X-ray crystallographic studies on the organotin anions $Me_3SnCl_2^-$ (17), $Ph_3SnCl_2^-$ (18) and $Bu_3SnCl_2^-$ (18), have all yielded trans-tbp structures, with the more electronegative chlorines in axial positions, and a near planar SnC_3 unit. Cl-Sn-Cl angles for the $Ph_3SnCl_2^-$ and $Bu_3SnCl_2^-$ anions are 177.5^o and 179.2^o respectively, showing little deviation from linearity (18). A cationic organotin species $Bu_3Sn(H_2O)_2^+$

has also been found to exhibit this geometry (19). Here the trans O-Sn-O angle is 178.4° (19).

Intramolecular chelation nearly always leads to a cis-tbp configuration for five coordinate organotins, but there are some unusual examples of a trans geometry being formed, such as the compound synthesised by Noltes (20) and shown in Fig. 1.4. In this compound the second donor atom is attached to one of the organic groups, and whereas the "chelating unit" bonds axially and equatorially, the more electronegative donor atoms are in trans-axial positions.

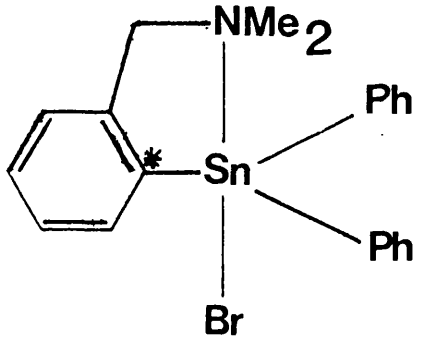

Fig. 1.4. C,N-[2{(dimethylamino)methyl}phenyl]diphenyltin bromide.

This compound however does show some distortions from ideal trans-tbp geometry, with a N-Sn-Br angle of 171° and N-Sn-C* angle of 75.3°.

In the case of a cis-geometry, the ligand has donor atoms in both axial and equatorial positions as exemplified by (1,3-diphenylpropane 1,3 dionato)triphenyltin (21), shown in Fig. 1.5. As a result of the narrow bite of the ligand (71.3°) there is significant deviation from ideal geometry. The trans-O-Sn-C angle has narrowed to 157.2°, while chelation is anisodentate with a longer Sn-O interaction in the axial position (2.308Å) than in the equatorial (2.091Å) (21).

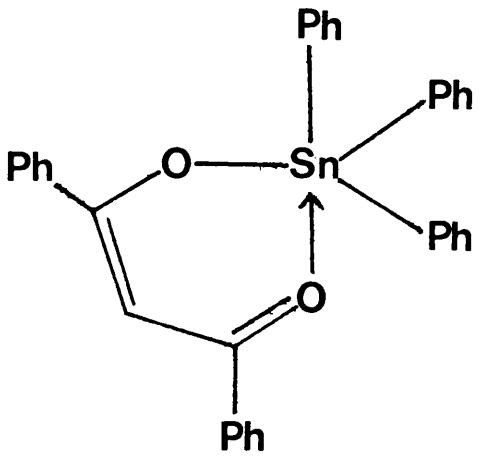

Fig. 1.5. (1,3-diphenylpropane-1,3-dionato)triphenyltin

If a ligand is bidentate it is also capable of bridging R_3Sn units, thus forming polymers. The overall appearance of this polymer chain will depend on the size and nature of the bridging group. Molloy and Quill (22) have suggested a classification system for such polymers which is illustrated in Fig. 1.6.

Class I polymers are "rod-like" with co-linear tin and X group, and occur when the bridging group is small such as in F, or CN. Me_3SnCN has planar Me_3Sn units equidistantly bridged by the CN group (23). Class II type polymers form zig-zag chains an example of which is Ph_3SnOH (24). The

hydroxy group bonds to tin in an almost isodentate fashion with Sn-O bonds of 2.197Å and 2.255Å. The SnC_3 unit is planar and the zig-zag structure arises from a Sn-O-Sn angle of 137.8° (24).

As the number of atoms in the bridging group increases a more flexible "S"-shaped polymer develops described in Fig. 1.6 as a class III polymer. This type of structure is commonly adopted by triorganotin carboxylates such as tribenzyltin acetate (25) and triphenyltin acetate (26).

Class IV type polymers are the most flexible, having a "concertina"-like shape. An example of this type of helical polymer is Me_3SnO_2SMe (27).

Diorganotin compounds are less likely to adopt five coordinate structures because of their greater Lewis acidity and therefore are inclined to expand to six coordination. Some examples of R_2SnX_3 compounds are found, however, such as the anion $Me_2SnCl_3^-$ (28), and diorganotin derivatives of tridentate Schiffs bases, e.g. [N-(2-hydroxyphenyl)-salicylaldimine]dimethyltin illustrated in Fig. 1.7 (29). In both these compounds the Sn-C bonds are in equatorial sites. Some five coordinate monorganotins also exist, such as the anion $MeSnCl_4^-$, which like the R_2SnX_3 species retains an equatorial R group (30).

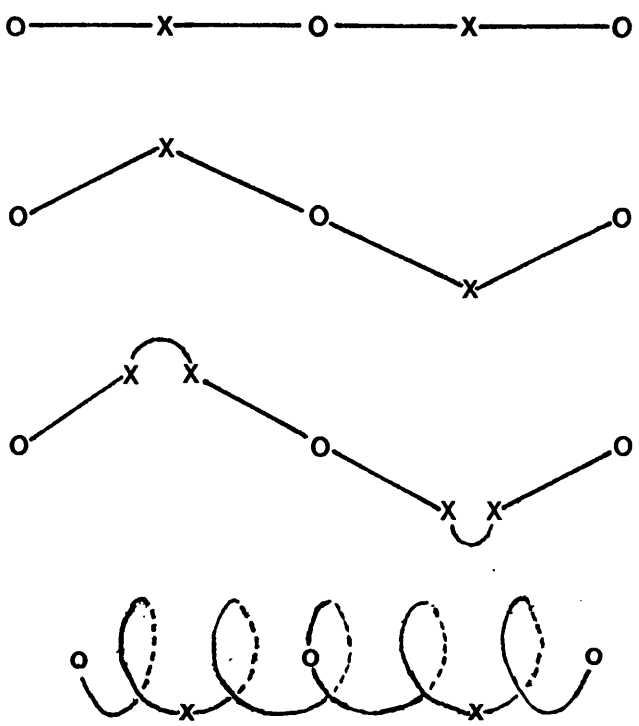

Fig. 1.6 Classification of Organotin Polymers

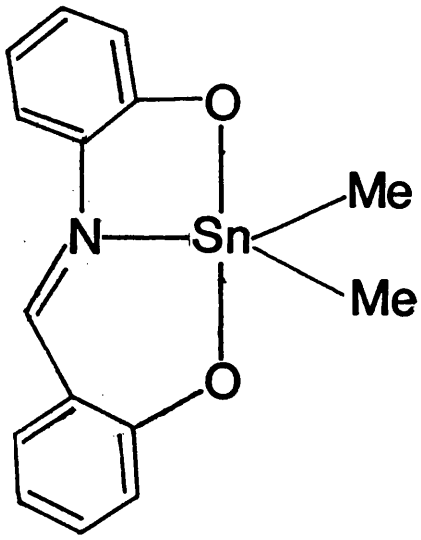

Fig. 1.7 [N-(2-hydroxyphenyl)salicylaldimine]dimethyltin

1.3.3. Six Coordinate Organotins

Diorganotin compounds, R_2SnX_2, have a strong tendency to increase their coordination number to six. This can arise from either intramolecular interactions to give molecular structures, or intermolecular interactions to give polymeric structures.

The octahedral organotin species R_2SnX_4, where all donor atoms (X) are the same can exist in two structural forms, as shown in Fig. 1.8, the cis (a) and trans (b) isomers.

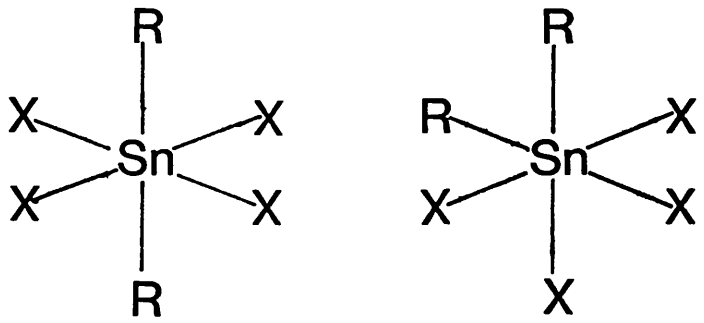

Fig. 1.8. (a) (b)

The trans-geometry is much more common than the cis. $Me_2Sn(acac)_2$ for example has trans-methyl groups with an ideal C-Sn-C angle of 180° (31). In cases where the cis-geometry is adopted the C-Sn-C angle narrows, as in $Me_2Sn(O.NH.CO.Me)_2$ to 109.1° (32) and in $Ph_2Sn(S_2CNEt_2)_2$ to 101.4° (33) but does not reach the ideal cis angle of 90°.

Distortion from ideal geometry, due to ligand repulsion or the presence of weak donor atoms, is the rule rather than the exception. In the case of bidentate ligands one donor atom often has a weaker interaction with tin than the other, and the R-Sn-R angle does not open out to the ideal trans value of 180°. This is illustrated in Fig. 1.9, and exemplified by the series, $Me_2Sn(S_2CNMe_2)_2$, C-Sn-C = 142.3° (34); $Me_2Sn(S_2CNEt_2)_2$, C-Sn-C = 136° (35) and $Me_2Sn(S_2CN(CH_2)_4)_2$, C-Sn-C = 129.7 (33).

For $R_2SnX_2Y_2$ organotin compounds where R groups are trans, then the X and Y donor atoms can be arranged either all trans or all cis. If either X_2 or Y_2 is bidentate then the cis-configuration of donor atoms is demanded, e.g. Ph_2SnCl_2.bipy (36). If all donor atoms are from monodentate ligands then a trans-arrangement is more common, as in $Me_2SnCl_2.2H_2O.4C_5H_4N_4$ in which Me, Cl and H_2O occupy the coordination sphere about tin, the purine molecules are H-bonded to the water and all trans-angles are 180° (37).

As with triorganotins, the nature of polymer formation in diorganotins, depends on the size of the bridging unit and the strength of the intermolecular interaction. The extent to which diorganotin halides form associated lattices has received particular attention. Dimethyltin difluoride (38) has the strongest interactions forming an infinite sheet polymer, the two-dimensional equivalent of class I polymers described in Fig. 1.6. The sheet is composed of co-planar Sn and F atoms while the methyl groups lie above and below the $(SnF_2)_n$ plane.

In the case of other diorganotin halides the intermolecular interaction is more ambiguous. Greene and Bryan (39) describe the structure of Ph_2SnCl_2 as essentially tetrahedral, though a rather long intermolecular Sn----Cl distance of 3.77Å is found. The fact that the C-Sn-C angle opens to 127° to accommodate such a lattice interattraction does not dilute their scepticism about halogen bridge formation in this and other diorganotin halides (39).

Davies et al (40) describes the structure of Me_2SnCl_2 as a weakly bridged zig-zag polymer. The C-Sn-C angle at 123.3° is no longer than that for Ph_2SnCl_2, but a shorter intermolecular distance of 3.54Å is found. The chlorines on each Me_2SnCl_2 unit bridge to another tin atom on either side as shown in Fig. 1.10. A different type of structure is found for Et_2SnI_2 (41) and $(ClCH_2)_2SnCl_2$ (42), (Fig. 1.11) in which bridging occurs in a chelating manner. Et_2SnBr_2 and Et_2SnCl_2 (41) bridge in the same manner as Me_2SnCl_2.

Only two six coordinate triorganotins have been demonstrated so far: Ph_3SnOAc which has a mer-Ph_3SnO_3 structure (26) and Me_3Sn[tris(pyrazoyl)borate] which has a distorted fac-Me_3SnN_3 geometry (43).

Six coordinate monoorganotins are also known, such as the dimeric species $[EtSn(OH)Cl_2H_2O]_2$ (44) which contain bridging hydroxide groups.

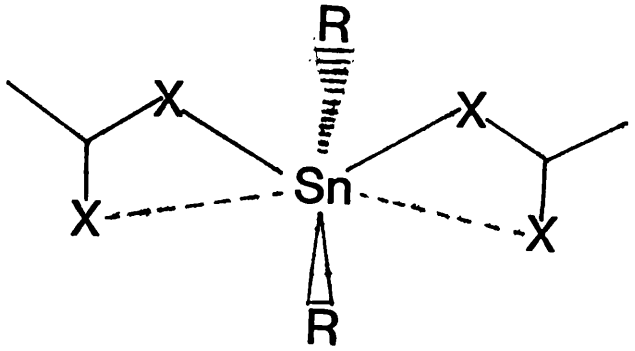

Fig. 1.9. As the longer Sn----X interaction weakens the R-Sn-R angle closes

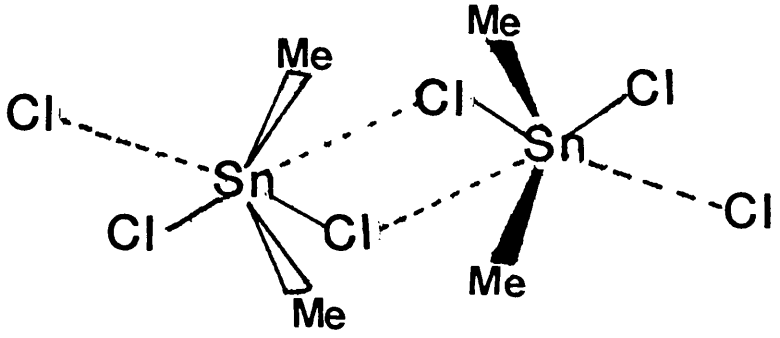

Fig. 1.10. Me_2SnCl_2

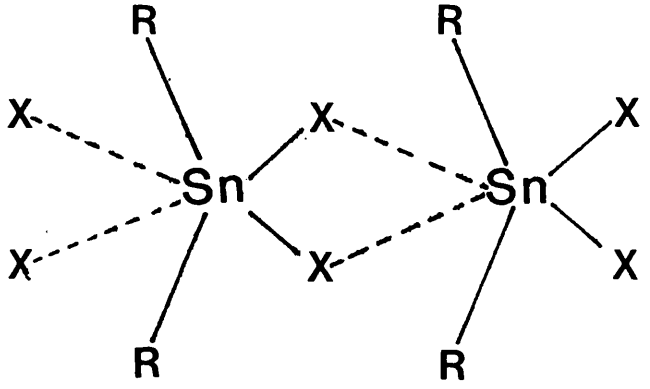

Fig. 1.11. R = Et; X = I, and R = $ClCH_2$; X = Cl

1.3.4. Seven Coordinate Organotins

Monoorganotins with three bidentate ligands readily adopt a seven coordinate structure. The preferred geometry for such $RSnX_6$ species is pentagonal bipyramidal, with apical R group. An example of this structure is $MeSn(S_2CNEt_2)_3$ (45) which contains two ligands chelating equatorially and one ligand bonding both axially and equatorially. Some diorganotins also form seven coordinate pentagonal bipyramids such as [2,6-diacetylpyridine bis(2-aminobenzoylhydrazone)]diphenyltin (46). In this structure (Fig. 1.12) the phenyl groups lie in a trans-axial position with a near ideal C-Sn-C angle (176.4°). The five donor atoms of the ligand occupy equatorial sites.

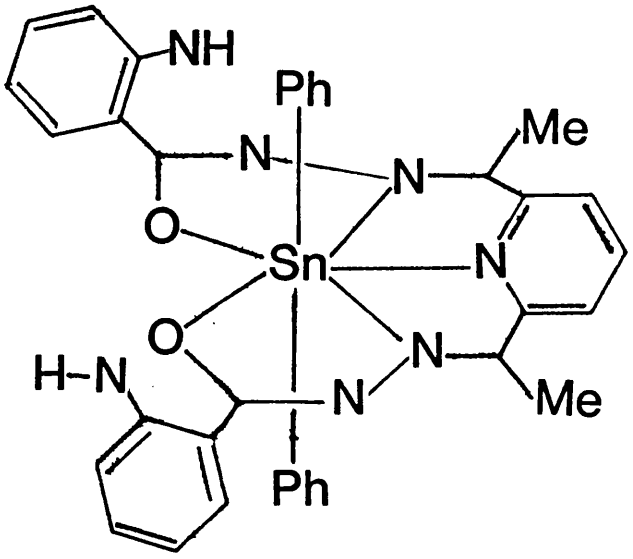

Fig. 1.12.

1.4. Spectroscopy and Analysis of Organotins

For the structural chemist, x-ray crystallographic studies are the definitive technique. However, due to the common difficulty in obtaining crystals of suitable quality or indeed a crystalline sample at all, supplementary structural probes are needed. Organotin chemistry is particularly blessed in this regard, because of the amenability of these compounds to a wide range of spectroscopic techniques. In addition to routine spectroscopic probes i.e. ir/Raman, uv, $^{13}C/^{1}H$ nmr, and mass spectrometry, the ^{119}Sn isotope (8.5% abundance) provides a particularly useful "handle" being both nmr ($I = \frac{1}{2}$) and Mössbauer active.

A common approach for the organotin chemist is the correlation of spectroscopic information with established crystal structures, to build up systematics which will allow the approximation of structure from spectroscopic techniques alone. This relationship although purely empirical has proved particularly useful in the case of ^{119}Sn Mössbauer spectroscopy.

1.4.1. ^{119}Sn Mössbauer spectroscopy.

Comprehensive and specialized reports on the Mössbauer phenomenon, and its application to tin compounds are available in many books (47,48) and reviews (49,50,51).

Mössbauer spectroscopy uses gamma-ray radiation to excite the nucleus of the ^{119}Sn isotope from ground to excited state. Isomer shift (δ) and quadrupole splitting are the two most accessible parameters obtained from the Mössbauer experiment.

The isomer shift is the energy difference between the nuclear transition in the absorber nucleus (sample), and that in a standard gamma-ray source (usually SnO_2 or $BaSnO_3$). It is quoted in mms^{-1}, which is the doppler acceleration required to match source and absorber nuclear transition energies.

The energy required to achieve this transition is very sensitive to the electron distribution at the nucleus of the absorber atom, and since only s electrons have a finite probability of existing at the nucleus, and only valence electrons are involved in chemical change, the following relation has been proposed:

$$\delta = k\, dR/R\, [|\Psi^2_{5s}(0)|^2_a - |\Psi^2_{5s}(0)|^2_s]$$

k is a constant for a particular isotope while dR/R is the change in the nuclear radius on going from excited to ground state, which is positive for tin . $|\Psi^2_{5s}(0)|_a$ is the 5s electron density at the absorber nucleus and $|\Psi^2_{5s}(0)|_s$, that for the source.

δ is therefore a probe of the valence shell s electron density at the tin nucleus, and should vary with oxidation state of the metal and the electronegativity of attached ligands. The isomer shift of α-Sn (2.10 mms^{-1}) is now considered to be the dividing line between SnIV and SnII compounds (51), with SnII derivatives lying to the high velocity side, but there are still some ambiguities in this schematic.

An increase in coordination number above four will necessitate the use of d orbitals in bonding, with a resultant drop in s electron density at the nucleus, and a fall in the value of δ. This is exemplified by the series $SnCl_4$ $\delta = 0.8 mms^{-1}$, $SnCl_5^-$ $\delta = 0.6 mms^{-1}$, and $SnCl_6^{2-}$ $\delta = 0.5 mms^{-1}$ (52).

As the electronegativity of an attached ligand increases so does the polarity of the Sn-L bond, and there is a decrease in the value of δ. A linear relationship between δ and the Mulliken electronegativity of the ligands has been found for the series $BuSnX_{5-n}Y_n^{2-}$ where X, Y = F, Cl, Br (53). The most electronegative ligand, F, gives the lowest δ ($BuSnF_5^{2-}$: $0.27 mms^{-1}$) whilst the least electronegative, Br gives the highest δ ($BuSnBr_5^{2-}$: $1.38 mms^{-1}$). The electron donating power of the R group also affects δ, with alkyl substituents leading to higher δ than aryl (electron withdrawing) groups e.g. Bu_4Sn ($1.35 mms^{-1}$) and Ph_4Sn ($1.15 mms^{-1}$) (50).

δ also shows some variation with geometry, for example in the R_2SnX_4 series the trans- R arrangement has higher δ than the cis- arrangement (54). This is explained by the fact that the near linear (sp) geometry of R groups in the trans-form has greater percentage s character.

Quadrupole splitting arises when the tin atom lies in a non-cubic arrangement of ligands. This leads to an electric field gradient (efg) at the nucleus, which lifts the degeneracy of the excited state and two transitions are then possible (Fig. 1.13). Two peaks are then seen in the Mössbauer spectrum the separation of which is the quadrupole splitting, ΔEq, and δ is then the midpoint of the two absorptions.

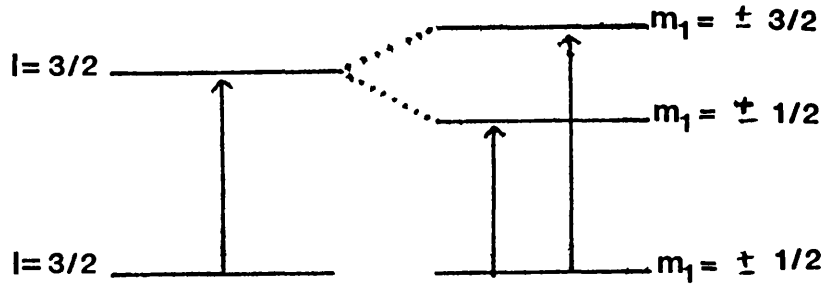

Fig. 1.13. $\Delta Eq = 0$ $\Delta Eq > 0$

Compound	C-Sn-C angle	ΔEq (mms^{-1})
$Me_2Sn(oxin)_2$	110.7 (59)	2.02
$Me_2Sn(S_2CN(CH_2)_4)_2$	129.7 (33)	2.85
$Me_2Sn(S_2CNEt_2)_2$	136.0 (35)	3.14
Me_2SnF	180.0 (38)	4.38
$Ph_2Sn(S_2CNEt_2)_2$	101.4 (33)	3.45
Ph_2SnCl_2.bipy	173.4 (36)	3.76

Table 1.1. The relationship between ΔEq and the C-Sn-C angle for R_2SnX_4 systems.

The quadrupole splitting is a good probe of the configuration of donor atoms about tin.

A model has been developed which treats each ligand as a point charge centred on the donor atom, to calculate theoretical values of ΔEq for ideal geometries (55). The first predictions of this model were that $RSnX_4$ and cis-R_2SnX_4 systems should have similar ΔEq values but that trans-R_2SnX_4 geometries should have ΔEq values twice as large (55). Some experimental agreement has been found with the former having ΔEq values of around $2mms^{-1}$ and the latter $4mms^{-1}$ (55). Deviations from these results often occur however, as a result of distortions from ideal geometry. The five coordinate R_3SnX_2 systems (Fig. 1.3) showed an even greater variation of ΔEq values, with the trans-X configuration having a range $3.0 - 3.9mms^{-1}$ and the cis-arrangement $1.7 - 2.3mms^{-1}$ (56).

A greater agreement between calculated and found ΔEq values has been obtained by applying different partial quadrupole splitting values for ligands in different coordinating geometries and environments e.g. axial and equatorial tbp sites (57). Results from this work still fail to deal with major distortions from ideal geometry.

The distortions in R_2SnX_4 octahedral systems, which lead to ΔEq values between 2 and $4mms^{-1}$ have, however, been the source of a much more accurate relationship between structure and ΔEq values. In such systems the partial quadrupole splitting contributions from the R group are much larger than those for the other donor atoms (58). As the C-Sn-C angle is the primary source

of distortions in such systems the following relationship has been proposed:

$$\Delta Eq = 4\{R\}\ [1-3Sin^2\theta Cos^2\theta]^{\frac{1}{2}}$$

{R} is the partial quadrupole splitting of the R group, and the C-Sn-C angle equals 180-2θ. Good agreement is found for dimethyl and diphenyltin compounds, where there is a steady increase in ΔEq values with increasing C-Sn-C angle, as shown in table 1.1 (58,50).

Mössbauer spectroscopy may also yield information about the lattice dynamics of an organotin. Because of the high energy of the gamma-ray much of the absorption-emission process is destroyed by recoil in either the source or absorber nucleus. The area under the Mössbauer resonance (A_T) depends on the recoil free fraction (f) of absorptions, which in turn is related to the vibrational motion of the tin atoms.

$$A_T \propto f = \exp(-E\gamma\langle x^2\rangle/(hc)^2)$$

where Eγ is the energy of the gamma-ray and $\langle x^2\rangle$, the mean square vibrational amplitude of the tin nucleus. If ln A_T is plotted against temperature, a straight line of negative slope is expected in the high temperature limit of the Debeye model, which forms the basis of the theory (51). This slope should be related to the tightness with which the tin atom is held in the lattice, and hence the degree of intermolecular interactions.

It should be possible to assign ranges of slopes which are indicative of monomers, one-dimensional polymers, H-bonded lattices etc. The separation of slope values for different structures has not, however, proven to be very clearly defined. $Ph_2Sn[S_2P(OiPr)_2]_2$, for example, has been shown by x-ray studies to be a very orderly packed yet still monomeric compound (60),but its variable temperature slope indicates it to be a strongly associated polymer (61). This material has been termed a "virtual polymer" (61) and probably owes its lattice dynamics to unusually strong packing forces.

Molloy and Quill (22) have noted a relationship between the nature of polymer propagation and variable temperature slope. They found that not all one-dimensional polymers gave similar slopes, and that helical polymers like Ph_3SnOAc (26) have slopes similar to monomers. This is accounted for by their "concertina"-like shape which makes the polymer more flexible.

1.4.2. Infra-red and Raman spectroscopy.

Infra-red spectroscopy is an important routine technique for identifying novel compounds. When a ligand coordinates to a metal atom, there is a redistribution of its electron density, causing bands to shift in the i.r. spectrum. New bands due to Sn-L bonds will also be found. Tanaka's comprehensive review (62) assigns bands to many Sn-L vibrations for organotin compounds.

As well as being an important analytical tool, i.r. can give additional information on both solid and solution phase structure. In halogen bridged lattices for example ν(Sn-X) for the bridging halogen occur at lower frequencies than for a terminal halogen, e.g. for $MeSnF_3$ ν(Sn-F) terminal occurs at 646cm^{-1} and ν(Sn-F) bridging at 425cm^{-1} (63).

Tin-carbon vibrations are of particular interest in elucidating structural information from i.r. studies. This is best illustrated by trimethyl and dimethyltin compounds. In tetrahedral compounds such as Me_3SnBr and Me_2SnBr_2 bands assigned to the symmetric and asymmetric Sn-C stretches are found at 506-516cm^{-1} and 528-536cm^{-1} respectively (64). However, when as in the case of Me_3SnOH the geometry is changed to <u>trans</u>-tbp (65) and the SnC_3 unit is planar, only the asymmetric band is found (66). The symmetry change has meant that the symmetric stretch no longer leads to a change in dipole moment and hence is not i.r. active, though it remains Raman active. In non-polar solvents Me_3SnOH forms a hydroxy bridged dimer, with <u>cis</u>-oxygen atoms, and Sn-C bonds which are no longer co-planar. Both symmetric and asymmetric Sn-C stretches are then found in the i.r. spectrum (66).

Similar results are found for dimethyltins when they extend their coordination to six-coordinate R_2SnX_4. In the aquo-dimethyltin cation $Me_2Sn(H_2O)_4^{2+}$ the C-Sn-C unit is linear and only the asymmetric band (582cm^{-1}) is found in the i.r. (67). The symmetric band is found in the Raman at 529cm^{-1} (67).

As the length of the alkyl chain increases the situation becomes more complicated in the i.r. with the chain adopting trans and gauche-isomers.

Similarly Sn-Ph stretches have been difficult to assign because of coupling with ring vibrations. A band found at around 1065cm^{-1}, thought to be an in plane C-H deformation perturbed by the tin atom is useful as a characteristic vibration of phenyltins (68). Bands at 260-280cm^{-1} and 225-240cm^{-1} have been assigned respectively to asymmetric and symmetric Sn-Ph stretches in tri- and diorganotin compounds (69).

1.4.3. N.m.r. Spectroscopy.

In addition to the now routine applications of ^{1}H and ^{13}C n.m.r., tin has ten naturally occurring isotopes of which three are n.m.r. active ($I = \frac{1}{2}$): ^{119}Sn (8.5% abundance), ^{117}Sn (7.57%), and ^{115}Sn (0.34%). ^{119}Sn n.m.r. is the preferred technique because of the greater sensitivity and abundance of this nucleus.

The coupling between $^{119/117}Sn$ nuclei and other n.m.r. active nuclei, particularly ^{1}H and ^{13}C yields valuable structural information. ^{2}J ($^{117/119}Sn$-C-^{1}H) coupling constants have a range of ca. 50 - 100Hz and can be observed in both ^{1}H and ^{119}Sn n.m.r. experiments. ^{1}H n.m.r. is the easiest source of these couplings, especially since ^{119}Sn n.m.r. spectra are generally proton-decoupled. $^{2}J(^{119}Sn$-C-$^{1}H)$ in the series Me_nSnX_{4-n} has been found to increase with the value of n, and the electronegativity of X (70) (Table 1.2). It was also found to increase when measured in donor solvents (71).

Table 1.2. Representative values for $^{2}J(^{119}Sn\text{-}C\text{-}^{1}H)$

Compound	Solvent	$^{2}J(^{119}Sn\text{-}C\text{-}^{1}H)$ (Hz)	Reference
Me_4Sn	CCl_4	54.0	(70)
Me_3SnCl	CCl_4	58.1	(70)
Me_3SnF	CCl_4	69.0	(70)
Me_2SnCl_2	CCl_4	69.0	(72)
$MeSnCl_3$	CCl_4	100.0	(72)
Me_3SnCl	H_2O	65.2	(71)
Me_2SnCl_2	H_2O	97.4	(71)

These variations in the coupling constant can be explained as a rehybridisation of bonding orbitals to put more p-character in bonds to electronegative ligands and more s-character in the Sn-C bonds (71). The $^{119}Sn\text{-}C\text{-}^{1}H$ coupling should therefore be a good indicator of geometry about tin in solution. For example in aqueous solution Me_3SnCl forms the tbp $Me_3Sn(H_2O)_2^{+}$ cation with co-planar and predominantly sp^2 hybridised Sn-C bonds. This increase in percentage s-character over sp^3 accounts for the increased coupling constant (71). Similarly the $Me_2Sn(H_2O)_4^{2+}$ cation has a linear SnC_2 unit utilising sp-hybrids on tin and therefore even greater percentage s-character in the Sn-C bonds, and a larger coupling constant.

It has also been possible to distinguish cis and trans-isomers of the octahedral complex Me_2Sn(salen) using ^{1}H n.m.r. The cis-isomer (bent SnC_2) has a coupling constant of 83.4Hz in $CDCl_3$, while the trans isomer (linear SnC_2) exhibits a larger

coupling of 113.1Hz (73).

^{119}Sn n.m.r. spectroscopy, is also diagnostic of the coordination number at tin in solution, and following the development of the double resonance technique (74), and Fourier transform methods (75), ^{119}Sn n.m.r. spectra can now be collected on a routine basis. Chemical shifts are quoted relative to Me_4Sn, with those downfield having a positive sign. The chemical shift is affected by both coordination number and the electronegativity of the donor atom. As the electronegativity of the ligand increases deshielding occurs and the chemical shift moves downfield (more positive), as in the following series: Me_3SnBr (-128ppm), Me_2SnBr_2 (-74ppm), $MeSnBr_3$ (+170ppm) (72).

An increase in coordination number to five or six produces a shift upfield (1), and hence ^{119}Sn n.m.r. can also be used to observe the autoassociation of monomers to polymers in solution, with increasing concentration. In the case of trimethyltin formate, a dilute (0.05M) solution in $CDCl_3$ has a chemical shift of +152.0ppm, but if the concentration is increased to 3M the shift moves upfield to +2.5ppm, indicating polymer formation.

1.4.4. Mass Spectrometry

Tin containing fragments give very distinctive patterns in their mass spectra, because of the large number of naturally occurring isotopes of tin. Expected patterns for mono- and di-tin fragments are shown in Fig. 1.14 (77).

Parent peaks are rarely found in any great abundance in the mass spectra of organotins because they readily lose an organic radical in the electron beam (78). The peaks found most often for triorganotins are the even electron ions: R_2SnX^+, R_3Sn^+, RSn^+ and SnX^+ (78).

1.5. Biocidal Action of Organotins

Because of their extensive and increasing industrial usuage, the biocidal action and toxicology of organotins have received considerable attention.

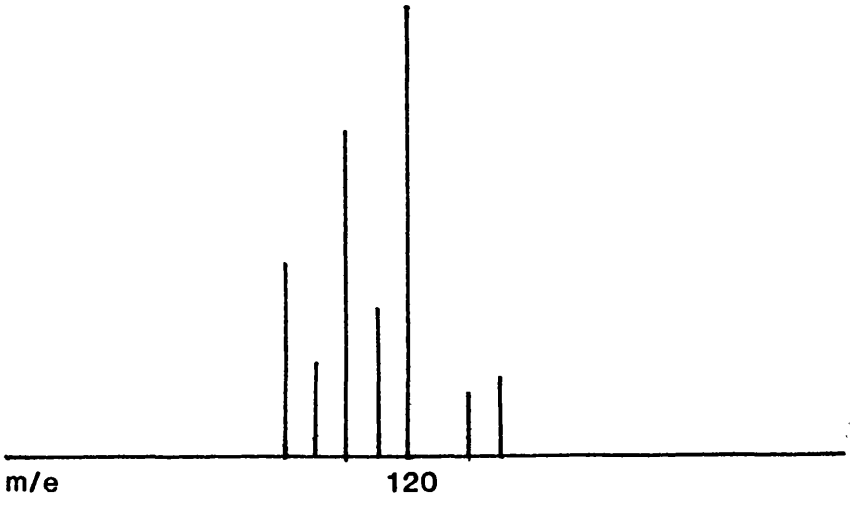

(a)

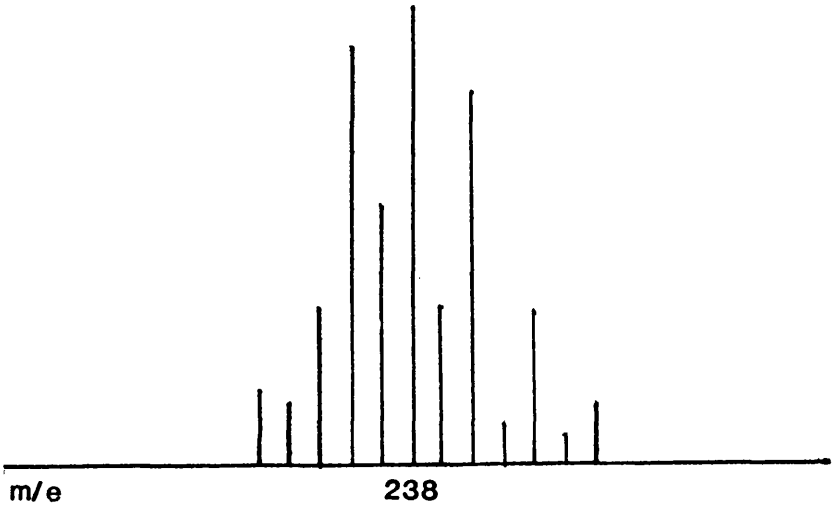

(b)

Fig. 1.14. Expected patterns for mono-tin (a) and di-tin (b) fragments in Mass Spectra.

1.5.1. General Patterns and Structure-activity Relationships

Variations in n, R, and X in the general formula R_nSnX_{4-n} reveal a marked activity-species dependence (79). Changes in n produce a maximum biocidal activity for most species when n = 3 (79). The nature of the R group, in particular the length of the alkyl chain, is also important. In mammals, the trimethyl and triethyltin compounds are most toxic (79). This is also true for insects (80), but in the case of fungi, gram positive bacteria and molluscs the tributyltin series are most toxic (81). This is illustrated in Fig. 1.15. for a series of trialkyltin acetates (80). Triphenyltin compounds are also active against fungi (81) and tricyclohexyltin and trineophyltin compounds are both effective acaricides (82,83).

Because of their high mammalian toxicity the lower trialkyltins are not used commercially. As the length of the alkyl chain increases there is a sharp drop in toxicity, with trioctyltin compounds being essentially non-toxic (79).

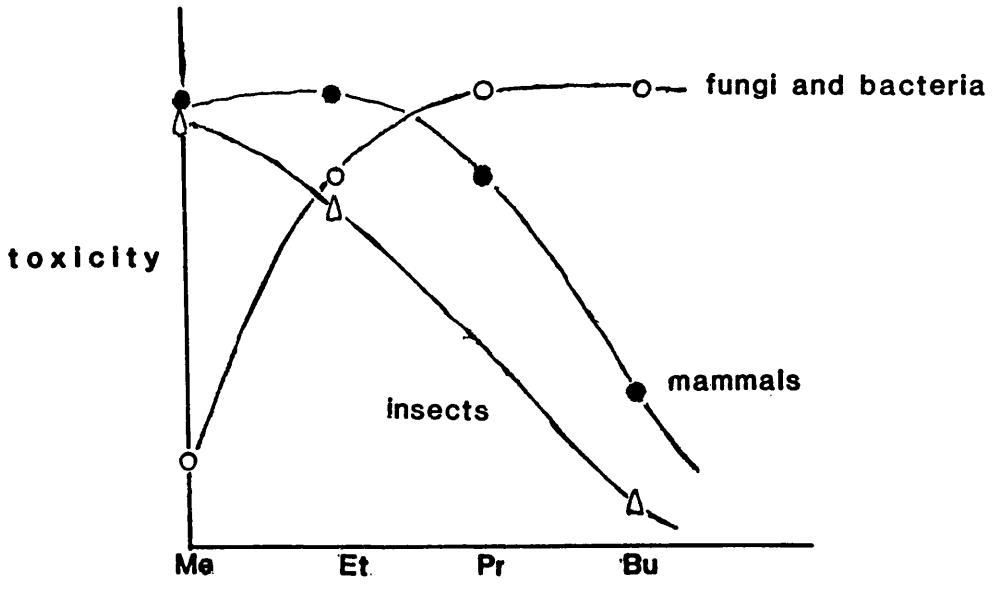

Fig. 1.15. Variation of toxicity with length of alkyl chain for R_3SnOAc compounds.

It has been generally held that the X group has no significant effect on the activity of organotins (81). However, this is not entirely true and a recent publication (84) shows how Ph_3SnX and Cy_3SnX derivatives of a chelating ligand are generally less active than the commercial biocides Ph_3SnOH and Cy_3SnOH. This difference in activity had been found to be structure related. The structure of commercial organotins are either monomeric with a tetrahedral configuration such as bis(tributyltin)oxide (85) or polymeric with a bridging X group and a trans-tbp configuration, such as Cy_3SnOH (86) and Ph_3SnOH (24), or bridging X with a distorted octahedral configuration e.g. Ph_3SnOAc (26).

The less active chelated compounds are known to adopt a cis-tbp, five-coordinate structure. A lower activity for such a structure has been observed previously by Tzschnanch et al who found that $Bu_3SnO(CH_2)_2NEt_2$ and $Bu_3SnOCH.Ph.CH_2NEt_2$, (Fig. 1.16) were less active than bis(tributyltin)oxide, (87). Tzschnanch suggests that this lower activity is due to a reduced tendency to exchange the chelating ligand for a donor atom at the active site (87). The non-labile ligands lead effectively to coordination saturation.

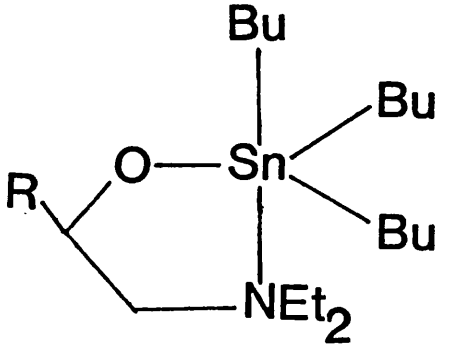

Fig. 1.16. Structure of $Bu_3SnOCH(R)CH_2NEt_2$, R = H, Ph.

Similar results were obtained by Farrow and Dawson (88) while studying the binding to protein of the five-coordinate, intramolecularly bonded complexes in Fig. 1.17, where compound 1.17 (a) has a much higher affinity than 1.17 (b). The crystal structure of closely related analogues of these compounds have been determined, for 1.17 (a) with the ethyl groups replaced by phenyl (20) (Fig. 1.4) and for 1.17 (b) with ethyl groups replaced by methyl groups (89). Both analogues were found to exhibit the trans-tbp structure shown in Fig. 1.17. The cationic species (1.17 (b)) was found to retain its structure in solution by n.m.r. studies (89), and the explanation for its lower activity is that it is coordinatively saturated and unable to form a bond to the active site (88), while the active compound contains a good leaving group (Br^-) which could facilitate such a bond (88).

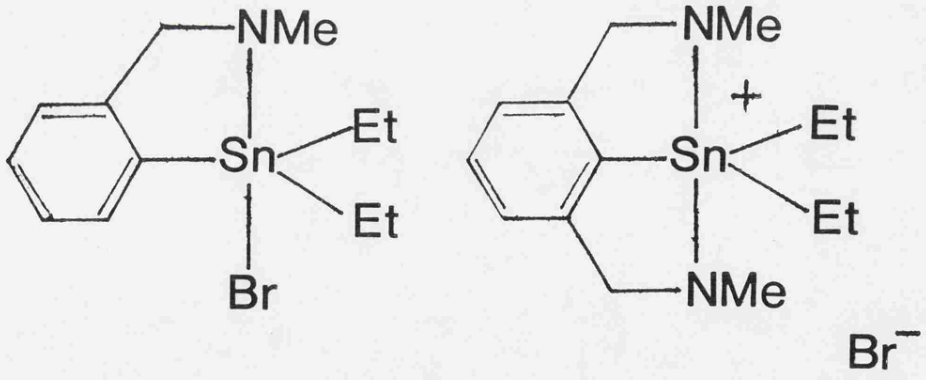

Fig. 1.17 17 (a) 17 (b)

At first appearance the commercial organotins which are polymeric such as Ph_3SnOAc would also appear to be coordinatively saturated. These compounds are, however, known to dissociate in organic solvents to form four coordinate monomers (90), and in water triorganotins are known to form hydrated cations

($R_3Sn(H_2O)_2^+$) (91), which would account for activity. That the polymer form is indeed inactive was shown by Ascher (92), who found that more concentrated solutions of Ph_3SnOAc, in acetone, and therefore containing more of the polymeric form, were less toxic than the dilute solutions.

1.5.2. Biochemical Mode of Action

Aldridge in 1955 (93) first established that trialkyltins lead to inhibition of mitochondrial oxidative phosphorylation, and also that dialkyltins have a different mode of action to the trialkyltins. Blunden et al (107) have reviewed what is currently known about the biochemical mode of action of triorganotins. Three general effects, all related to a dearrangement of mitochondrial function are noted:

(a) Interaction with mitochondrial membranes leading to swelling and disruption (94).

(b) Mediation of a Cl^-/OH^- exchange across the mitochondrial membrane (95).

(c) Inhibition of oxidative phosphorylation, leading to a breakdown in the energy conservation process.

Process (a) and (b) are interelated but (c) is independent (96). Stockdale (95) found that organotins also mediate an anion/hydroxide exchange across smectic mesophases, indicating that artificial carriers are not involved in process (b). The Cl^-/OH^- exchange is very dependent on the ions present in the medium, with Cl^- leading to rapid exchange, and sulphide inhibiting exchange by the formation of unreactive organotin sulphides (97,98).

Swelling occurs as a result of the exchange, discharging the pH difference across the membrane initially caused by the process of respiration (97). Effect (c) was found to be independent of the nature of the anion, and hence not related to the anion/hydroxide exchange.

Triethyltin compounds have been found to bind to a large variety of proteins, especially those associated with mitochondrial function, and also haemoglobulins (91). Binding to haemoglobulin could not, however, be the source of activity, because Et_3SnCl does not bind to haemoglobulins from species towards which it is still toxic (99). It was found that binding to a high affinity site in rat liver mitochondrion was directly related to the ability of Et_3Sn/Me_3Sn to inhibit oxidative phosphorylation.

Attempts have been made to try and identify the amino acids involved in the binding of organotins to proteins. Rose (101) found evidence for histidine residues in the binding site of Et_3SnCl to a protein fraction from guinea pig liver, and proposed the active site structure shown in Fig. 1.18.

Further studies agreed with the presence of a histidine residue, but ruled out the trans-structure shown in Fig. 1.18. Elliot et al. (102) concluded that both histidine and cysteine were involved in binding Et_3Sn to cat haemoglobulin. From Mössbauer data on the bound species they ruled out a trans-configuration of donor atoms. A ΔEq value of $1.74 mms^{-1}$ was obtained, which would suggest a cis-R_3SnX_2 geometry with X-groups at approximately 90^{o} (102, 56) (Fig. 1.19).

Farrow and Dawson have also carried out Mössbauer studies on the binding of organotins to proteins (88,103). The Mössbauer spectrum of the Et_3Sn/rat liver mitochondrion complex is shown in Fig. 1.20 (88). The doublet with the largest resonance area and ΔEq is attributed to Et_3Sn partitioned into the membrane, the intermediate doublet to the low affinity site, and the narrowest doublet to high affinity site responsible for oxidation inhibition. This high affinity doublet has a ΔEq of $1.57 mms^{-1}$ and isomer shift of $1.22 mms^{-1}$ (103). This quadrupole splitting could be explained by the tin atom being in either a tetrahedral or cis-R_3SnX_2 geometry (56). The authors favour a tetrahedral arrangement because of the activity of compound 1.17(a) which can only form one bond to the active site, making the postulation of a cis-R_3SnX_2 configuration unnecessary. Though they find evidence for cysteine in the low affinity site, they consider the high affinity site to consist exclusively of histidine residues (88).

The biochemical mode of action of the diorganotins is entirely different to that of the triorganotins. They also **(104)** inhibit oxygen uptake by the mitochondrion, but do so by combining with enzymes, such as lipoic acid, which are involved in α-keto acid oxidation (105). Diorganotins probably combine with dithiol groups on these enzyme systems (2). A drop in activity occurs, as in triorganotins, when coordination saturation of the tin atom is present (2). The compound in Fig. 1.21 is thirty times less toxic than Et_2SnCl_2, for example (79).

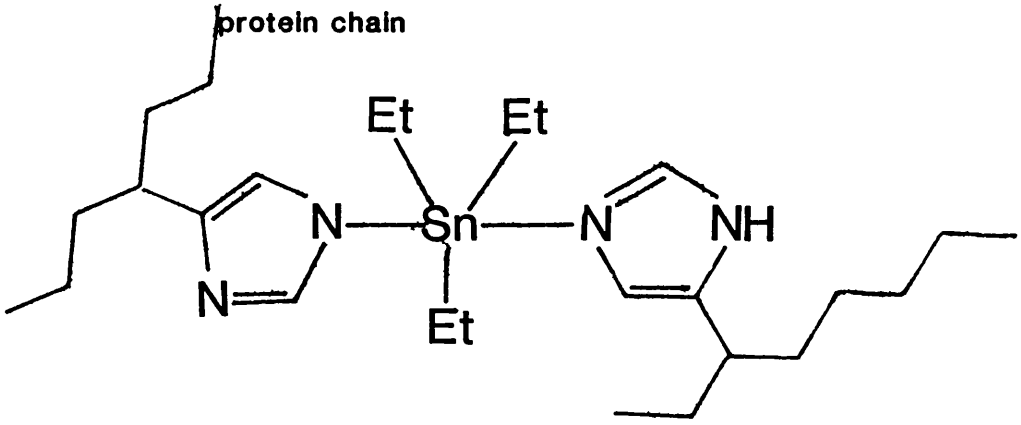

Fig. 1.18

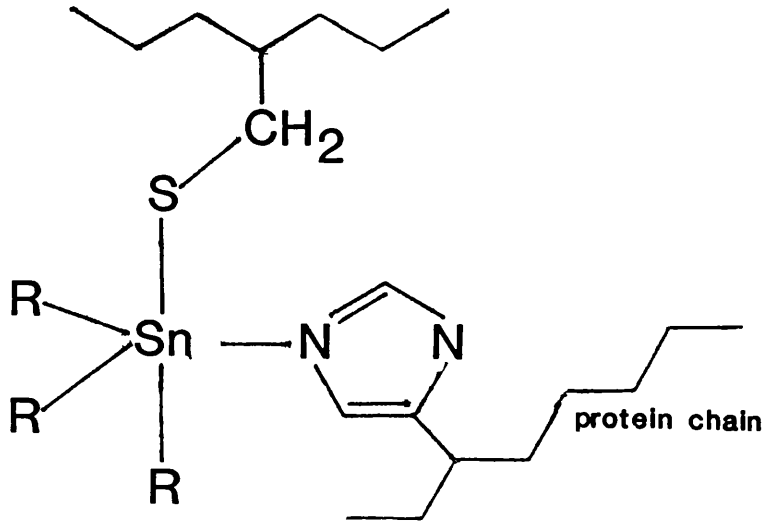

Fig. 1.19

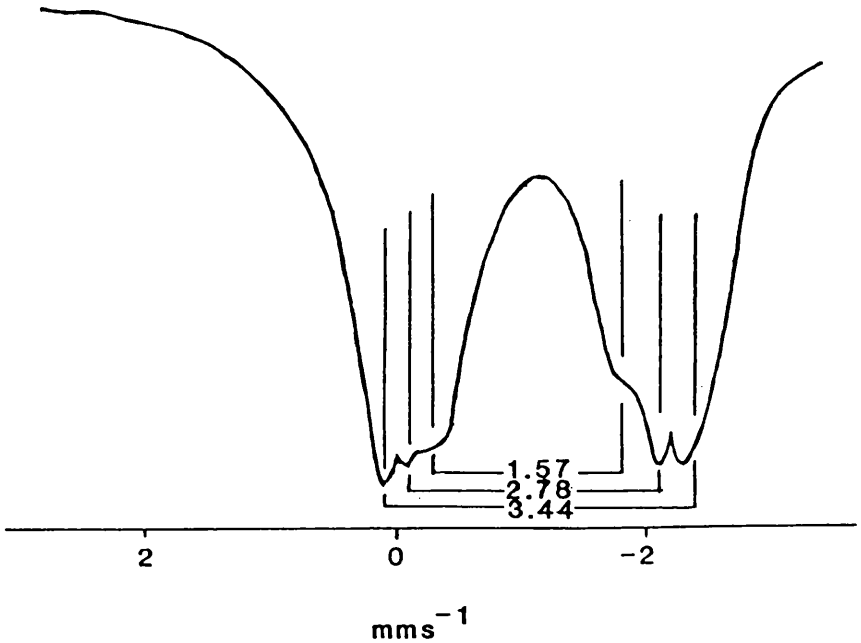

Fig. 1.20

Mössbauer spectrum of Et_3Sn/rat liver mitochondrion

Monorganotin compounds and inorganic tin are considered non-toxic, whereas tetraorganotins show a delayed toxicity and are believed to be converted to triorganotins in the liver (106).

1.5.3. Environmental degradation of organotins

That organotins eventually degrade to non-toxic tin (IV) species has been a major selling point for the industrial use of these compounds (107), especially as the inorganic forms of competing biocides such as organolead and organomercurials are still very toxic. In the environment leaching of organotins into waterways should not be a major problem because of their low water solubility (108). However, this would not be the case when organotins are applied in aqueous environments, such as in marine anti-fouling paints and there is rising concern over their toxicity towards fish and commercial molluscs like oysters (109).

Ph_3SnOAc in soil was found to have a half-life of 140 days in soil and was degraded to di- and monorganotins, and eventually inorganic tin via photochemical and microbiological pathways (110). Bis-(tributyltin)oxide readily absorbs CO_2 from the atmosphere to form $(Bu_3Sn)_2CO_3$ (111). The inclusion of a chromophore (C=O) may speed up its photochemical breakdown (2). Sheldon (112) proposed the pathway for the breakdown of phenyl and butyltins shown in Scheme 1.2.

Because of the breakdown to non-toxic Sn(IV) species there should be no long term build-up of organotins in the environment. The danger of biomethylation does exist however, leading to the formation of the more toxic, and more mobile, methyltins.

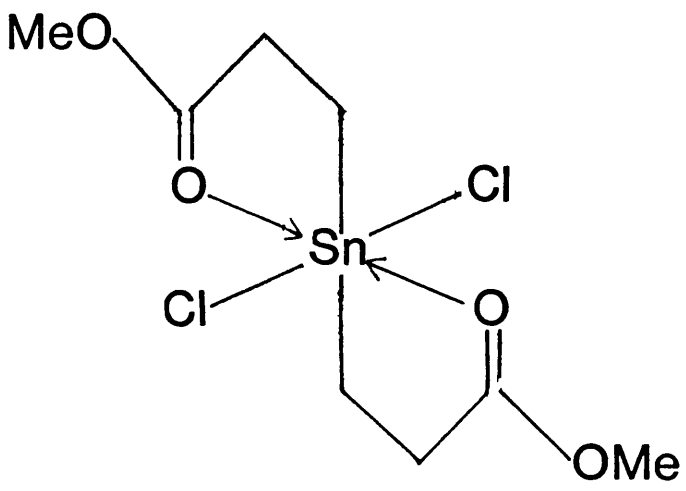

Fig. 1.21

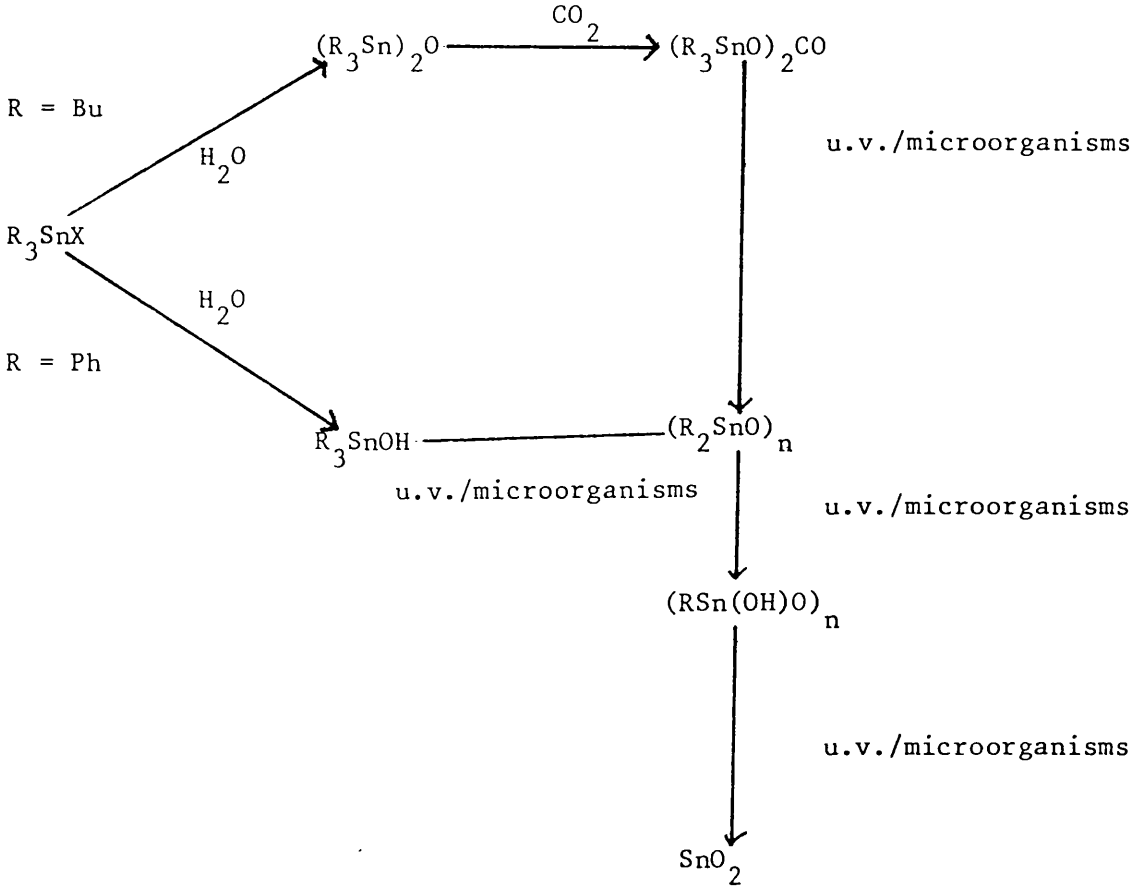

Scheme 1.2.

Wood et al.(113) have found evidence for the biomethylation of a tin(II) species to a monoorganotin (IV) species using methylcobalamin as a methylating agent. The reaction requires the presence of an oxidizing agent (e.g. Fe(III) or Co(III)), and did not occur for tin(IV) compounds (113).

Brinckman et al. (107), however, did obtain evidence for the biomethylation of tin(IV) species to a diorganotin using pseudomonas bacteria isolated from Cheasapeake Bay. A recent paper by Craig (114) states that the specialized conditions required for biomethylation of inorganic tin to tri- or tetraorganotins would be difficult to find in the environment.

1.5.4. Industrial uses of Organotin Compounds

The largest single application of organotin compounds is in the stabilisation of PVC (115, 8). Diorganotins are mostly used for this purpose especially dioctyltin compounds with S-bonded ligands, because of their low mammalian toxicity (115). Several triorganotins are now marketed for plant protection, including Ph_3SnOAc (Brestan*, Hoechest A.G.), and Ph_3SnOH (Du-ter*, Philips Dunphar N.V.) which are successful fungicides, Cy_3SnOH (Plictran*, Dow Chemicals), bis(trineophyltin)oxide (Vendex*, Shell Chemicals), and 1-tricyclohexyltin-1,2,4-triazole (Peropal*, Bayer A.G.) which are used as acaricides.

Several tributyltin compounds are used as wood preservatives, in marine anti-fouling paints and as molluscides. In aqueous application the Bu_3Sn moiety is often attached to a polymeric elastomer to give a controlled release biocide (8).

* Trade name

CHAPTER 2

Derivatives of 3-Indolyl Acetic acid and N-methyl-3-Indolyl acetic acid

2.1. Introduction

3-Indolyl acetic acid (IAAH) is a plant growth hormone, important for cell enlargement in shoots and lateral root initiation (Fig. 2.1). It is believed to act by stimulating polysaachride synthesis, which leads to loosening of the cell membrane, making cell enlargement easier (116).

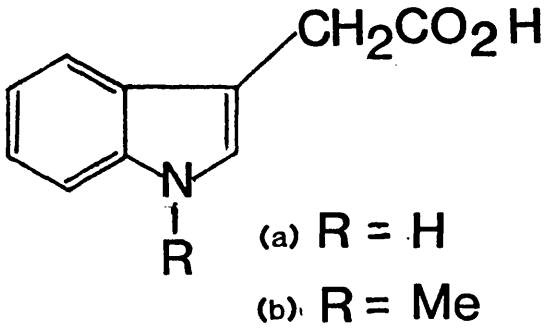

Fig. 2.1. (a) 3-Indolyl acetic acid, (b) N-Methyl, 3-Indolyl acetic acid.

Organotin carboxylates, which derivatives of these ligands will be, are known to have biological activity, in particular triphenyltin acetate which is a commercial biocide (2).

This chapter will describe the synthesis and characterisation of triorganotin derivatives of this ligand and its N-methyl analogue (Fig. 2.1).

2.2. Experimental

3-Indolyl acetic acid was purchased from Aldrich and used without further purification. The N-methyl analogue was synthesised by the method of Rosemund et al. (117). Trimethyllead chloride was obtained from Octel Ltd. Syntheses of organotin starting materials are described in Appendix 1.

All but two derivatives were synthesised using an organotin oxide or hydroxide as starting material. Method (a) describes the general technique employed for these syntheses with individual conditions given in Table 2.1.

$Me_3Sn(IAA)$ and $Me_3Pb(IAA)$ were the only derivatives synthesised using an organotin halide or organolead halide as starting materials, and method (b) describes the technique employed. Conditions for $Me_3Pb(IAA)$ are in Table 2.1.

Method (a): Tricyclohexyltin hydroxide (3.0g, 7.8mmol) and 3-Indolyl acetic acid (1.39g, 7.9mmol) were refluxed in toluene (100mls) for 45 mins. Water formed was removed using a Dean and Stark apparatus. The solution was cooled to ca. 55°C before filtering and was then concentrated to ca. 40% of its volume. Overnight crystallisation yielded 2.42g (55% yield) of the title compound, which was subsequently recrystallised from hot toluene.

Method (b): 3-Indolyl acetic acid (1.0g, 5.8mmol) was dissolved in a methanolic solution (20mls) containing sodium (0.13g, 6.2mmol). To this was added trimethyltin chloride (1.13g, 5.7mmol) in methanol (10mls). The resulting mixture was

Table 2.1

Preparation conditions for the synthesis of

Organotin derivatives of IAA, and N-Me IAA

Starting materials	Reflux solvent	Reflux time	Recrystallisation solvent	Yield %	Product
Cy_3SnOH, (7.8mmol) IAAH, (7.8mmol)	toluene	45 mins	toluene	55	Cy_3Sn(IAA)
Cy_3SnOH, (5.1mmol) N-Me, IAAH, (5.2mmol)	toluene	1 hr	methanol	50	Cy_3Sn(N-Me, IAA)
$(Bu_3Sn)_2O$, (4.2mmol) IAAH(8.5mmol)	toluene	2½ hr	pet ether (40/60)	93	Bu_3Sn(IAA)
$(Bu_3Sn)_2O$, (2.6mmol) N-Me, IAAH(5.3mmol)	toluene	45 mins	pet ether (40/60)	91	Bu_3Sn(N-Me, IAA)
Me_3SnOH(5.5mmol) N-Me, IAAH(5.5mmol)	toluene	1½ hrs	ethanol	73	Me_3Sn(N-Me, IAA)
Me_3SnCl(5mmol) IAAH(5.8mmol) Na (6.2mmol)	methanol	2 hrs	ethanol	26	Me_3Sn(IAA)
Me_3PbCl(5mmol) IAA(5.8mmol) Na (6.2mmol)	methanol	1 hr	ethanol	30	Me_3Pb(IAA)

Table 2.2

Physical data for Organotin derivatives of Indole-3-Acetates

Compound	m.p. °C	Calculated %C	Calculated %H	Calculated %N	Found %C	Found %H	Found %N
Me_3Sn(IAA)	166-168	46.20	5.07	4.14	45.87	4.90	3.95
Bu_3Sn(IAA)	58-60	56.92	7.59	3.02	55.80	7.32	2.94
Cy_3Sn(IAA)	150-152	62.01	7.62	2.58	61.82	7.59	2.50
Me_3Sn(N-Me,IAA)	150-152	47.77	5.44	3.98	47.09	5.30	3.89
Bu_3Sn(N-Me,IAA)	75-76	57.76	7.80	2.92	57.84	7.95	3.23
Cy_3Sn(N-Me,IAA)	89-90	62.60	7.81	2.52	61.80	7.71	2.50
Me_3Pb(IAA)	180 d	36.61	4.02	3.28	36.26	3.93	3.14

stirred for 1hr. at room temperature and then refluxed for 2hrs., before being evaporated to dryness and redissolved in hot toluene. The solution was then filtered to remove NaCl and left to stand. The solid obtained was recrystallised further from ethanol to yield 0.5g (26% yield) of crystalline trimethyltin 3-indolylacetate.

Physical data for all the compounds are given in Table 2.2.

2.3. Results and discussion.

2.3.1. Mass spectrometry

Mass spectral details are given in Table 2.3. Parent ions are in low abundance as expected (118), as they rapidly lose an odd electron neutral fragment to give the even electron ions R_3Sn^+ and R_2SnL^+. The mass spectrum of $Bu_3Sn(IAA)$ was also obtained using chemical ionisation (isobutene). In this technique the amount of fragmentation occurring is reduced (119) and the parent ion is observed, as well as greater abundances of the high mass ions R_2SnL^+ and R_3Sn^+.

The even electron ions decompose with loss of a neutral group to give other even electron fragments. Loss of odd electron radicals from even electron ions is not common as indicated by the absence of the odd electron ions $R_2Sn^{+\cdot}$ and $RSnL^{+\cdot}$. R_2SnH^+ species have been found however, [e.g. for $Bu_3Sn(N\text{-}Me,IAA)$, Bu_2SnH^+ m/e = 235, 6.9%], indicating preferred loss of alkene as shown in equation I.

$$Bu_3Sn^+ \rightarrow Bu_2SnH^+ + CH_3CH_2CH{=}CH_2 \qquad \text{I}$$

Table 2.3

Fragments found in Mass Spectra (electron ionisation) of organotin derivatives of IAA and N-Me,IAA

Compound	Parent$^{+\cdot}$	R_2SnL^+	R_3Sn^+	LSn^+	RSn^+	$Sn^{+\cdot}/SnH^+$
Cy_3Sn(IAA)						
m/e	-	460	369	294	203	120/121
abundance(%)		85.5	3.3	19	30	10/12
Cy_3Sn(N-Me,IAA)						
m/e	-	474	369	308	203	120/121
abundance(%)		15	1	3	24	3.2/6
Bu_3Sn(IAA)						
m/e	-	408[a]	291	294	177	120/121
abundance(%)		60	8	3	18	3/5
Bu_3Sn(N-Me,IAA)						
m/e	479	422	291	308	177	120/121
abundance(%)	1.3	35	5	4.5	10	2/4
Me_3Sn(IAA)						
m/e	339	324	165	295[b]	135	120/121
abundance(%)	3.2	4	12.6	1	2	1/0
Me_3Sn(N-Me,IAA)						
m/e	353	338	165	308	135	-
abundance(%)	3.2	3	5	1	1	
C.I.						
Bu_3Sn(IAA)						
m/e	466	408[a]	291	-	-	120/121
abundance	44	60	94			3.6/4.2

a Parent$^{+\cdot}$ - butane

b $HSnL^{+\cdot}$ (from $(CH_3)_2SnL^+ \rightarrow HSnL^{+\cdot} + CH_3CH_2^{\cdot}$)

This is also shown by the general higher abundance of SnH^+ over $Sn^{+\cdot}$ except in the case of methyltins where the formation of an alkene is not possible.

The most abundant (100%) peak for all spectra is the ligand fragment shown in Fig. 2.2

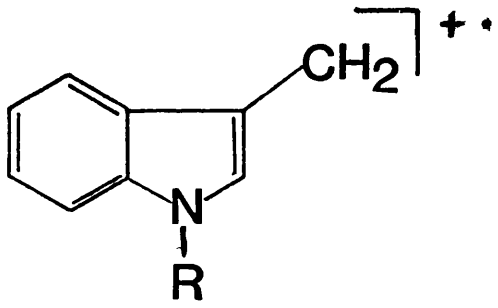

Fig. 2.2 R = H; m/e = 130, R = Me; m/e = 144.

2.3.2. Infra-red and Raman spectroscopy

The results obtained from vibrational studies on the derivatives of IAA and N-Me,IAA are given in Tables 2.4 and 2.5

The bonding of the carboxylate unit of the ligand to a tin atom should lead to a decrease in the frequency of $\nu_{asym}(CO_2)$ because of the mass effect of the R_3Sn unit. The extent to which this stretching frequency decreases will also depend on the structure adopted by the compound. Chelation or bridging by the carbonyl group will lower electron density in the C=O bond and cause a further decrease in frequency. The more isobidentate the nature of the bridging or chelation the lower $\nu_{asym}(CO_2)$ is

found. In Me_3SnOAc which has two strong Sn-O interactions [2.205Å and 2.391Å (120)], $\nu_{asym}(CO_2)$ is found at 1558cm^{-1} (120). In the weakly bridging Cy_3SnOAc [Sn---O , 3.84Å (122)] the $\nu_{asym}(CO_2)$ band is found at the higher frequency of 1645cm^{-1} (122). It would appear that in weak chelation by the carboxylate group $\nu_{asym}(CO_2)$ is also found at a higher frequency. Triphenyltin derivatives of various substituted benzoic acids which have been shown to have a distorted cis-Ph_3SnO_2 structure exhibit $\nu_{asym}(CO_2)$ between 1615cm^{-1} and 1630cm^{-1} (nujol) (123,124).

The free acid form of the ligands used here have $\nu_{asym}(CO_2)$ bands at ca. 1700cm^{-1} (Table 2.4). On coordination with Me_3Sn- and Bu_3Sn- groups the band drops to frequencies of between 1565cm^{-1} - 1575cm^{-1} (Tables 2.3 and 2.5), typical of strongly bidentate acetates such as Me_3SnOAc [1558cm^{-1}, (121)] and $(CH_2{=}CH_2)_3SnOAc$ [1565cm^{-1}, (125)]. Coordination of the ligands to Cy_3Sn, however, give $\nu_{asym}(CO_2)$ values of 1615cm^{-1} (IAA) and 1640cm^{-1} (N-Me,IAA) which are more typical of a cis-R_3SnO_2 or weakly bridging structure, though the possibility of a monodentate tetrahedral configuration cannot be ruled out. The change in frequency of these bands upon dissolution further highlights the structural difference between the Cy_3Sn- derivatives and those of Me_3Sn- and Bu_3Sn-. The latter show an increase in $\nu_{asym}(CO_2)$ upon dissolution in $CHCl_3$ to 1640-1645cm^{-1} indicative of break-up of the coordination polymer. This is also observed in the known polymers Me_3SnOAc and $Me_3SnO_2CCF_3$ (120), which are considered tetrahedral monomers in solution[$\nu_{asym}(CO_2)$: 1650cm^{-1} and 1720cm^{-1} respectively in $CHCl_3$].

$Cy_3Sn(IAA)$ does show a slight shift ($20cm^{-1}$) and $Cy_3Sn(N\text{-}Me,IAA)$ no shift in $\nu_{asym}(CO_2)$ on dissolution, indicating little or no change in structure. This pattern was also found for the triphenyltin benzoates mentioned earlier, which adopt a distorted cis-tbp geometry (123,124).

The N-H group on the indole ring acts as an additional i.r. probe for derivatives of IAAH. For $Me_3Sn(IAA)$ and $Bu_3Sn(IAA)$, a drop of only $30cm^{-1}$ in the ν(N-H) stretching frequency is observed on coordination and in solution the band returns to a higher frequency. The solid state pattern is most likely due to packing factors. The ν(N-H) band in $Cy_3Sn(IAA)$ however shows a drop in frequency of $95cm^{-1}$ and also marked broadening. In solution it returns to $3480cm^{-1}$ and sharpens, behaviour similar to the ν(N-H) band found for the free ligand in $CHCl_3$, which corresponds to free N-H. This would seem to indicate hydrogen bonding involving the N-H group in the solid-state for $Cy_3Sn(IAA)$. The small shift in $\nu_{asym}(CO_2)$ for $Cy_3Sn(IAA)$ on dissolution suggests that the carbonyl band is also involved in the hydrogen-bond.

It was because of this apparent hydrogen-bonding that the N-methyl analogue of IAAH was also used as a ligand. Spectroscopic behaviour was found, however, to be segregated along the lines of Me_3Sn- and Bu_3Sn- derivatives versus Cy_3Sn- derivatives, rather than between IAA and N-Me,IAA derivatives.

$Me_3Pb(IAA)$, whilst showing $\nu_{asym}(CO_2)$ patterns similar to its Me_3Sn- analogue has the additional anomaly in that it exhibits two ν(N-H) bands. One at $3275cm^{-1}$ is broad and indicative of hydrogen-bonding, and the other at $3395cm^{-1}$ is narrow, and typical of a free N-H. The lattice may consist of alternate H-bonded and non-H-bonded ligand moieties.

The ν(Sn-C) region for trimethyltins yields further structural information. $Me_3Sn(IAA)$ shows the asymmetric Sn-C stretch at $558cm^{-1}$ in the i.r. but the symmetric band is absent, indicating the presence of a planar SnC_3 unit. This was also found for Me_3SnOAc and $Me_3SnO_2CCF_3$ which exhibit ν_{asym}(Sn-C) at $553cm^{-1}$ and $555cm^{-1}$ respectively (121). Similar results were obtained for Me_3Sn(N-Me,IAA) which shows ν_{asym}(Sn-C) at $542cm^{-1}$ in the i.r., while Raman studies revealed the symmetric band at $518cm^{-1}$.

Solution studies in this region are more ambiguous and for Me_3Sn(N-Me,IAA) what appears to be only one band at $541cm^{-1}$ is found. This is not what is expected for the break up of the polymer and hence the non-planarity of the SnC_3 unit. For example, Me_3SnOAc and Me_3SnO_2CH (126) show weak, though much stronger than that obtained here, ν_{sym}(Sn-C) bands at $515cm^{-1}$ and $513cm^{-1}$ respectively in the solution i.r. indicating the formation of tetrahedral monomers in this phase. Zuckerman et al. noted a similar problem for a bis-tricarbonyl chromium complex of Me_2SnPh_2 (127,128) which although tetrahedral failed to exhibit a

Table 2.4

I.R. Spectroscopic data for Cy_3Sn- and Bu_3Sn derivatives of IAA and N-Me,IAA

Compound	Solvent	ν(N-H)	$\nu_{asym}(CO_2)$	$\nu_{sym}(CO_2)$
IAAH	KBr	3390n	1690br	1400
	$CHCl_3$	3470n	1710n	1410
Cy_3Sn(IAA)	KBr	3295br	1615	1445
	$CHCl_3$	3480n	1635	1440
Bu_3Sn(IAA)	KBr	3350br	1575br	1380
	$CHCl_3$	3370	1637n	1340
N-Me,IAAH	KBr		1700	
Cy_3Sn(N-Me,IAA)	KBr		1640	1340
	$CHCl_3$		1640	1340
Bu_3Sn(N-Me,IAA)	KBr		1575br	1390
	$CHCl_3$		1642n	1335

asym - asymmetric

sym - symmetric

n - narrow

br - broad

Table 2.5

I.R. and Raman data for $Me_3Sn(IAA)$ and $Me_3Sn(N\text{-}Me,IAA)$

Compound	Technique	ν(N-H)cm^{-1}	ν_{asym} CO_2 cm^{-1}	ν_{sym} CO_2 cm^{-1}	ν_{asym} Sn-C cm^{-1}	ν_{sym} Sn-C cm^{-1}
$Me_3Sn(IAA)$	i.r.(KBr)	3358n	1574br	1400	558	absent
	i.r.($CHCl_3$)	3470n	1640	1330	550	545
$Me_3Sn(N\text{-}Me,IAA)$	i.r.(KBr)	-	1565	1400	542	520vw
	i.r.($CHCl_3$)	-	1645	1330	542	540
	Raman	-			543vw	518
$Me_3Pb(IAA)$	i.r.(KBr)	3395n	1562	1380	495	488w
		3275br			(ν_{asym} Pb-C)	(ν_{sym} Pb-C)

asym: asymmetric
sym : symmetric
n : narrow
br : broad
vw : very weak

ν_{sym}(Sn-C) in the i.r. of solution or solid phases. One rationale is that the ν_{sym}(Sn-C) and ν_{asym}(Sn-C) bands are becoming degenerate, an explanation strengthened by the fact that the solution i.r. of Me_3Sn(IAA) shows a doublet in the ν(Sn-C) region with peaks at 550cm^{-1} (ν_{asym}(Sn-C)) and 545cm^{-1} (ν_{sym} (Sn-C)). Re-examination of the Me_3Sn(N-Me,IAA) band at 541cm^{-1} gives a strong band at 542cm^{-1} with a shoulder at 540cm^{-1}.

2.3.3. N.m.r. spectroscopy

N.m.r. data for the compounds are given in Table 2.6. ^2J (^{119}Sn-C-^{1}H) coupling constants in solution give useful information about the geometry of the Me_3Sn- moiety in that phase. Me_3Sn(IAA) and Me_3Sn(N-Me,IAA) have values of 60Hz and 56Hz respectively which are typical of four coordination at tin (1). Similar values are found for Me_3SnOAc (58.4Hz) and $Me_3SnO_2CCF_3$ (60Hz) (129). That these values are higher than the indisputably four-coordinate Me_4Sn (54Hz) (1), is the result of rehybridisation to increase p-character in the bond to the more electronegative oxygen and s-character in bonds to carbon. The larger coupling constant (67Hz) in d^6-acetone for Me_3Sn(IAA) is probably due to coordination by the carbonyl group of the solvent.

^{119}Sn chemical shifts for Cy_3Sn(IAA) (+5.1ppm) and Cy_3Sn(N-Me,IAA) (+3.6ppm) are typical of four-coordinate tricyclohexyltin species in solution, and can be compared with $[Cy_3Sn]_2O$ (-7.9ppm) and Cy_3SnOAc (-1.3ppm) (130). Five-coordinate species have chemical shifts much more upfield, e.g. $Cy_3SnCl_2^-$ (-85.6ppm) (130). As the i.r. spectrum of Cy_3Sn(N-Me,IAA) changes little on going from solid to solution it is fair to deduce from n.m.r. results that it is a tetrahedral monomer in

Table 2.6.

N.m.r. data for Cy_3Sn- and Me_3Sn- derivatives of IAAH and N-Me,IAAH

Compound	Solvent	δH-C-M (ppm)	δ^{119}Sn (ppm)	$^2J(^{119}Sn-C-^1H)$ (Hz)	$^2J(^{207}Pb-C-^1H)$ (Hz)
Cy_3Sn(IAA)	toluene		+5.1		
Cy_3Sn(N-Me,IAA)	toluene		+3.6		
Me_3Sn(IAA)	$CDCl_3$	0.57		60	
"	d^6 acetone	0.48		67	
Me_3Sn(N-Me,IAA)	$CDCl_3$	0.56		56	
Me_3Pb(IAA)	d^4MeOH	1.36			84

both solution and solid state. The slight change found for $Cy_3Sn(IAA)$ between solid state and solution i.r. is assigned to hydrogen bonding and this compound is similarly expected to have a close to tetrahedral geometry in the solid-state.

The $^2J(^{207}Pb\text{-}C\text{-}^1H)$ value of 84Hz found for $Me_3Pb(IAA)$ is typical of coordination expansion of four to five at lead (131). Coupling constants for Me_3PbCl in donor solvents occur at similar values e.g. in pyridine:81Hz, and in acetone: 78Hz (131). The value obtained here (84Hz) is probably due to solvation by d^4MeOH, but the fact that the material is only soluble in a strong donor solvent is itself indicative of a polymeric lattice in the solid.

2.3.4. Mössbauer Spectroscopy

The spectroscopic evidence so far reviewed supports a five-coordinate trans-R_3SnO_2 configuration for the Me_3Sn and Bu_3Sn-derivatives and either a tetrahedral or cis-R_3SnO_2 configuration for the Cy_3Sn derivatives. This is further supported by Mössbauer studies (Table 2.7). Expected quadrupole splittings for triorganotins with a trans-R_3SnX_2 geometry are in the range 3.00-4.00mms^{-1}, with isobidentate bridging pushing ΔEq towards the higher value (1). The values obtained for Bu_3Sn- and Me_3Sn-derivatives fall within this range and compare well with polymers such as Me_3SnOAc [3.68mms^{-1}, (121)], $Me_3Sn(O_2CCH_2NH_2)$ which is bridged via N [3.14mms^{-1}, (132)] and Cy_3SnOAc [3.33mms^{-1}, (133)]. The cis-configuration gives ΔEq values in the range 1.70-2.40mms^{-1} (1) e.g. $Ph_3Sn[O_2CC_4H_4,p(N{=}N\text{-}C_6H_3,o,OH,p,Me)]$

[2.36mms^{-1}, (134)] and $Me_3SnON.Ph.CO.Ph$ [2.36mms^{-1}, (135)], whilst tetrahedral values fall in a similar range, 1.00 - 2.40mms^{-1} (1). Some tricyclohexyltin compounds known to be tetrahedral show larger ΔEq values than this. Monomeric Cy_3SnBr and Cy_3SnI for example have quadrupole splittings of 2.90mms^{-1} and 2.76mms^{-1} respectively (136), and values obtained for $Cy_3Sn(IAA)$ (3.01mms^{-1}) and $Cy_3Sn(N\text{-}Me,IAA)$ (2.67mms^{-1}) correspond to the upper limits of either the tetrahedral or <u>cis</u>-R_3SnO_2 ranges.

Carboxylates with a <u>trans</u>-arrangement of donor atoms are invariably polymeric, whilst those with a <u>cis</u>-arrangement, excluding other possible interactions, should be monomeric. It should then be possible to distinguish the two using the variable temperature Mössbauer experiment. Five coordinate monomers such as $Me_3SnON.Ph.CO.Ph$ (135) exhibit <u>a</u>-values (-slope of plot of $\ln A_T/A_{78}$ versus T) of 1.74 x $10^{-2}K^{-1}$ (137) indicating a rapid fall off in resonant absorption. Polymers such as $Cy_3Sn(triazole)$(1.31 x $10^{-2}K^{-1}$) and Cy_3SnF(0.91 x $10^{-2}K^{-1}$) show slower fall-off in resonant absorption and therefore lower <u>a</u>-values (22). It has however, been found that due to the nature of polymer propagation, certain polymers give <u>a</u>-values typical of monomers. Ph_3SnOAc has a polymeric lattice, but exhibits an <u>a</u>-value of 1.91 x $10^{-2}K^{-1}$ (26). The helical nature of its lattice gives the tin atom an enhanced freedom of motion (26).

Variable temperature data for the compounds studied are given in Tables 2.8-2.10. $Me_3Sn(IAA)$ was found to have <u>a</u> of

Table 2.7.

Mössbauer data for Organotin derivatives of IAA and N-Me,IAA

Compound	Isomer Shift (mms^{-1}) δ	Quadrupole Split(mms^{-1}) ΔEq	Γ_1 (mms^{-1})	Γ_2 (mms^{-1})	$\underline{a}$ (K^{-1})
$Cy_3Sn(IAA)$	1.55	3.01	0.95	0.94	1.75×10^{-2}
$Cy_3Sn(N\text{-}Me,IAA)$	1.48	2.67	0.99	1.01	1.78×10^{-2}
$Me_3Sn(IAA)$	1.32	3.61	1.06	1.05	1.36×10^{-2}
$Me_3Sn(N\text{-}Me,IAA)$	1.35	3.43	0.93	0.91	1.60×10^{-2}
$Bu_3Sn(IAA)$	1.44	3.46	0.87	0.82	
$Bu_3Sn(N\text{-}Me,IAA)$	1.35	3.46	0.87	0.82	

Γ_1 : full width at half height for first peak

Γ_2 : full width at half height for second peak

$\underline{a}$: slope of plot of $\ln A_T/A_{78}$ v T

Table 2.8

Variable temperature Mössbauer Spectroscopic Data for Me_3SnIAA

T(K)	Area	ln A_T/A_{78}	$\underline{a}$ (K^{-1})
78	5.763	0	1.36×10^{-2}
90	4.874	-0.168	correlation factor:
110	3.717	-0.439	-0.998
125	3.108	-0.617	
140	2.370	-0.889	
150	2.202	-0.962	

Table 2.9

Variable temperature Mössbauer Spectroscopic Data for Me_3Sn(N-Me,IAA)

T(K)	Area	ln A_T/A_{78}	$\underline{a}$ (K^{-1})
78	1.900	0	1.60×10^{-2}
85	1.694	-0.115	correlation factor:
95	1.460	-0.266	-0.999
100	1.347	-0.344	
110	1.134	-0.516	
120	0.982	-0.659	
130	0.810	-0.840	

Table 2.10

Variable temperature Mössbauer Spectroscopic Data for $Cy_3Sn(IAA)$

T(K)	Area	$\ln A_T/A_{78}$	$\underline{a}$ (K^{-1})
78	9.90	0	1.75×10^{-2}
95	7.73	-0.247	correlation factor: 0.996
110	6.22	-0.465	
132	4.32	-0.829	
150	2.99	-1.197	
165	2.13	-1.536	

Table 2.11

Variable temperature Mössbauer Spectroscopic Data for $Cy_3Sn(N\text{-}Me,IAA)$

T(K)	Area	ln A_T/A_{78}	$\underline{a}(K^{-1})$
78	3.697	0	1.78×10^{-2}
90	3.068	-0.187	correlation factor: 0.998
105	2.425	-0.422	
120	1.759	-0.743	
135	1.406	-0.967	
145	1.116	-1.200	

Figure 2.3

Plots of ln A_T/A_{78} versus temperature for $Me_3Sn(IAA)$ and $Me_3Sn(N\text{-}Me,IAA)$

(○) (●)

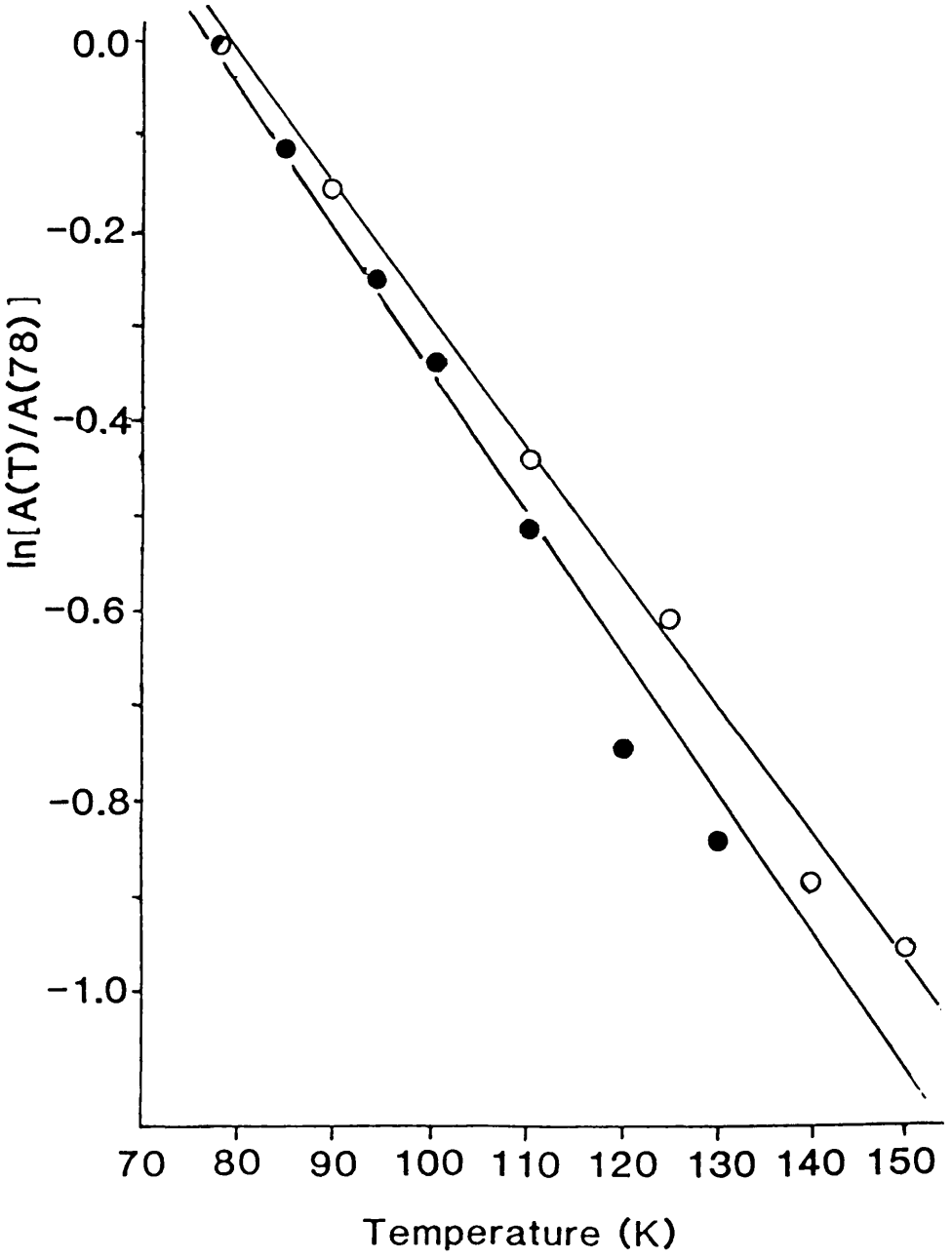

Figure 2.4:

Plots of ln A_T/A_{78} versus temperature for $Cy_3Sn(IAA)$ (○) and $Cy_3Sn(N\text{-}Me,IAA)$ (●)

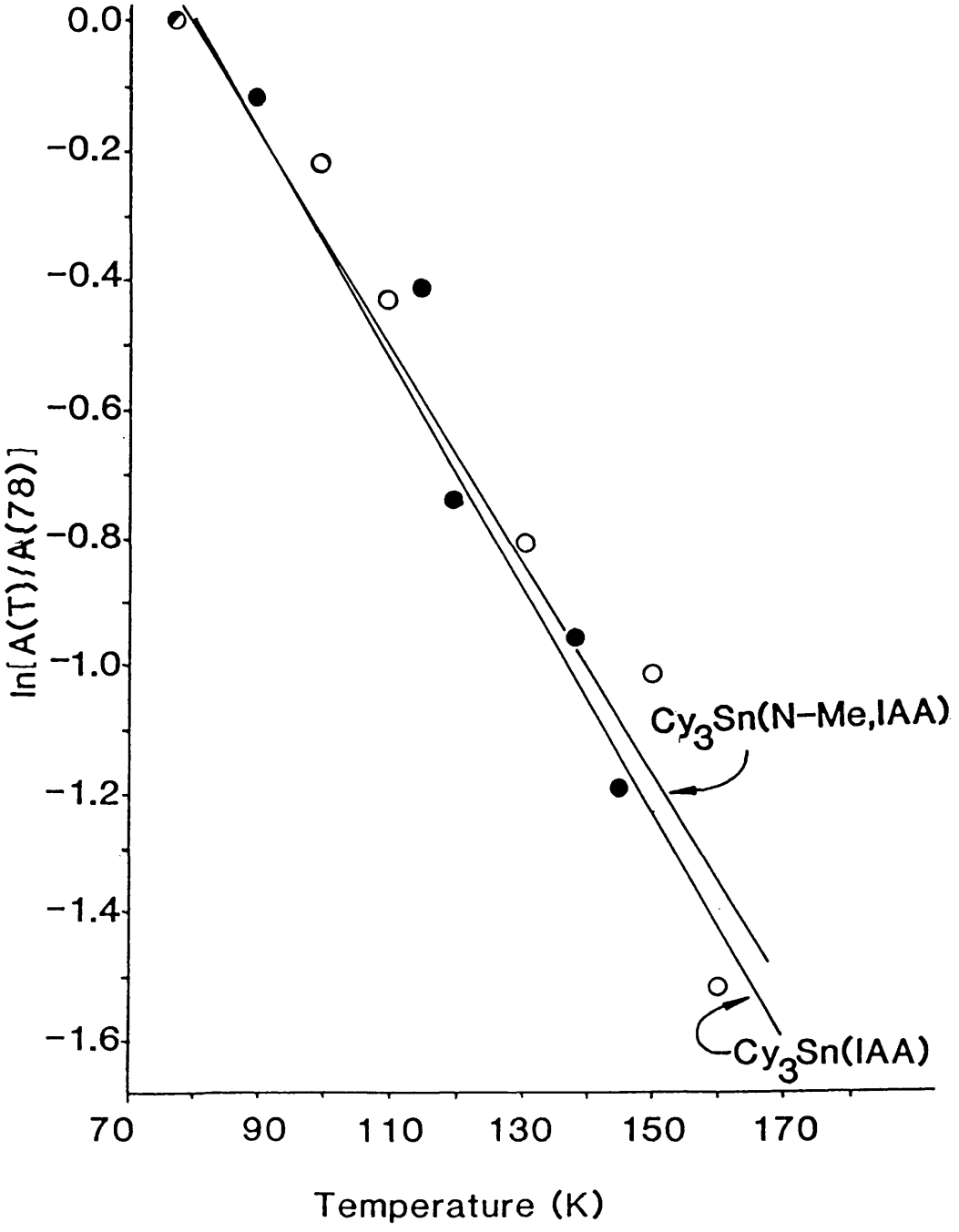

$1.36 \times 10^{-2}K^{-1}$ (plot in Fig. 2.3) which is on the interface of polymers and monomers, and a lot lower than that found for other polymeric carboxylates e.g. Ph_3SnOAc ($1.91 \times 10^{2}K^{-1}$) and Cy_3SnOAc ($1.59 \times 10^{-2}K^{-1}$) (22). A possible explanation is that this carboxylate adopts a more rigid lattice closer to a Class II type (zig-zag) polymer as described by Molloy et al (22) than to the more helical Class III polymer typical of polymeric carboxylates. Me_3Sn(N-Me,IAA) with its higher $\underline{a}$ of $1.60 \times 10^{-2}K^{-1}$ (Fig. 2.3) should adopt the "s-shaped" Class III structure. The Cy_3Sn- derivatives also show higher values of $\underline{a}$, $1.75 \times 10^{-2}K^{-1}$ for Cy_3Sn(IAA) and $1.78 \times 10^{-2}K^{-1}$ for Cy_3Sn(N-Me,IAA) (Fig. 2.4), which are similar to those obtained for the known monomers (136) Cy_3SnI ($1.60 \times 10^{-2}K^{-1}$) and Cy_3SnBr ($1.64 \times 10^{-2}K^{-1}$) (22). The values obtained are also similar to that for the weakly bridged polymer Cy_3SnOAc ($1.59 \times 10^{-2}K^{-1}$) (22), but this latter structure is ruled out by other spectroscopic evidence.

2.4. Crystal and molecular structure of Cy_3Sn,IAA

Crystals suitable for X-ray diffraction were obtained through recrystallisation from hot toluene. Details of crystallographic analysis and structure refinement are given in Appendix 2. Final atomic positional parameters are listed in Table 2.12. Tables 2.13 and 2.14 list interatomic distances and bond angles. Fig. 2.5 shows the numbering scheme and local geometry about tin, while Fig. 2.6 is a view along the z-axis. Table 2.15 lists selected structural data for other triorganotin compounds for comparison.

The local geometry about tin is best described as distorted tetrahedral. The carboxylate group is considered monodentate despite an intramolecular approach of 2.929Å by the carbonyl oxygen to tin, well within the sum of the respective van der Waals radii (3.70Å), and the opening of <C(1)-Sn-C(13) to 124.9° (from ≃ 109°). This opening (at least in part) is due to the proximity of the carbonyl oxygen, however there is no systematic change in bond angles to suggest that a cis-tbp configuration is being formed, with O(2) and O(7) in trans-axial positions. The sum of the would-be equatorial angles involving O1, C1 and C13, total only 332.5°, compared with an ideal tbp angle of 360°, and is only slightly distorted from the sum of ideal tetrahedral angles of 328.5°.

In addition the Sn-C(7) bond is the shortest tin-carbon contact at 2.147(5)Å whereas in an axial-tbp position it would be expected to be the longest. Further proof that the positioning of the carbonyl oxygen close to the tin atom is not the result of an electronic interaction comes from the C(19)-O(1) and C(19)=O(2) bond distances. The C(19)=O(2) bond at 1.213Å retains its double bond character, despite the fact that it is involved in a hydrogen-bond to the N-H group of a neighbouring indole ring (Fig. 2.6). This carbonyl bond length is in fact shorter than that for the free ligand which is a H-bonded dimer (-CO----HO) (138).

In the presence of bidentate ligands organotin carboxylates prefer to expand their coordination number and adopt bridging or chelated structures, hence genuine tetrahedral geometries are rare.

Trimethyltin carboxylates invariably form polymer chains e.g. Me_3SnOAc (120). Some trimethyltin carboxylates contain monodentate carboxylate groups such as $Me_3Sn(O_2CCH_2NH_2)$ (139) and $Me_3SnO_2CC_5H_4N.H_2O$ (140), but still achieve a trans-tbp structure by additional interactions (-N:→Sn, and H_2O:→Sn respectively in these cases).

Triphenyltin acetate also adopts a polymeric structure but a rather unique one. The geometry about tin is described as distorted six coordinate, mer-Ph_3SnO_3 (26). The carbonyl group bonds to both neighbouring tin atoms, evidence coming from additional angle openings and an unusually long C=O bond (1.251Å) (26).

Unlike Ph_3SnOAc just described many triphenyltin compounds adopt a cis-tbp configuration. They are more likely to adopt this structure than Me_3Sn- or Cy_3Sn derivatives, phenyl groups being more electronegative they more readily accept the axial position in a tbp geometry. An example of such a structure is $Ph_3SnO_2CC_6H_4(N_2R)$-o (R = 2 hydroxy-5-methylphenyl), which forms discrete five coordinate cis-R_3SnO_2 monomeric units (134). The Sn----O intramolecular interaction (2.463(7)Å) is considerably stronger than in Cy_3Sn(IAA) despite the fact that like Cy_3Sn(IAA) the carbonyl oxygen is involved in a hydrogen bond, though in this case a three-centred one. The sum of the equatorial angles is only 340.7° but the angular changes are indicative of a molecule approaching a cis-R_3SnO_2 geometry.

A closer analogy to the structure obtained for Cy_3SnIAA are the substituted benzoates studied by Holmes et al (123,124), $Ph_3SnO_2C_6H_4X$ (=o-OH,o-NMe_2, p-SMe, o-NH_2, o-OMe, p-NH_2). These compounds have intramolecular Sn----O contacts varying from 3.071Å (o-OH) (123) to 2.564Å (o-NMe_2) (124). The geometry about tin is tetrahedral, distorted towards cis-R_3SnO_2, and in some cases this distortion is very slight.

Tricyclohexyltin carboxylates, because of their reduced Lewis acidity at tin, arising from the electron donating nature of the C_6H_{11} group, tend to form more weakly associated polymers than the trimethyltin carboxylates (122, 133, 134). The weak intermolecular interactions found in Cy_3SnOAc and $Cy_3SnO_2CCF_3$ (Table 2.15) are however, sufficient to cause the angles about tin to open towards a trans-tbp structure. The sum of the equatorial angles for these structures are 349° (Cy_3SnOAc) and 352° ($Cy_3SnO_2CCF_3$) compared with only 332.5° for $Cy_3Sn(IAA)$.

The lattice structure of $Cy_3Sn(IAA)$ is composed of chains of molecules linked intermolecularly by hydrogen bonds which join -NH----OC- subunits of the 3-indolylacetate ligands (Fig. 2.6). The polymer is propagated in a helical fashion. The N-H(1) and H(1)-O(2') bond distances are 0.88(6)Å and 2.00(6)A° respectively but are not co-linear, having a < N-H(1)-O(2') of 163(4)°. Normalisation of the N-H bond to a standard length of 1.03Å (141) the H(1)-O(2') distance becomes 1.85Å and < N-H(1)-O(2') 162°. The hydrogen-bond is therefore quite strong, when compared to an average H----O approach of 1.895Å (142). It would appear therefore that the effect of organostannylation of 3-indolylacetate

on the latter's lattice structure is to convert a dimeric OH----OC (O----O, 2.665Å (138)) into a N-H----OC polymer (O----N, 2.88Å) from which the Cy_3Sn- moiety is pendant. This explains the a-value obtained in the variable temperature Mössbauer experiment ($1.75 \times 10^{-2} K^{-1}$) which is indicative of a monomer with respect to tin.

It is worth considering whether the hydrogen-bonding found for $Cy_3Sn(IAA)$ and other organotin carboxylates listed in Table 2.15 is responsible for the monodentate behaviour of the carboxylate group. This would not appear to be entirely the case. In $Ph_3SnO_2CC_6H_4(N_2R)$-o, (Table 2.15) for example although the carbonyl group is involved in a hydrogen bond, it makes quite a close approach to the tin atom [2.463(7)Å, (134)], and the ligand is considered bidentate. Also in the case of Holmes' substituted benzoates (123,124), while those derivatives not capable of H-bonding show the strongest intramolecular interactions (e.g. o-NMe_2, 2.564Å) the ligands are not necessarily bidentate. It appears that hydrogen-bonding involving the carbonyl group, though playing an important role in determining the crystal and molecular structure of these compounds, does not appear to be a pre-requisite for monodentate carboxylate bonding.

In conclusion, the structure of $Cy_3Sn(IAA)$ contains tin in a distorted tetrahedral environment. Angular distortions at tin are due to a rehybridisation to increase p-character in the bond to the more electronegative oxygen atom and particularly large angle changes are due to the proximity of another oxygen atom, a steric though not electronic phenomenon.

Table 2.12 Final Positional Parameters for

$(C_6H_{11})_3SnOC(O)CH_2(C_8H_6N)$ $(x10^4)$[a]

Atom	x	y	z
Sn	-2379.8(2)	-1742.1(4)	-4092.6(3)
C1	-3328(4)	-530(6)	-4593(4)
C2	-3632(4)	362(7)	-3859(4)
C3	-4244(4)	1288(6)	-4227(5)
C4	-4950(4)	628(6)	-4688(4)
C5	-4659(4)	-246(7)	-5422(4)
C6	-4049(4)	-1197(6)	-5061(4)
C7	-1209(3)	-866(6)	-4038(4)
C8	-656(4)	-1459(7)	-3336(5)
C9	173(4)	-832(8)	-3312(6)
C10	115(4)	546(7)	-3169(4)
C11	-413(4)	1164(7)	-3880(5)
C12	-1258(4)	552(7)	-3897(5)
C13	-2264(4)	-3714(5)	-4410(4)
C14	-3014(4)	-4290(6)	-4865(4)
C15	-2870(4)	-5645(6)	-5105(4)
C16	-2634(4)	-6400(5)	-4277(4)
C17	-1890(4)	-5846(6)	-3806(4)
C18	-2040(4)	-4486(6)	-3570(4)
O1	-2565(2)	-1648(4)	-2700(2)
O2	-3691(3)	-2720(4)	-2958(3)
C19	-3255(4)	-2131(6)	-2453(5)
C20	-3506(4)	-1822(7)	-1477(4)
C21	-3922(5)	-583(7)	-1489(4)
C22	-4746(5)	-394(7)	-1504(4)
N	-4905(4)	856(6)	-1584(4)
H1[b]	-539(4)	118(6)	-165(4)
C23	-4815(5)	1507(7)	-1638(4)
C24	-3561(5)	624(7)	-1574(4)
C25	-2751(5)	1054(8)	-1634(4)
C26	-2622(6)	2299(9)	-1752(4)
C27	-3259(6)	3155(8)	-1811(4)
C28	-4060(5)	2774(7)	-1756(4)

[a] Estimated standard deviations of the last significant digit are given in parentheses.

[b] H1 is bonded to N and is the only hydrogen atom with refined positional parameters. Positional parameters for H1 are multiplied by 10^3.

Table 2.13. Bond distances (Å) for

$(C_6H_{11})_3SnOC(O)CH_2(C_8H_6N)$[a]

Intramolecular bond distances

Sn - C1	2.161(6)	C1 - C2	1.529(8)
Sn - C7	2.147(5)	C2 - C3	1.514(8)
Sn - C13	2.165(6)	C3 - C4	1.522(7)
Sn - O1	2.086(3)	C4 - C5	1.510(8)
O1 - C19	1.302(7)	C5 - C6	1.525(8)
O2 - C19	1.213(7)	C6 - C1	1.550(8)
C19 - C20	1.538(8)	C7 - C8	1.521(7)
C20 - C21	1.489(9)	C8 - C9	1.523(8)
C21 - C22	1.374(8)	C9 - C10	1.489(9)
C22 - N	1.365(8)	C10 - C11	1.517(8)
C23 - N	1.377(8)	C11 - C12	1.539(8)
H1 - N	0.88(6)	C12 - C7	1.530(8)
C23 - C24	1.398(8)	C13 - C14	1.537(7)
C24 - C21	1.425(9)	C14 - C15	1.508(8)
C24 - C25	1.415(9)	C15 - C16	1.519(8)
C25 - C26	1.357(8)	C16 - C17	1.530(8)
C26 - C27	1.395(9)	C17 - C18	1.514(8)
C27 - C28	1.383(9)	C18 - C13	1.536(7)
C28 - C23	1.380(9)		

Intermolecular bond distances

H1 - O2'[b]	2.00(6)

[a] Estimated standard deviations of the last significant digit are given in parentheses.

[b] Primed atoms represent transformed coordinates of the type -1-x, 1/2+y, -1/2-z.

Table 2.14 Bond Angles (deg) for $(C_6H_{11})_3SnOC(O)CH_2(C_8H_6N)$[a]

Intramolecular Angles

C1 - Sn - C7	113.7(2)	C1 - C2 - C3	111.6(5)
C1 - Sn - C13	124.9(2)	C2 - C3 - C4	111.7(5)
C1 - Sn - O1	101.7(2)	C3 - C4 - C5	111.4(5)
C7 - Sn - C13	110.6(2)	C4 - C5 - C6	111.6(5)
C7 - Sn - O1	94.2(2)	C5 - C6 - C1	110.8(5)
C13 - Sn - O1	105.9(2)	C6 - C1 - C2	110.7(5)
Sn - O1 - C19	112.8(4)	C7 - C8 - C9	111.8(5)
O1 - C19 - O2	123.3(6)	C8 - C9 - C10	112.3(6)
O1 - C19 - C20	114.5(6)	C9 - C10 - C11	111.6(6)
O1 - C19 - C20	122.1(7)	C10 - C11 - C12	110.2(6)
C19 - C20 - C21	107.6(5)	C11 - C12 - C7	112.0(5)
C20 - C21 - C22	125.9(7)	C12 - C7 - C8	110.5(6)
C21 - C22 - N	109.6(7)	C13 - C14 - C15	111.1(5)
C22 - N - C23	109.4(6)	C14 - C15 - C16	111.1(5)
C22 - N - H1	125(4)	C15 - C16 - C17	111.6(5)
C23 - N - H1	125(4)	C16 - C17 - C18	110.2(5)
N - C23 - C24	106.9(6)	C17 - C18 - C13	111.5(5)
C23 - C24 - C21	108.0(7)	C18 - C13 - C14	109.5(5)
C24 - C21 - C22	106.2(7)		
C24 - C21 - C20	127.7(7)	Intermolecular Angles	
C23 - C24 - C25	118.2(7)	N - H1 - O2'[b]	163(4)
C24 - C25 - C26	118.3(9)	H1 - O2' - C19'	158(4)
C25 - C26 - C27	122.1(9)		
C26 - C27 - C28	121.5(8)		
C27 - C28 - C23	116.0(8)		
C28 - C23 - C24	124.0(8)		

[a] Estimated standard deviations of the last significant digit are given in parentheses.

[b] Primed atoms represent transformed coordinates of the type -1-x, 1/2+y, -1/2-z.

Table 2.15. Bond distances (Å) for selected Organotin Carboxylates

Compound	Sn - O	Sn----O Intra	Sn----O Inter	C=O	C-O	H-bond[a]	Ref
3-Indolyl-acetic acid				1.223	1.298	2.665	138
$Cy_3Sn(IAA)$	2.086	2.929		1.213	1.302	2.891	this work
Cy_3SnOAc	2.12(3)	2.94(4)	3.84	1.25(9)	1.39(8)		122
$Cy_3SnO_2CCF_3$	2.08(4)	3.11	3.70	1.20(5)	1.28(4)		133
$Ph_3SnO_2CC_6H_4(N_2R)$-o[b]	2.070	2.463		1.224	1.296	2.94[c]	134
$Ph_3SnO_2CC_6H_4(OH)$-o	2.083	3.071	3.035	1.232	1.301	2.71	123
Ph_3SnOAc	2.185	3.206	2.349	1.251	1.263		26
$Me_3SnO_2CCH_2NH_2$	2.21	3.23	2.46[d]	1.23(3)	1.34(3)	2.74	139

a CO----HO, or CO----HN

b R = 2 hydroxy-5-methyl phenyl

c CO----HO distance, also contains two O----H----N hydrogen bonds (2.62Å and 2.58Å)

d N:→Sn bond

Figure 2.5. Pluto drawing of one molecule of $(C_6H_{11})SnOC(O)CH_2(C_8C_6N)$, showing the employed numbering scheme. Hydrogen atoms are omitted for clarity.

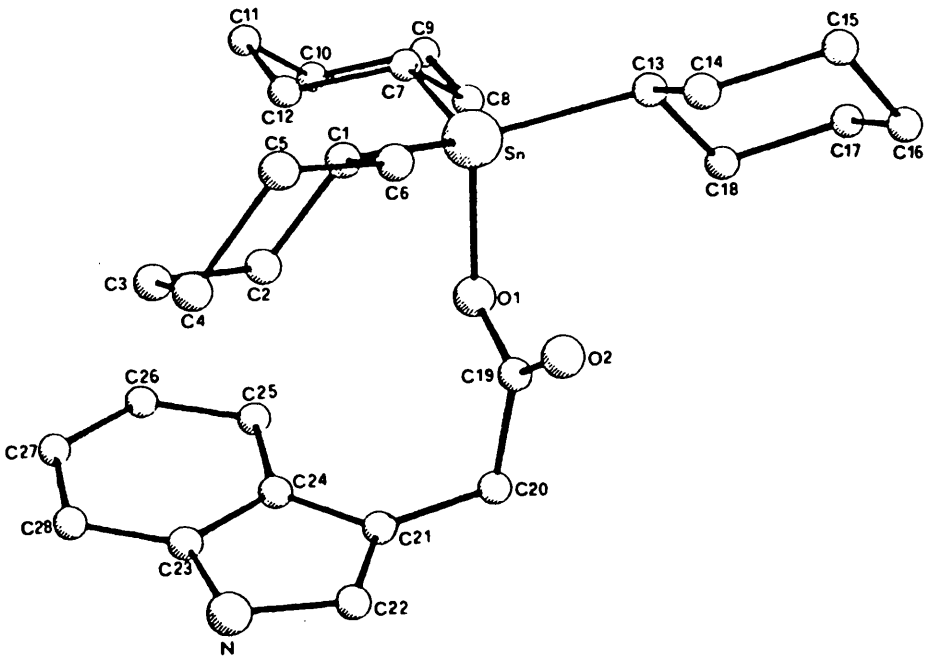

Figure 2.6. Stereoview of the helix, viewed down the z-axis (plotting range x: 0.0 - 1.0, y: -1.0 - 1.0, z: 0.0 - 0.5. The cyclohexyl groups on tin have been omitted for clarity.

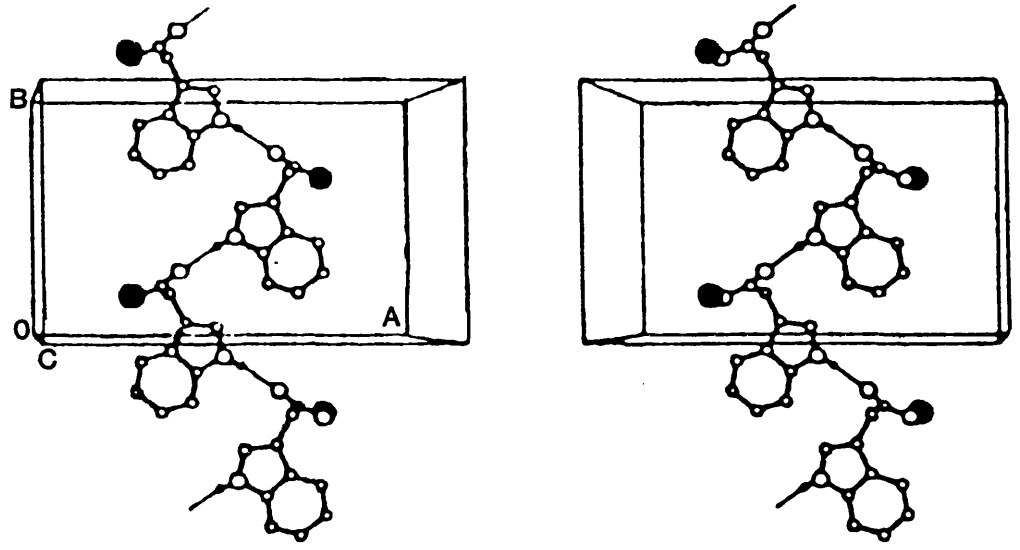

● = Sn

Figure 2.7. Suggested structure for

R = Bu, Me, R^1 = H, Me

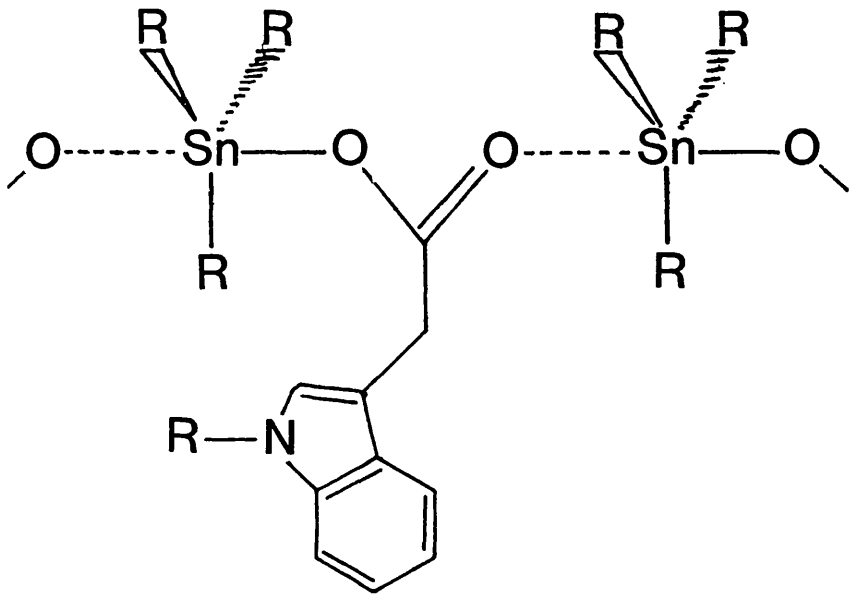

In the light of this result it is possible to make the following predictions about the structures of the other derivatives of 3-indolylacetate. From its related spectroscopic behaviour Cy_3Sn(N-Me,IAA) should adopt a similar structure to Cy_3Sn(IAA) i.e. a tetrahedral monomer. Bu_3Sn- and Me_3Sn- are expected to have similar structures, namely bridged polymers as shown in Fig. 2.7. From the variable temperature Mössbauer work Me_3SnIAA is expected to have a more tightly held lattice, probably less helical in nature than that for Me_3Sn(N-Me,IAA) or organotin carboxylates in general. The lack of spectroscopic evidence obtained for Me_3Pb(IAA) makes structure prediction difficult but most likely has a structure similar to that in Fig. 2.7, possibly with alternate N-H groups involved in H-bonding. Definitive evaluation of these compounds awaits crystallographic analysis.

2.5. Biocidial Activity of some 3-indolylacetate derivatives

Tables 2.16, 2.17 and 2.18 show biocidial activity of Me_3Sn(IAA) and Cy_3Sn(IAA) against selected organisms, carried out by ICI Plant Protection (Jealotts Hill). Though both compounds show activity, Me_3Sn(IAA) is clearly the most active. Me_3Sn(IAA) however, would also be expected to have a higher mammalian toxicity, which may prevent commercial exploitation.

That both derivatives are active is consistent with previous work (84) which associates activity with R_3Sn-species which are four-coordinate at tin in solution.

Table 2.16 Pesticidal Activity

Organism	ppm	$Me_3Sn(IAA)$	$Cy_3Sn(IAA)$
Tetranychus	500	9	9
Myzus	500	9	0
Musca	500	9	0
Chilo	500	9	0
Nilaporvata	500	0	0
Blatella	500	0	9

0 = 0 - 49% kill

9 = 80 - 100% kill

Table 2.17 Fungicidal and Bactericidal activity of $Cy_3Sn(IAA)$

Organism	ppm	Activity
Claudosporium sphaerospermum	25	2
Aspergillus niger	25	0
Botrytis cinera	25	0
Septoria nodurum	25	4
Plasmopara viticola (vine)†	100	4
Ventura ina qualis (apple)†	100	4
Pyricularia orgzae (rice)†	100	3*

4 = No disease

3 = trace - 5%

2 = 6 - 25%

0 > 60% disease

* slightly phytotoxic

† in vivo tests

Table 2.18 Herbicidal activity*

Compound	kg ha^{-1}	lettuce	Tomato	Oat
$Me_3Sn(IAA)$	8	3(3)	3(3)	3(3)
$Cy_3Sn(IAA)$	10	0(0)	0(3)	0(0)

* Pre-emergence with post emergence in brackets

0 = within 5% of control

3 = > 60% decrease in size

Chapter Three

Synthesis and structure of organotin derivatives of 2-mercaptobenzothiazole, 2-mercaptobenzoxazole and 2-mercaptobenzimidazole

3.1. Introduction

The ligand 2-mercaptobenzothiazole (Fig. 3.1(a))was chosen for study because of its known fungicidal activity (143), and its potential for multidentate bonding. The mode of action of this fungicide is not fully understood, but is thought to involve an opening of the thiazole ring to yield toxic dithiocarbamates (143). It was found that substituents on the thiazole ring that increase the lipophilicity of the molecule increases its activity.

These ligands can exist in two tautomeric forms, the thione and thiol structures (Fig. 3.2). The thione structure is illustrated in Fig. 3.1 for all ligands as it has been found by X-ray studies to be the preferred structure for mbtH and mbiH (148,149).

Some work on organotin derivatives of 2-mercaptobenzothiazole (mbtH) and 2-mercaptobenzoxazole (mboH) has already been reported in the literature (144-147). Czerwinska et al. (144) and Ison et al. (145) report fungicidal activity for $Ph_3Sn(mbt)$, $Ph_3Sn(mbo)$ and $Bu_3Sn(mbo)$, but carried out no structural studies. Domazetis et al. (146,147) report spectroscopic studies on $Bu_3Sn(mbt)$ and $Bu_2Sn(mbt)_2$.

In this chapter a more comprehensive study of the structure and spectroscopy of organotin derivatives of mbtH and its analogues shown in Fig. 3.1 is presented, and structures proposed by Domazetis et al. (146,147) are reappraised.

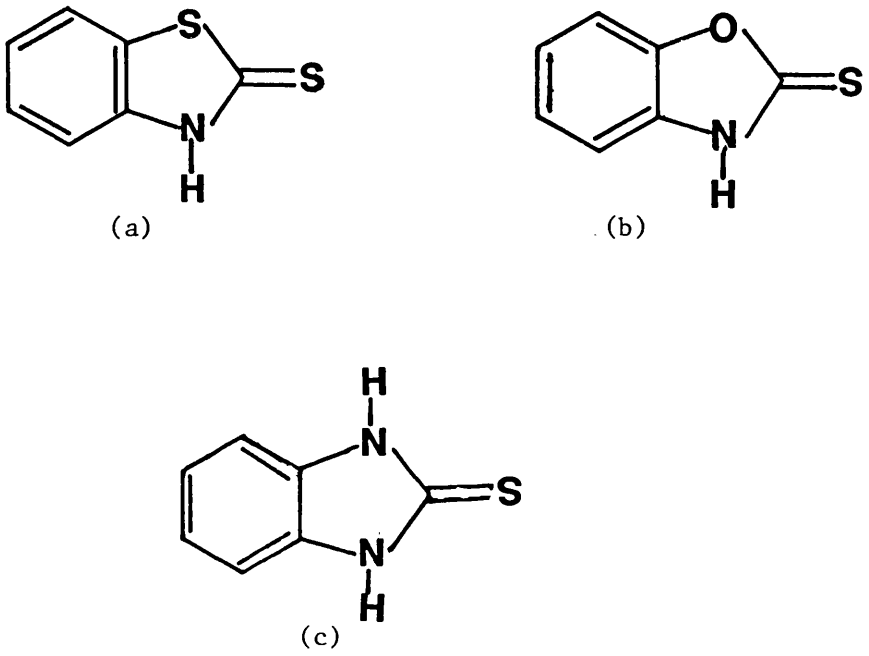

Fig. 1.3 (a) 2-mercaptobenzothiazole,

(b) 2-mercaptobenzoxazole (mboH)

(c) 2-mercaptobenzimidazole (mbiH)

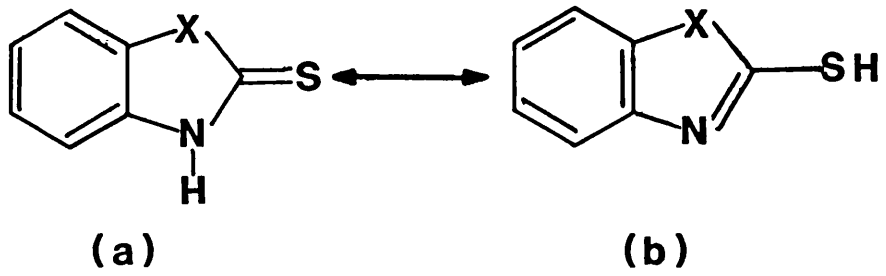

Fig. 3.2. Thione (a) thiol(b)tautomerisation. X = O, S, NH

3.2. Synthesis

Synthesis of organotin starting materials is described in appendix 1. The ligands were purchased from Riedel de Haen A.G. and used without further purification. Solvents were dried before use. Method (a) describes the general technique for synthesising the compounds shown in Table 3.1. An organotin halide was used as precursor in the preparation of $Me_3Sn(mbt)$, details are given in method (b).

Method (a): Tricyclohexyltin hydroxide (3.45g, 9mmol) and 2-mbtH (1.5g, 9mmol) were refluxed in toluene for 2hrs. Water produced was removed from the reaction using a Dean and Stark apparatus. The solution was then cooled to room temperature and filtered. The filtrate was evaporated to dryness, to give a yellow oil, which when triturated with a small volume of cold ethanol yielded a solid (3.85g, 80%). This material was

recrystallised from Et_2O/MeOH (30/70).

Method (b): 2-mbtH (2.0g, 12mmol) was dissolved in an ethanolic solution (15mls) containing sodium (0.22g, 13mmol). To this was added trimethyltin chloride (2.4g, 12mmol) in ethanol (10mls). The mixture was refluxed for 2hrs and then evaporated to dryness. The oil obtained was dissolved in petroleum ether (40/60) and filtered to remove unreacted ligand and NaCl formed. The filtrate was again evaporated to dryness to return the oil. The oil was purified by repeatedly dissolving in hot ethanol, reprecipitating by cooling and decanting off the supernatant. Prolonged drying under vacuum removed the last trace of solvent.

The purification of other oils synthesised was by the technique in method (b), as attempts to distil them lead to decomposition. Physical data for all derivatives is given in Table 3.2.

3.3. Results and discussion

3.3.1. Mass Spectrometry

Mass spectral data obtained under EI conditions (70eV) are given in Table 3.3. As with the derivatives of 3-indolyl-acetate (Chapter 2) parent ions $[P^{+\cdot}]$ are in low abundance in the EI spectra, with the exception of triphenyltin compounds. $[P + H]^{+\cdot}$ peaks are found in high abundance in the CI (iso-butene) spectra (Table 3.4) of Bu_3Sn- and Me_3Sn- derivatives and Cy_3Sn(mbO), due to the lesser tendency to fragment under CI conditions.

Table 3.1.

Preparation conditions for the synthesis of organotin derivatives of mbt, mbo, and mbi

Starting materials	Solvent	reflux time	Recrystallisation solvent	Yield %	Product
Cy_3SnOH(6mmol) mbtH (6mmol)	toluene	2hrs	Et_2O/MeOH	80	Cy_3Sn(mbt)
Ph_3SnOH (2.7mmol) mbtH (2.7mmol)	toluene	2hrs	$CHCl_3$/EtOH	40	Ph_3Sn(mbt)
Bz_3SnOH(2mmol) mbtH (2mmol)	toluene	1½hrs	EtOH	79	Bz_3Sn(mbt)
$[Bu_3Sn]_2O$ (3.6mmol) mbtH (7.2mmol)	toluene	1½hrs	EtOH	41	Bu_3Sn(mbt)
Me_3SnCl(12mmol) mbtH(12mmol) Na(13mmol)	EtOH	2hrs	EtOH	28	Me_3Sn(mbt)
Cy_3SnOH(4.6mmol) mboH (4.6mmol)	toluene	1hr	Et_2O/EtOH	40	Cy_3Sn(mbo)
Ph_3SnOH(10mmol) mboH (10mmol)	toluene	1hr	CH_2Cl_2/EtOH	50	Ph_3Sn(mbo)
$[Bu_3Sn]_2O$(6.6mmol) mboH (13.2mmol)	toluene	1½hrs	EtOH	52	Bu_3Sn(mbo)
Cy_3SnOH(6.7mmol) mbiH (6.7mmol)	toluene	1½hrs	toluene	32	Cy_3Sn(mbi)
Bu_2SnO(4.5mmol) mbtH (9mmol)	toluene	1½hrs	EtOH	32	$Bu_2Sn(mbt)_2$

Table 3.2

Physical data for organotin derivatives of 2-mbtH, 2-mboH, and 2-mbiH.

		Calculated			Found		
Compound	m.p.	C	H	N	C	H	N
$Cy_3Sn(mbt)$	72°	56.19	6.80	2.62	56.36	6.56	2.59
$Ph_3Sn(mbt)$	92-93°	58.16	3.71	2.71	58.14	3.52	2.66
$Bz_3Sn(mbt)$	80-81°	60.10	4.51	2.50	59.96	4.80	2.56
$Bu_3Sn(mbt)$	oil	50.02	6.85	3.07	50.00	7.09	3.00
$Me_3Sn(mbt)$	oil	36.28	3.96	4.23	36.21	3.95	4.18
$Cy_3Sn(mbo)$	46-47	56.93	7.37	2.77	56.59	7.11	2.48
$Ph_3Sn(mbo)$	96-98	59.91	3.82	2.72	60.03	3.81	2.69
$Bu_3Sn(mbo)$	oil	51.84	7.10	3.18	51.60	7.25	3.06
$Cy_3Sn(mbi)$	165-166	58.04	7.04	5.42	57.80	7.10	5.49
$Bu_2Sn(mbt)_2$*	68-70	46.65	4.64	4.95	45.03	5.13	4.51

* contains traces of Bu_2SnO impurity (Mössbauer spectrum) which would be expected to depress the C and N and raise the H content of the sample, as observed in the microanalytical data.

Table 3.3

Fragments found in E.I. (70ev) spectra of organotin derivatives of mbt, mbo and mbi

	$P^{+\cdot}$	R_2SnL^+	R_3Sn^+	SnL^+	RSn^+	LH^+	$Sn^{+\cdot}/SnH^+$
Cy_3Sn(mbt)							
m/e	absent	452	absent	286	203	167	120/121
abundance(%)		100		89	21	22	1/6
Ph_3Sn(mbt)							
m/e	517	440	351	286	197	167	120/121
abundance(%)	14	100	16	11	37	8	16/2
Bz_3Sn(mbt)							
m/e	absent	468	absent	286	211	167	120/121
abundance(%)		58		100	10	10	3/0
Bu_3Sn(mbt)							
m/e	absent	400	391	286	177	167	120/121
abundance(%)		100	8	45	14	12	5/10
Me_3Sn(mbt)							
m/e	absent	316	165	286	135	167	120/121
abundance(%)		100	9	40	7	3	4/1
Cy_3Sn(mbi)							
m/e	absent	435	369	269	203	150	120/121
abundance(%)		100	3	85	22	43	1/12
Cy_3Sn(mbo)							
m/e	absent	436	369	270	203	151	120/121
abundance(%)		100	10	85	20	10	20/19
Ph_3Sn(mbo)							
m/e	501	424	351	270	197	151	120/121
abundance(%)	24	100	67	12	72	49	43/1
Bu_3Sn(mbo)							
m/e	absent	384	291	270	177	151	120/121
abundance(%)		100	25	45	50	70	11/28

Table 3.4. Selected data from CI mass spectra of mbo- and mbt- derivatives

Assignment	Bu_3Sn(mbo) m/e (%)	Bu_3Sn(mbt) m/e (%)	Me_3Sn(mbt) m/e (%)	Cy_3Sn(mbo) m/e (%)	Ph_3Sn(mbt) m/e (%)
$P^{+\cdot}$ + i-butane	498(2.3)	514(2.1)			
$P^{+\cdot}$ + n-propene	482(3.4)	498(4.1)	373(3.8)		
$PH^{+\cdot}$	442(45)	458(48)	332(91)	520(26)	
$P^{+\cdot}$					517(2)
R_2SnL^+	384(31.2)	400(35)	316(70)	436(35)	440(21)
R_3Sn^+	391(27)	391(31.2)	165(12.2)	369(26)	351(16)

Also present in the CI spectra are $P^{+\cdot}$ +57 (iso-butane) and $P^{+\cdot}$ +41 (n-propene) peaks as a result of reaction with the ions of the ionising gas. $P^{+\cdot}$ peaks are in fact in lower abundance in the CI spectra for Ph_3Sn- compounds, as was found by Fish et al (150) which is consistent with their reduced stability in an acid environment.

In the EI spectra the even electron ions are in highest abundance as expected (78). The most common odd electron ion fragment for all compounds examined under EI is $Sn^{+\cdot}$. The ratio of SnH^+ to $Sn^{+\cdot}$ is an indication of which compounds can fragment by alkene elimination and those which cannot. Compounds containing a β-methylene group (e.g. butyl and cyclohexyltins) can lose an alkene to give greater abundance of SnH^+, whereas phenyl, methyl and benzyltins give a higher abundance of $Sn^{+\cdot}$ over SnH^+. Phenyltins decay from Ph_3Sn^+ by loss of biphenyl to give $PhSn^+$ and then by loss of a phenyl radical to give Sn^+ (78).

Some fragments in the EI are due to decomposition of the ligand while still attached to the tin atom. A possible structure for the peak found at 179 in the EI spectra of Bu_3Sn(mbt), Bu_3Sn(mbo) and Me_3Sn(mbt) is $SnSCNH^+$ (abundances, 10%, 5% and 40% respectively) and a peak at 254 (6%) in the spectrum of Me_3Sn(mbt) could be assigned to $SnCSNC_6H_4^+$ (i.e. loss of S).

3.3.2. Infra-red Spectroscopy

The crystal structures of the mbtH and mboH ligands (148,149) give bond distances for the thioamide group (S=C-NH) which do not correspond to pure single or double bonds. This suggests a resonant structure, which accounts for the difficulty in assigning bands in the i.r. Very few bands arise from simple "one-bond" vibrations, the majority being due to the coupling of one or more vibrations. There has been some ambiguity in the literature as to which bands various important vibrations contribute to (153-157).

The bands due to ν(N-H) are clearly visible in the i.r. spectra of the free ligands (Table 3.5). These bands move to a higher frequency in solution indicating the disruption of the H-bonding that exists in the solid state (151). These ν(N-H) bands disappear on coordination as do bands at 643-740cm^{-1} (Table 3.5), which have been assigned to Δ(N-H) (an out of plane vibration), on the basis of deuteration experiments (152). While this indicates the loss of the N-H group, it does not necessarily mean that coordination occurs via nitrogen.

A band at 1595cm^{-1} in mbtH has been assigned by several authors to a pure ν(C=N) vibration (153,154). This band was found at 1616cm^{-1} in mboH and 1620cm^{-1} in mbiH. That it weakens and drops in frequency on coordination with transition metals to 1565-1590cm^{-1} (153,154), was seen as an indication that the nitrogen coordinated the metal atom. However, in the

complex $Ru(mbt)_2py_2(CO)_2$, which was shown to have monodentate mbt moieties coordinating via the exocyclic sulphur, a band at $1565cm^{-1}$ (weak) was observed (155). This is the same band assigned to $\nu(C=N)$ in other complexes. In this compound though the N atom does not coordinate the metal, and the C⋯N bond in fact shortens with respect to the free ligand (148), which should give $\nu(C=N)$ at a higher frequency, than in the ligand. In the organotin-mbt complexes examined here a similar weak band is found at $1560-1585cm^{-1}$ (Table 2.5), but from the above example, this cannot be taken as evidence for coordination via N.

Other bands related to the thioamide group are given in Table 3.5. The bands shown have contributions from $\nu(C-N)$, ν (C-S) and $\delta(N-H)$, and they all show either a drop in frequency or intensity or in most cases both, upon complexation. This is the same pattern as found in transition metal complexes of mbt (153-157). In most of these complexes the ligand is considered bidentate through N and S (exo) , with the exception of the Ru complex mentioned earlier, which was found to be monodentate via S(exo) and exhibited similar i.r. patterns.

Selenation studies by Devillonova et al (152) help shed some light on this ambiguous i.r. data. By replacing S(exo) with Se in all three ligands under investigation, Devillonova identified bands which contained significant contributions from C=S(exo) [about 80% double bond character in the free ligand (148,149)]. These bands are listed in Table 3.6 along with

Table 3.5.

Infra-red data for derivatives of mbt, mbo, and mbi

Compound	ν(N-H) cm^{-1}	Thioamide bands cm^{-1}			ΔN-H cm^{-1}	ν_{asym} (Sn-C) cm^{-1}	ν_{sym} (Sn-C) cm^{-1}
mbtH	3105m	1595m	1597s	1282m	705br		
$Cy_3Sn(mbt)$	absent	1555vw	1466	1280w	absent		
$Ph_3Sn(mbt)$	"	1580vw	1470sh	1270w	"		
$Bz_3Sn(mbt)$	"	1560vw	1466sh	1280w	"	453s	439m
$Bu_3Sn(mbt)$	"	1560vw	1465m	1278w	"		
$Me_3Sn(mbt)$	"	1560vw	1480sh	1275w	"	440s	413m
$Bu_2Sn(mbt)_2$	"	1555vw	1462sh	1270w	"		
mboH	3225br	1616m	1500s	1280m	645br		
$Cy_3Sn(mbo)$	absent	1580vw	1480sh	1272w	absent		
$Ph_3Sn(mbo)$	"	1600vw	1490s	1280vw	"		
$Bu_3Sn(mbo)$	"	1600vw	1480s	1275w	"		
mbiH	3155	1620m	1510s	1260m	705br		
$Cy_3Sn(mbi)$	3135* br	1615vw	1515w	1270s	absent		

s = strong

m = medium

w = weak

vw = very weak

sh = shoulder

br = broad

* This band is 50% intensity of original band corresponding to the remaining N-H group.

Table 3.6.

I.r. bands corresponding to large contributions from ν(C=S), and ν(Sn-S) bands

Compound	ν(C=S) containing bands (cm^{-1})					ν_{asym} (Sn-S)	ν_{sym} Sn-S
mbtH	1032s	1012s	602s	526w	391w		
$Cy_3Sn(mbt)$	1001s	995s	601vw	505vw	absent*	398sh	335s
$Ph_3Sn(mbt)$	1008s	993s	600vw	505vw			
$Bz_3Sn(mbt)$	1008s	1002s	604vw	510vw	absent*	400sh	322m
$Bu_3Sn(mbt)$	995s	982s	602w				
$Me_3Sn(mbt)$	998s	980m	602vw	515m	absent*	396sh	325m
$Bu_2Sn(mbt)_2$	1005s	1000s	602w	505vw	absent*		325m
mboH	1410s	813m	675m	480m	430s		
$Cy_3Sn(mbo)$	absent	813m	675vw	absent	422m	392vw	330s
$Ph_3Sn(mbo)$	"	810m	665vw	"	417m	397vw	338m
$Bu_3Sn(mbo)$	"	810m	absent	"	419m		
mbiH	658m	598s	480m	418m			
$Cy_3Sn(mbi)$	658w	600w	479w	414m			318m

s = strong

m = medium

w = weak

vw = very weak

sh = shoulder

* ligand and ν(Sn-S) band in this region

the changes that occur on coordination. All the relevant bands showed either a drop in intensity, some disappearing altogether, or a drop in frequency. This would seem to indicate a considerable drop in electron density in the C=S(exo) bond, which could be explained by coordination to tin via S(exo) and this is corroborated by the appearance of bands attributable to ν(Sn-S) (Table 3.6) (147,158).

The ν(Sn-C) region of the i.r. for $Me_3Sn(mbt)$ and $Bz_3Sn(mbt)$ show both ν_{asym}(Sn-C) and ν_{sym}(Sn-C) bands (Table 3.5) indicating a tetrahedral geometry and hence four coordination for these compounds. It would seem likely that a similar structure is adopted by the other derivatives.

3.3.3. N.m.r. spectroscopy

^1H n.m.r. and ^{119}Sn n.m.r. data are given in Table 3.7. ^2J ($^{119}Sn-Cl-^1H$) values obtained for $Me_3Sn(mbt)$ and $Bz_3Sn(mbt)$ are indicative of four coordination (1). The coupling constant for $Me_3Sn(mbt)$ is in good agreement with that obtained by Domazetis et al (63Hz) (147), and is also consistent with values obtained for the tetrahedral mercaptides $Me_3SnS-C_6H_4X-p$ (X = H, Me, Bu^t, Cl, Br, NH_2, NO_2, OMe) of 55.5Hz $\pm$ 0.3 (159). Bidentate chelation via S(exo) and N would give similar coupling constants as found for the five coordinate complex Me_3Sn(ON.Ph.CO.Ph) [54Hz, (197)].

Table 3.7

N.m.r. data for organotin derivatives

of mbt, mbo, and mbi

Compound	δCH-Sn (ppm)	$J^{119}Sn-C-^{1}H$ (H_3)	$\delta^{119}Sn$ (ppm)
$Bz_3Sn(mbt)$, $CDCl_3$	2.53	65	
$Me_3Sn(mbt)$, $CDCl_3$	0.65	59	
$Cy_3Sn(mbt)$,toluene			+37.7
$Cy_3Sn(mbo)$,toluene			+37.7
$Cy_3Sn(mbi)$,toluene			+26.6

^{13}C n.m.r. studies carried out by Domazetis et al (146,147) on tri- and dibutyltin derivatives of mbtH indicate four coordination for $Bu_3Sn(mbt)$ $^1J(^{119}Sn-^{13}C)$ = 336Hz, and five coordination for $Bu_2Sn(mbt)_2$ $^1J(^{119}Sn-^{13}C)$ = 505Hz. The structure proposed for $Bu_2Sn(mbt)_2$ in solution was that in which one mbt is bidentate [N and S(exo)] and the other monodentate [S(exo)], with interchange of bonding modes between the two ligands (146). Another possibility however is that of a tetrahedral R_2SnS_2 system distorted by two long Sn---N contacts towards an octahedral configuration with trans-R groups e.g. $Bu_2Sn(S-C_5H_4N-2, NO_2-5)$ which has been shown by X-ray studies to have a distorted tetrahedral structure (C-Sn-C = 129.2°, Sn---N = 2.77Å) and exhibits $^1J(^{119}Sn-^{13}C)$ = 523Hz (161).

^{119}Sn chemical shifts for cyclohexyltin derivatives of these ligands are all quite similar (ca. +30ppm) and indicative of four coordinate tin in solution e.g. Cy_3SnBr (+69.1ppm) and Cy_3SnI (+56.7ppm) (160). Five coordinate values of $\delta^{119}Sn$ would be expected to be found more upfield e.g. $Cy_3Sn(trop)$ δ = -62.8ppm(160).

3.3.4. Mössbauer spectroscopy

Mössbauer data for derivatives of these ligands are given in Table 3.8. Data from variable temperature experiments are in Tables 3.9. and 3.10 and are depicted in Fig. 3.3.

Quadrupole splitting data for the triorganotin compounds with the exception of $Bu_3Sn(mbo)$ fall in the range 1.80 - 2.35mms^{-1} which are typical of a tetrahedral geometry about tin but could also result from a cis-tbp configuration (range 1.70 - 2.40mms^{-1}) (1). Mössbauer studies have been carried out on various organotin mercaptides. R_3SnSR^1 and $R_2Sn(SR^1)_2$ (R^1 = Me, Ph, or C_6H_4-x) and ΔEq values found were similar to those obtained here (158,159,162). These compounds were all considered tetrahedral monomers with monodentate S-bonded ligands. $Ph_3SnSC_6H_4$-Bu^t-p [ΔEq = 1.41, (159)] has been shown by X-ray studies to adopt such a structure (163).

Phenyltin derivatives were found to exhibit lower ΔEq values (1.80 - 2.03 mms^{-1}) than the alkyltins (2.22 - 2.40mms^{-1}). This is explained by the fact that ΔEq arises from an imbalance in the tin-ligand σ bonds and since phenyl groups are more electronegative than alkyl groups this imbalance is least in this case (159).

Five coordinate polymeric structures containing trans N and S donor atoms are ruled out (except for $Bu_3Sn(mbo)$) as these would give ΔEq's of over 2.80mms^{-1} e.g. $Me_3SnSC_6H_4NH_2$-p [2.85mms^{-1} (159)] and $Me_2ClSnS(CH_2)_2NH_2$ [2.83mms^{-1} (147)]. Domazetis et al (147) proposed a cis-R_3SnNS (S axial) geometry for one of the tin sites in $(Me_3Sn)_2$ (1,3,4-thiazole-2,5 dithiolate) for which he assigns the doublet at δ1.31 mms^{-1}, ΔEq 2.35 mms^{-1}, and they also suggest that there may be a short Sn---N interaction in $Bu_3Sn(mbt)$ to give a similar structure. The Mössbauer data obtained here for $Bu_3Sn(mbt)$ (δ 1.48mms^{-1}, ΔEq 2.37mms^{-1}) agrees well with those found by Domazetis (147) (δ 1.41mms^{-1}, ΔEq 2.39mms^{-1}), however on

the basis of i.r. results we are inclined to rule out a cis-R_3SnNS structure for the compounds studied here and ΔEq values obtained are considered the result of monodentate coordination via S(exo).

The quadrupole splitting obtained for $Bu_3Sn(mbo)$ ($3.26mms^{-1}$) is quite different from that of the other derivatives and clearly indicates an increase in coordination number from four to five. The value is too high to be the result of a cis-R_3SnNS, or cis-R_3SnOS structure [range 1.70 - $2.40mms^{-1}$ (1)] and instead appears to indicate the formation of five coordinate polymer with trans-donor atoms (1). This phenomenon is the result of a change in structure on solidification at the low temperature of the Mössbauer experiment and has been noted before for other oils such as $Me_3SnS_2P(OR_2)$ (R = Et, i-Pr) (173). The $Me_3Sn(mbo)$ analogue should behave in a similar manner but attempts to synthesise it failed. Either the nitrogen or oxygen atoms on the benzoxazole ring could cause this coordination expansion, but the latter is favoured as the same phenomenon is not observed in $Bu_3Sn(mbt)$ which lacks an oxygen atom.

For the dibutyltin derivative $Bu_2Sn(mbt)_2$ Domazetis et al. claimed two doublets in the Mössbauer spectrum, one at $\delta 1.48mms^{-1}$, ΔEq $3.00mms^{-1}$ corresponding to a distorted octahedron with two strong Sn-S bonds and two Sn---N bonds, and the other at $\delta 0.98mms^{-1}$, ΔEq $2.07mms^{-1}$ which they claim corresponds to a cis-$Bu_2SnN_2S_2$

structure with strong Sn-N and weak Sn-S bonds. Whereas the first assignment appears correct with similar parameters obtained in this work for $Bu_2Sn(mbt)_2$ (δ1.48mms^{-1}, ΔEq 2.37mms^{-1}), the other peak is most likely due to Bu_2SnO (starting material) impurities [δ1.04mms^{-1}, ΔEq 2.09mms^{-1} (50)] which are difficult to eliminate entirely, and is also found in the spectrum obtained in this work (δ 1.00mms^{-1}, ΔEq 2.04mms^{-1}). ΔEq for $Bu_2Sn(mbt)_2$ (2.37mms^{-1}) though higher than that found for tetrahedral $Bu_2Sn(SR)_2$ systems [1.91mms^{-1} (158)] is well short of that expected for an octahedron with two bidentate (N and S) ligands and trans-Bu groups, such as Bu_2Sn(6-thiopurine) ΔEq = 3.26mms^{-1} (164). Distortions of the tetrahedral geometry at tin are likely to be minor, and < C-Sn-C anticipated to be only slightly in excess of 110°.

The variable temperature data for $Cy_3Sn(mbt)$ (Fig. 3.3) gives a rather shallow slope, but this is not inconsistent with being a tetrahedral monomer. The $\underline{a}$-value of 1.35 x $10^{-2}K^{-1}$ is at the interface of monomers and compounds with a polymeric lattice such as Cy_3Sn(triazole) [$\underline{a}$ = 1.31 x $10^{-2}K^{-1}$ (22)] and the weakly bridging Cy_3SnCl (165) [$\underline{a}$ = 1.40 x $10^{-2}K^{-1}$ (136)]. As other spectroscopic data do not suggest polymer formation in the solid state the only explanation for such a low value of $\underline{a}$ is that very strong packing factors exist. Tetracyclohexyltin which is also a monomer exhibits similar variable temperature behaviour with $\underline{a}$ = 1.14 x $10^{-2}K^{-1}$ (22).

$Cy_3Sn(mbi)$ exhibits a steeper slope with $\underline{a}$ = 1.68 x $10^{-2}K^{-1}$ typical of a monomeric lattice, e.g. Cy_3SnBr (136)

Table 3.8

Mössbauer data (78K) for organotin derivatives of mbt, mbo and mbi

Compound	δ	ΔEq	Γ_1 (b)	Γ_2 (b)
$Cy_3Sn(mbt)$	1.54	2.22	0.940	0.899
$Ph_3Sn(mbt)$	1.31	1.80	0.864	0.875
$Bz_3Sn(mbt)$	1.51	1.91	1.020	0.971
$Me_3Sn(mbt)$	1.35	2.40	1.030	0.993
$Bu_3Sn(mbt)$	1.48	2.37	1.030	1.020
$Cy_3Sn(mbo)$	1.57	2.35	0.984	0.988
$Ph_3Sn(mbo)$	1.34	2.03	0.990	1.002
$Bu_3Sn(mbo)$	1.28	3.26	1.17	1.203
$Cy_3Sn(mbi)$	1.57	2.30	0.935	0.952
$Bu_2Sn(mbt)_2$ (a)	1.48	2.37	0.977	0.919

(a) Contains impurity peak

δ1.00mms^{-1} ΔEq 2.04mms^{-1}

(b) Γ = Full-width at half-height of absorption

Table 3.9

Variable temperature Mössbauer Spectroscopic Data for $Cy_3Sn(mbt)$

T(K)	Area	$\ln A_T/A_{78}$	$\underline{a}$ (K^{-1})*
78	9.166	0.000	1.35×10^{-2}
95	7.189	-0.243	correlation factor =
110	5.988	-0.426	-0.999
125	4.794	-0.648	
140	3.975	-0.835	

* $\underline{a} = -d\ln A_T/dT$

Table 3.10

Variable temperature Mössbauer spectroscopic Data for $Cy_3Sn(mbi)$

T(K)	Area	$\ln A_T/A_{78}$	$\underline{a}(K^{-1})$*
78	7.100	0.000	1.68×10^{-2}
95	5.155	-0.320	correlation factor =
110	4.215	-0.521	-0.998
125	3,388	-0.740	
140	2.490	-1.048	
155	1.901	-1.318	

* $\underline{a} = -d\ln A_T/dT$

Fig. 3.3. Variable temperature plots for $Cy_3Sn(mbt)$ (o) and $Cy_3Sn(mbi)$ (●)

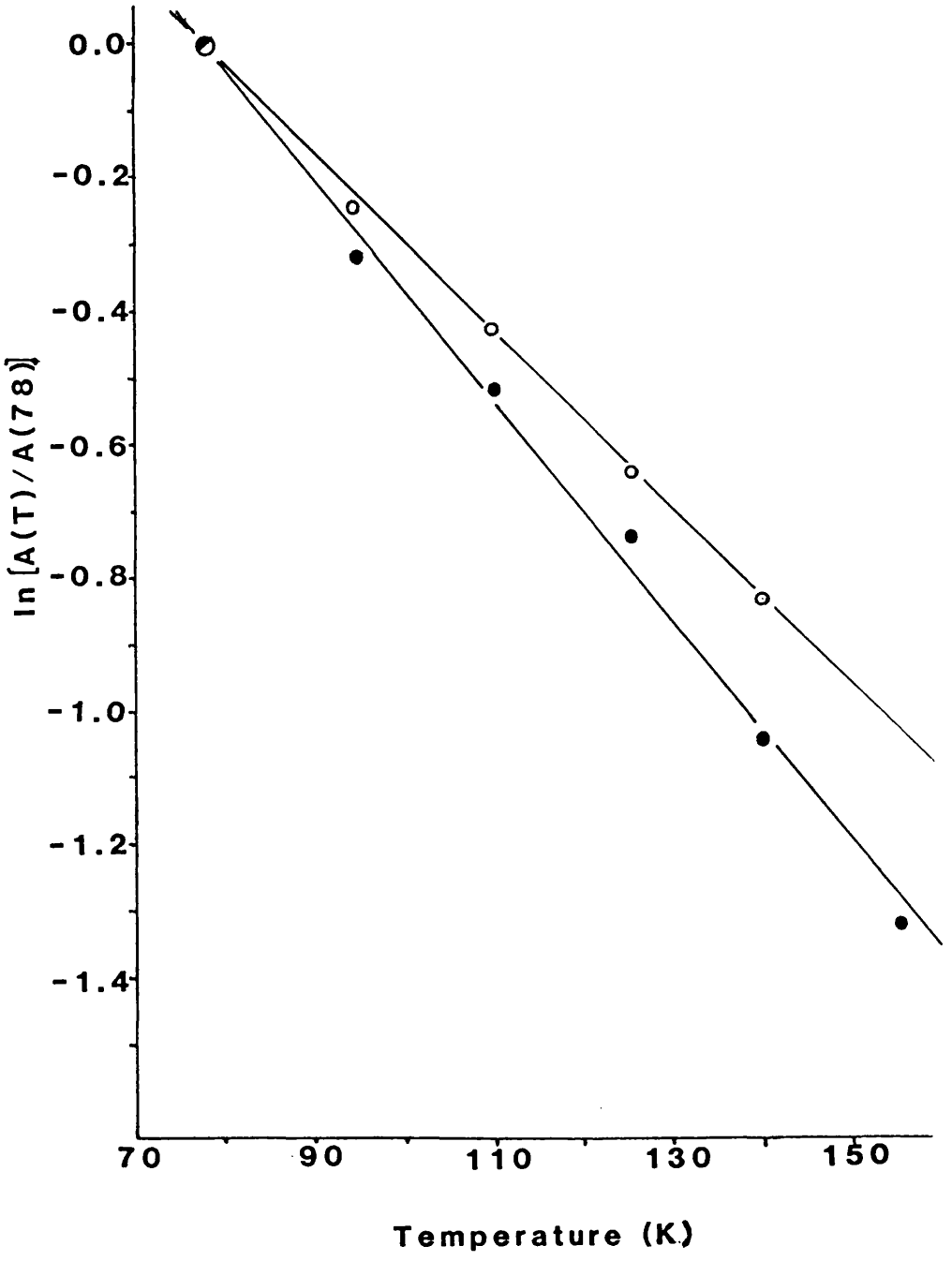

[$\underline{a}$ = 1.64 x $10^{-2}K^{-1}$(22)]. This compound may contain a H-bonded lattice as suggested by ν(N-H) of 3135cm^{-1} (broad) in the i.r. (Table 3.5) and a lower solubility than the other derivatives in apolar solvents. The high value of $\underline{a}$ does not necessarily discount this as the Cy_3Sn- moiety would be pendant to such a H-bonded lattice and behave as a monomer as in Cy_3SnIAA (a = 1.75 x $10^{-2}K^{-1}$) (Chapter 2).

3.4. Crystal and molecular structure of $Cy_3Sn(mbt)$

Suitable crystals were obtained by recrystallisation from a diethyl ether/methanol solvent mixture. Details of crystallographic analysis and structure refinement are given in Appendix 3. Final atomic positional parameters are given in Table 3.11, Fig. 3.4 shows the local geometry about Sn and the numbering system, while Fig. 3.5 gives a view of the unit cell. Table 3.12 gives the bond lengths and Table 3.13 the bond angles. Table 3.14 lists bond distances of analogous compounds for comparison.

The local geometry about tin is best described as a distorted tetrahedron. A long Sn-----N contact of 3.055Å which is within the sum of the respective van der Waals radii of 3.67Å does exist however, but is a lot longer than the bonding Sn-N distances found in $Me_3SnO_2CCH_2NH_2$ [2.46Å(139)] and $Ph_3SnSC_5H_4N$-p [2.62Å (166)], which form N-bridged polymers.

A similar though shorter Sn---N intramolecular interaction is found in $Bu_2Sn(SC_5H_4N\text{-}2,NO_2\text{-}5)_2$ (2.77Å) which causes the complex to distort considerably from a R_2SnS_2 geometry with <C-Sn-C expanding to 129.2° (161). In the case of $Cy_3Sn(mbt)$ distortions are much weaker with no systematic change in angles about Sn to suggest the formation of a cis-R_3SnNS configuration with axial N and C(8). The sum of the angles in the would be equatorial plane in such a structure is only 334.9° compared with 360.0 for ideal tbp, and 328.5 for ideal tetrahedral.

Deviations from tetrahedral angles are very slight in most cases with the exception of C(8)-Sn-S(1) which decreases to 96.6°. Rehybridisation to increase p-character in the bond to sulphur would lead to an increase in all <C-Sn-C (towards 120°) and a narrowing of all <C-Sn-S (towards 90°). Such systematics are not observed here, unlike in Cy_3SnIAA (Chapter 2), where more electronegative oxygen is the donor atom. The electronegativity of S(2.58) is similar to that of carbon (2.55) and rehybridisation schemes are less clear-cut. In $Ph_3SnSC_6H_4Bu^t\text{-}p$ (163) a similar singular <C-Sn-S angle narrowing is observed (98.5°) which is attributed to crystal packing requirements.

The Sn-S(1) bond at 2.472Å agrees well with those found for other organotin mercaptides e.g. $Ph_3SnSC_6H_4Bu^t\text{-}p$ [2.613Å, (163)], and dithiocarbamates e.g. $Me_3Sn(S_2CNMe_2)$ [2.47Å, (167)] and is somewhat shorter than that found for the bridged thiopyridine derivative $Ph_3SnSC_5H_4N\text{-}p$ [2.567Å(166)]. The Sn-C bond lengths

agree well with each other and the mean value of 2.167Å compares favourably with those found in $Cy_3Sn(IAA)$ (mean 2.157Å, Chapter 2), Cy_3SnCl [2.096Å, (165)] and Cy_3SnI [2.17Å, (136)]. The Sn-C(8) bond is only slightly longer (2.183Å) than the other tin carbon bond lengths (2.15, 2.17Å) so it is unlikely to be in the axial position of a cis-R_3SnNS structure.

In its non-complexed form the ligand adopts a thione structure (Fig. 3.1) i.e. the C(1)-S(1) bond (1.662Å) has mostly double bond and the C(1)-N bond (1.353Å) single bond character (148). The crystal structure of $Cy_3Sn(mbt)$ shows a redistribution of electron density on the ligand molecule towards a thiol structure. The C(1)-S(1) bond has lengthened to 1.743Å consistent with a decrease in bond order, though it is not as long as the C-S (single) bond lengths in Ph_3SnSMe [1.77Å, (168)] or $Ph_3SnSC_6H_4Bu^t$-p [1.784Å, (163)]. The C(1)-S(2) bond distance, involving the endo-sulphur does not change on going from uncomplexed [1.734, (148)] to complexed form (1.734Å) retaining its mostly single bond character. The C(1)-N bond length concomittantly shortens to 1.29Å from 1.353Å (148). A similar pattern is found when the ligand coordinates to transition metals. In cases where the ligand is bidentate via N and S(exo) the C(1)-S(1) bond lengthens to ca. 1.69 - 1.72Å and the C-N bond shortens to ca. 1.29 - 1.31Å (169-171). In the case of the ligand coordinating in a monodentate fashion via S(exo), the C(1)-N bond has shortened further to 1.287Å (155), indicating almost pure C=N. If the ligand were to coordinate only via the N atom then the C(1)-S(1) and C(1)-N bonds would be expected to retain their thione arrangement, as found in a series of zinc complexes where C-S= 1.67-1.69Å and C-N=

Table 3.11

Fractional atomic coordinates and thermal parameters (A^o) for $Cy_3Sn(mbt)$

Atom	x	y	z	U_{iso} or U_{eq}
Sn1	0.27094(5)	0.01442(6)	0.27575(6)	0.0516(4)
S1	0.1192(2)	0.0274(3)	0.1081(3)	0.067(2)
S2	0.0291(2)	0.2845(3)	-0.1213(3)	0.080(2)
N1	0.1718(6)	0.2801(8)	0.0718(9)	0.066(2)
C1.1	0.1151(7)	0.2034(10)	0.0271(10)	0.061(2)
C2.1	0.0757(8)	0.4381(11)	-0.1224(11)	0.072(3)
C3.1	0.0418(10)	0.5685(13)	-0.2148(14)	0.091(3)
C4.1	0.0884(10)	0.6694(15)	-0.1876(15)	0.099(4)
C5.1	0.1625(10)	0.6477(14)	-0.0792(15)	0.100(4)
C6.1	0.1964(9)	0.5208(12)	0.0098(13)	0.083(3)
C7.1	0.1491(8)	0.4122(11)	-0.0124(11)	0.070(3)
C1.2	0.2827(9)	-0.2046(11)	0.3716(13)	0.081(3)
C2.2	0.3780(10)	-0.2504(13)	0.4736(14)	0.091(3)
C3.2	0.3892(12)	-0.4016(16)	0.5391(19)	0.119(5)
C4.2	0.2890(15)	-0.4820(22)	0.5920(23)	0.158(7)
C5.2	0.2030(14)	-0.4365(17)	0.4840(20)	0.139(6)
C6.2	0.1883(12)	-0.2877(15)	0.4327(18)	0.117(5)
C1.3	0.2431(8)	0.0895(10)	0.4290(11)	0.069(3)
C2.3	0.1328(9)	0.0901(12)	0.4581(13)	0.079(3)
C3.3	0.1207(11)	0.1509(13)	0.5626(14)	0.095(4)
C4.3	0.1887(11)	0.0906(15)	0.7010(16)	0.109(4)
C5.3	0.2963(11)	0.0876(15)	0.6743(16)	0.106(4)
C6.3	0.3086(10)	0.0272(12)	0.5697(13)	0.088(3)
C1.4	0.4061(8)	0.1160(10)	0.1483(10)	0.063(2)

Table 3.11 contd.

C2.4	0.3912(9)	0.1549(12)	-0.0122(12)	0.081(3)
C3.4	0.4854(10)	0.2229(13)	-0.0997(15)	0.095(4)
C4.4	0.5309(11)	0.3332(14)	-0.0724(14)	0.097(4)
C5.4	0.5479(10)	0.2981(13)	0.0884(13)	0.093(3)
C6.4	0.4497(9)	0.2360(12)	0.1710(13)	0.081(3)

Table 3.12

Intramolecular Bond lengths (Å) for $Cy_3Sn(mbt)$

Sn-S(1)	2.472(2)	C(14)-C(15)	1.494(15)
Sn-N	3.055(8)	C(15)-C(16)	1.526(16)
Sn-C(8)	2.183(11)	C(16)-C(17)	1.502(18)
Sn-C(14)	2.150(10)	C(17)-C(18)	1.457(19)
Sn-C(20)	1.170(9)	C(18)-C(19)	1.529(18)
		C(19)-C(14)	1.502(15)
C(1)-S(1)	1.743(10)		
C(1)-N	1.290(12)	C(20)-C(21)	1.486(14)
C(1)-S(2)	1.734(10)	C(21)-C(22)	1.502(16)
C(7)-N	1.364(13)	C(22)-C(23)	1.443(16)
C(2)-S(2)	1.753(11)	C(23)-C(24)	1.500(17)
C(2)-C(3)	1.407(16)	C(24)-C(25)	1.515(16)
C(3)-C(4)	1.355(17)	C(25)-C(20)	1.509(14)
C(4)-C(5)	1.353(18)		
C(5)-C(6)	1.372(17)		
C(6)-C(7)	1.406(15)		
C(2)-C(7)	1.352(15)		
C(8)-C(9)	1.515(17)		
C(9)-C(10)	1.514(19)		
C(10)-C(11)	1.498(22)		
C(11)-C(12)	1.453(24)		
C(12)-C(13)	1.515(21)		
C(13)-C(8)	1.461(17)		

Table 3.13

Intramolecular bond angles for $Cy_3Sn(mbt)$

C(8)-Sn-C(20)	108.6(4)	C(8)-C(9)-C(10)	112.9(11)
C(14)-Sn-C(8)	115.7(4)	C(9)-C(10)-C(11)	111.9(14)
C(20)-Sn-C(14)	112.4(4)	C(10)-C(11)-C(12)	114.3(17)
C(8)-Sn-N	153.6(3)	C(11)-C(12)-C(13)	110.9(16)
C(14)-Sn-N	78.3(3)	C(12)-C(13)-C(8)	116.8(13)
C(20)-Sn-N	83.8(3)	C(13)-C(8)-C(9)	114.2(11)
C(14)-Sn-S(1)	112.3(3)		
C(8)-Sn-S(1)	96.6(3)	C(14)-C(15)-C(16)	112.4(9)
C(20)-Sn-S(1)	110.2(3)	C(15)-C(16)-C(17)	112.8(11)
		C(16)-C(17)-C(18)	114.1(13)
C(1)-S(1)-Sn	95.7(3)	C(17)-C(18)-C(19)	112.7(12)
C(1)-N-Sn	82.8(6)	C(18)-C(19)-C(14)	112.7(12)
N-C(1)-S(1)	124.1(8)	C(19)-C(14)-C(15)	113.3(10)
S(2)-C(1)-S(1)	119.7(6)		
C(1)-N-C(7)	109.9(9)	C(20)-C(21)-C(22)	110.7(9)
N-C(7)-C(2)	117.1(1)	C(21)-C(22)-C(23)	114.1(10)
C(7)-C(2)-S(1)	108.8(8)	C(22)-C(23)-C(24)	112.5(11)
C(2)-S(2)-C(1)	87.9(5)	C(23)-C(24)-C(25)	114.5(11)
C(2)-C(3)-C(4)	115.5(13)	C(24)-C(25)-C(20)	111.1(11)
C(3)-C(4)-C(5)	122.9(15)	C(25)-C(20)-C(21)	111.1(9)
C(4)-C(5)-C(6)	121.7(14)		
C(5)-C(6)-C(7)	117.6(12)		
C(6)-C(7)-C(2)	119.0(11)		
C(7)-C(2)-C(3)	123.4(11)		

Fig. 3.5

View of unit cell of $Cy_3Sn(mbt)$

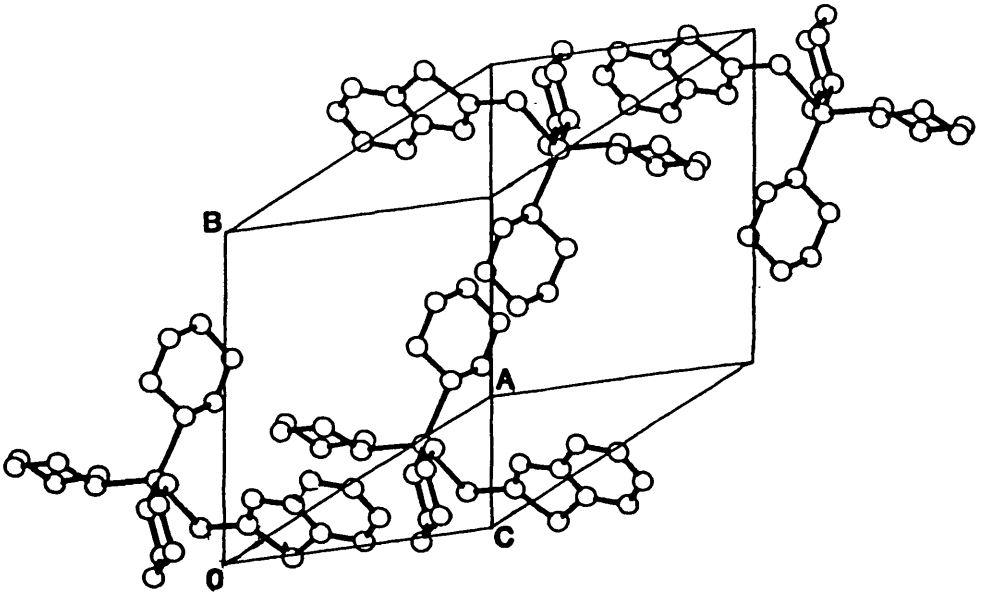

Fig. 3.4.

Local geometry about Sn in $Cy_3Sn(mbt)$

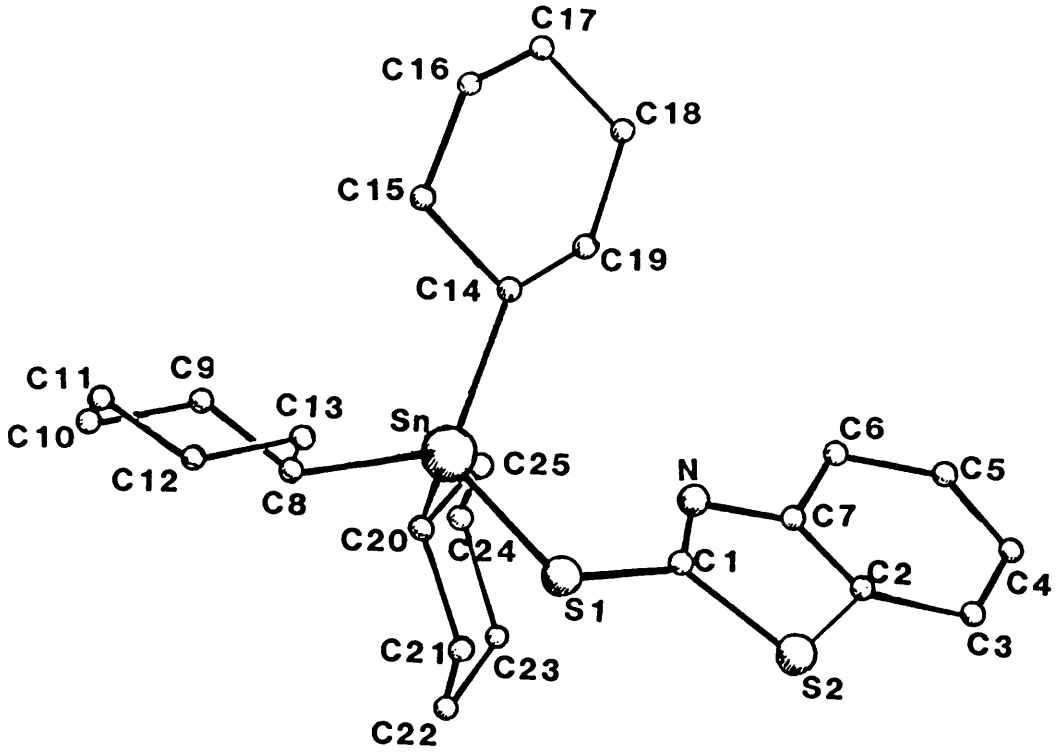

Table 3.14. Selected bond distances for compounds related to $Cy_3Sn(mbt)$ (Å)

Compound	Sn-S(1)	Sn-N	Sn-C (mean)	S-C(1)	C(1)-N(1)	Ref.
$Cy_3Sn(mbt)$	2.472	3.055	2.167	1.743	1.290	This work
$Bu_2Sn(SC_5H_4N\text{-}2,NO_2\text{-}5)_2$	2.477	2.77	2.162	1.73	1.32	161
$Ph_3SnSC_6H_4Bu^t\text{-}p$	2.413		2.126	1.784		163
Ph_3SnSMe	2.391		2.137	1.770		168
$Ph_3SnSC_6H_4N\text{-}p$	2.567	2.62				166
$Co(mbt)_2py_2$				1.709	1.304	169
$[Cd(mbt)_3][NEt_4]$				1.693	1.303	170
$Ru_2(mbt)_2py_2(CO)_2$				1.719*	1.306*	171
$[Zn(mbt)_3H_2O][NBu_4]$				1.725*a 1.690b	1.301*a 1.331b	172
$[Zn(mbt)(S_2CNMe_2)_2]EtOH[NBu_4]$				1.679	1.328	172
$[Zn(mbt)_2(S_2CNMe_2)][NBu_4]$				1.681	1.318	172
$Ru(mbt)_2py_2(CO)_2$				1.724	1.287	155
mbtH				1.662	1.353	148

* - average of two ligands in similar sites

a - N of ligand H-bonded to water molecule

b - different site (N-bonded)

1.31-1.33Å (172). The ligand bond distances found for $Cy_3Sn(mbt)$ favour a thiol structure and the short length found for C(1)-N (1.29Å) dictates a non-bonding interaction between Sn and N.

From spectroscopic behaviour similar to $Cy_3Sn(mbt)$, it is proposed that all the other triorganotin derivatives of mbt-, mbo- and mbi adopt a similar four coordinate structure.

3.5 Biocidial activity

Pesticidal activity of $Ph_3Sn(mbo)$, $Ph_3Sn(mbt)$ and $Cy_3Sn(mbt)$ against selected species is given in Table 3.15; while fungicidal/ bactericidal activity in Table 3.16. The cyclohexyltin derivative showed the greatest pesticidal activity which was expected since cyclohexyltins are used as commercial acaricides (1). $Ph_3Sn(mbo)$ shows no pesticidal activity, while all three show fungicidal activity with the phenyltins most active, in agreement with their existing commercial use in this area.

All three, but especially the mercapto-benzoxazole derivative showed activity as plant growth regulators, being phytotoxic towards specific crop species (particularly maize, soya, tomato and sugar beet).

Again, the four coordinate nature of the compounds under study is consistent with this geometry being a pre-requisite for high activity (84).

Table 3.15.

Pesticidal activity of $Ph_3Sn(mbo)$, $Ph_3Sn(mbt)$ and $Cy_3Sn(mbt)$

Species	ppm	$Cy_3Sn(mbt)$	$Ph_3Sn(mbt)$	$Ph_3Sn(mbo)$
Tetranychus	500	9	9	0
Musca	500	9	0	0
Chilo	500	9	9	0
Nilapravata	500	0	0	0

0 = 0-49% kill

9 = 80-100% kill

Table 3.16.

Fungicidal and bactericidal activity of

$Ph_3Sn(mbo)$, $Ph_3Sn(mbt)$ and $Ph_3Sn(mbo)$

Species	ppm	$Cy_3Sn(mbt)$	$Ph_3Sn(mbt)$	$Ph_3Sn(mbo)$
Aspergillus Niger*	25	2	4	4
Botrytis Cinerea*	25	2	4	4
Septoria Nodorum*	25	2	4	0
Penicillium digitatum*	25	2	4	4
Plasmopora viticola (vine)≠	100	4	4	4
Venturia inaequdlis (apple)≠	100	3	3	4
Xanthomonas oryzae (ground nut)≠	100	1	4	3

* in vitro

≠ in vivo

4 = No disease

3 = trace - 5% disease

2 = 6-25% disease

1 = 26-60% disease

Chapter Four

Synthesis and Characterisation of Organotin Derivatives of Piperazine bis-Dithiocarbamate

4.1. Introduction

Bis-dithiocarbamates have been in use as commercial fungicides for a long time. In terms of commercial use, metal salts of ethylenebisdithiocarbamate [patented 1943] such as Maneb (Mn) and Zineb (Zn) are the most popular form of this series (143). The mode of action of these compounds is not entirely clear but like 2-mercaptobenzothiazole discussed in Chapter 3, it is thought to be related to a decomposition to toxic by-products especially isothiocyanates (143). Activity may also be due, in part, to an exchange of the metal atom in the fungicide for a metal in a metalloprotein leading to a disruption of enzyme systems. Zinc and copper dialkyldithiocarbamates for example displace Fe^{2+} in aconitase, an enzyme involved in the Krebs cycle (143).

In this chapter the synthesis and characterisation of organotin derivatives of piperazine bis-dithiocarbamate (pipdtc) (Fig. 4.1) will be presented. The synthesis of trimethyl-, tributyl, and triphenyltin derivatives of this ligand have been reported before (174). The compounds synthesised by Siddiqi et al. (174) however give substantially different physical data from those reported here and a re-evaluation of one of these derivatives is made.

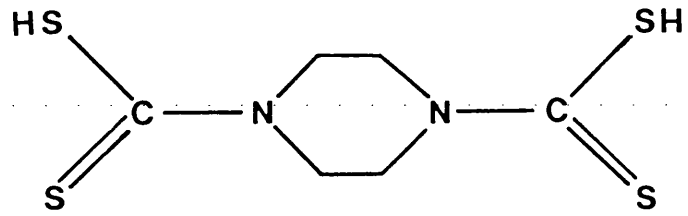

Fig. 4.1. Piperazine bis-dithiocarbamate

4.2. Synthesis

Organotin starting materials were obtained as described in Appendix 1. Piperazine hexahydrate was purchased from Merck and used without further purification. Piperazine bis-dithiocarbamate (disodium salt, dihydrate) was synthesised by the method of Tombeux et al. (175) and recrystallised from ethanol. All solvents were dried before use.

The derivatives were synthesised using organotin halides as starting materials and the general procedure used is described by Method (a). Conditions for individual reactions are given in Table 4.1, and physical data for the products in Table 4.2.

Method (a): Tricyclohexyltin chloride (0.97g, 2.43mmol) was dissolved in ethanol (20mls). To this was added with stirring a warm ethanolic solution (20mls) of Na_2pipdtc.$2H_2O$ (0.39g, 1.22mmol).

Table 4.1.

Reaction conditions for the synthesis of organotin derivatives of piperazine bis-dithiocarbamates.

Starting materials	Solvent	Reaction time	Recrystall. solvent	% Yield	Product
Cy_3SnCl(2.43mmol) $Na_2pipdtc.2H_2O$ (1.22mmol)	EtOH	15 mins	Toluene	50	$(Cy_3Sn)_2$ pipdtc
Ph_3SnCl(7.6mmol) $Na_2pipdtc.2H_2O$ (3.8mmol)	EtOH	10 mins	Toluene	50	$(Ph_3Sn)_2$ pipdtc
Me_3SnCl(15mmol) $Na_2pipdtc.2H_2O$ (7.5mmol)	MeOH	10 mins	$CHCl_3$/EtOH	30	$(Me_3Sn)_2$ pipdtc
Bu_3SnCl (15.2mmol) $Na_2pipdtc.2H_2O$ (7.6mmol)	EtOH	30 mins	EtOH	25	$(Bu_3Sn)_2$ pipdtc
$Octyl_2SnCl_2$(3.4mmol) $Na_2pipdtc.2H_2O$ (3.4mmol)	EtOH	15 mins	-	72	$Octyl_2Sn$ pipdtc
Me_2SnCl_2(5.1mmol) $Na_2pipdtc.2H_2O$ (5.1mmol)	EtOH	1½ hrs	-	76	Me_2Sn pipdtc
Bu_2SnCl_2(8.6mmol) $Na_2pipdtc.2H_2O$ (8.4mmol)	EtOH	30 mins	-	87	Bu_2Sn pipdtc
			EtOH	(60mg)*	$(Bu_2ClSn)_2$ pipdtc
Ph_2SnCl_2(6.8mmol) $Na_2pipdtc.2H_2O$ (6.8mmol)	EtOH	30 mins	-	76	Ph_2Sn pipdtc

* 78% of molar excess of Bu_2SnCl_2

Table 4.2. Physical data for organotin derivatives of piperazine bis-dithiocarbamate

Compound	m.p. (°C)	Calculated			Found		
		C	H	N	C	H	N
$(Cy_3Sn)_2$pipdtc	233-234	51.86	7.67	2.88	52.16	7.79	2.84
$(Ph_3Sn)_2$pipdtc	244-246	53.87	4.09	2.99	54.33	4.09	2.89
$(Me_3Sn)_2$pipdtc	182-184	25.56	4.65	4.97	25.50	4.46	4.67
$(Bu_3Sn)_2$pipdtc	oil	44.46	6.72	3.46	44.80	7.74	3.08
$(Bu_2ClSn)_2$pipdtc [a]	133-134	34.20	5.73	3.62	34.49	5.96	3.65
Me_2Snpipdtc	d > 270	24.94	3.60	7.27	22.61	3.44	5.95
Bu_2Snpipdtc	d > 220	35.83	5.58	5.97	35.38	5.63	5.04
Ph_2Snpipdtc	d > 200	42.45	3.56	5.50	41.7	3.41	4.24
$Octyl_2$Snpipdtc	d > 225	45.60	7.30	4.83	45.54	7.38	4.51

a Cl: calc'd 9.15, found 9.02

An instantaneous white precipitate developed, and the reaction mixture was stirred for a further 15 mins before filtering off a white solid. This solid (which contained both product and NaCl) was recrystallised from toluene, yielding 0.55g of white crystals (50% yield) m.p. 233-234°C.

$(Bu_3Sn)_2$pipdtc was found to be an oil, and as attempts at distillation lead to decomposition the compound is purified by repeatedly dissolving the oil in hot ethanol and reprecipitating it by cooling, decanting of the supernatant. Prolonged drying under vacuum removed the last traces of solvent. The R_2Sn(pipdtc) derivatives were found to be insoluble in all solvents and so were purified by washing alternately with H_2O (to remove NaCl, and unreacted ligand) and Et_2O (to remove unreacted organotin).

4.3. Discussion and Results

4.3.1. Synthesis

The triorganotin derivatives were all obtained in a 2:1 organotin to ligand ratio as shown in eqn. (a). Siddiqi et al (174) failed to obtain such derivatives except in the case of $(Ph_3Sn)_2$pipdtc despite using 2:1 ratios of starting materials. From C, H and N microanalytical results they formulated their tributyl and trimethyltin derivatives as $R_3SnS_2CNNCS_2Na$. This would account for the high melting points and general insolubility reported for these compounds. $(Ph_3Sn)_2$pipdtc however, in disagreement with the results presented here, was also reported to be insoluble in several organic solvents and have a m.p. 300°d. That this compound was not recrystallised would suggest the presence of NaCl in the isolated product [eqn. (a)] and this could explain the high m.p. but not the microanalytical results obtained

which were in perfect agreement with the proposed structure. It is worth noting that they also report a synthesis of $Ph_3SnS_2CNEt_2$ and give its m.p. as being >200°C, but which has been previously reported as melting at 132-133° (176)

$$2\ R_3SnCl + Na_2(S_2CNNCS_2).2H_2O \rightarrow R_3SnS_2CNNCS_2SnR_3 + 2\ NaCl + 2H_2O \qquad \text{[eq (a)]}$$

The diorganotin derivatives all yielded 1:1 complexes [eqn (b)] in high yield. $(Bu_2ClSn)_2$pipdtc was obtained in small quantities as a by-product of the reaction of Bu_2SnCl_2 with Na_2pipdtc.$2H_2O$. Its formation is probably due to the presence of an excess of Bu_2SnCl_2 in the reaction mixture. This compound was easily isolated from the main product of the reaction as it remained in the reaction solution while the polymeric Bu_2Sn(pipdtc) rapidly precipitated.

$$R_2SnCl_2 + Na(S_2CNNCS_2).2H_2O \rightarrow [-Bu_2SnS_2CNNCS_2-]_n + 2NaCl + 2H_2O \qquad \text{[eqn (b)]}$$

4.3.2. Mass spectrometry

Table 4.3. lists some of the fragments identified in the El (70ev) and CI (isobutene) mass spectra of the triorganotin derivatives of pipdtc. The diorganotin derivatives were not examined by this technique because of their involatile nature.

Parent peaks ($P^{\cdot+}$) are absent from all spectra, even under CI conditions. The ligand appears to decompose rapidly in the electron or ionising-gas beam. The only high mass peak identified with any certainty was the $P^{\cdot+}$-methyl peak for $(Me_3Sn)_2$pipdtc. Because the ligand fragments in a complex fashion it is difficult to assign structures accurately. Ditin peaks are found in the CI spectra of all derivatives but only in the EI spectra of $(Me_3Sn)_2$pipdtc.

Along with expected R_3Sn^+ and RSn^+ peaks certain other fragment types are common to all spectra. Sulphur bridged ditin species such as $R_3SnSSnR_2^+$ are found in nearly all the spectra and fragments containing a tin-nitrogen bond such as $MeSn\overset{S}{\underset{S}{NN}}SnMe^+$ are found in the spectra of the Me_3Sn- and Cy_3Sn-derivatives. These latter fragments could arise from a reaction involving the elimination of CS_2 which would be a reversal of the known insertion reaction shown in eqn (c).

$$R_3SnNR'_2 + CS_2 \rightarrow R_3SnS_2CNR'_2 \qquad \text{[eqn (c)]} \quad (177)$$

Another very common fragment is the monotin species $R_2SnS_2CNNH^+$ found in all but two spectra [$(Cy_3Sn)_2$pipdtc and $(Bu_2ClSn)_2$pipdtc].

It was possible to identify several chlorine containing fragments ($SnCl^+$, Bu_2SnCl^+) in the spectrum of the by-product from the reaction of Bu_2SnCl_2 and Na_2pipdtc.$2H_2O$ which rationalises its formulation as $(Bu_2ClSn)_2$pipdtc.

Table 4.3. Suggested assignments for mass spectral fragments of organotin derivatives of pipdtc

$(Me_3Sn)_2$pipdtc (70eV)

m/e	abundance(%)	assignment
551	60	$Me_3SnS_2CNNCS_2SnMe_2^+$
475	17	$Me_3SnS_2CNNSnMe_2^+$
355	23	$HMeSnNNSnMe^+$
347	30	$Me_3SnSSnMe_2^+$
311	28	$Me_2SnS_2CNNH^+$
185	7	$HSnS_2^+$
183	16	Me_2SnSH^+
165	100	Me_3Sn^+
135	24	$MeSn^+$
120	7	Sn^+

$(Ph_3Sn)_2$pipdtc

657	trace	$Ph_3SnSSnPh_2^+$
435	trace	$Ph_2SnS_2CNNH^+$
351	4	Ph_3Sn^+
309	4	? monotin
197	3	$PhSn^+$
120	2	Sn^+

Table 4.3. contd.

$(Bu_3Sn)_2$pipdtc

m/e(CI)	abundance(%)	m/e (EI, 70ev)	abundance	assignment
743	2	-	-	? ditin
615	7	-	-	$Bu_3SnSC(N)SSnBu_2^+$
599	4	-	-	$[Bu_3SnS(C)SSnBu_2-2H]^+$
557	2	-	-	$Bu_3SnSSnBu_2^+$
541	2	-	-	? ditin
395	8	-	-	$Bu_2SnS_2CNNH^+$
347	6	347	3	? monotin
291	100	291	25	Bu_3Sn^+
177	3	177	50	$BuSn^+$
155	1	155	20	H_3SnS^+
121	1	121	20	HSn^+
-	-	269	100	$H_2BuSnS_2CN^+$
-	-	235	24	$BuSnSCN^+$
-	-	213	28	H_3SnSCN^+
-	-	120	10	Sn^+

Table 4.3 (contd)

$(Cy_3Sn)_2pipdtc$

m/e (CI)	abundance(%)	m/e (EI,70ev)	abundance (%)	assignment
796	2.5	-	-	? ditin
769	2	-	-	$[Cy_3SnSSnCy_3\text{-}H]^+$
514	2	-	-	? monotin
401	8	401	6.5	Cy_3SnS^+
369	15	369	1	Cy_3Sn^+
203	1	203	18	$CySn^+$
		331	3	Cy_2SnSCH^+
		321	9	$SnNNSnH^+$
		287	3	Cy_2SnH^+
		235	2	$CySnS^+$
		120	2	Sn^+

$(Bu_2ClSn)_2pipdtc$

573	1	-	-	? ditin
325	1.5	-	-	$Bu_2SnS_2CNH^+$
269	100	269	2	Bu_2SnCl^+
185	3	-	-	$HSnS_2^+$
177	2	177	15	$BuSn^+$
120	1.2	120	2	Sn^+
-	-	247	7	$H_2ClSnS_2CN^+$
-	-	155	6.2	$SnCl^+$

4.3.3. Vibrational spectroscopy

The position of selected bands in the i.r. and Raman spectra of the derivatives of pipdtc are given in Tables 4.4 and 4.5.

The band assigned to ν(C=N) is due to the significant contribution of canonical form III in Fig. 4.2 to the overall structure of the dithiocarbamate (175).

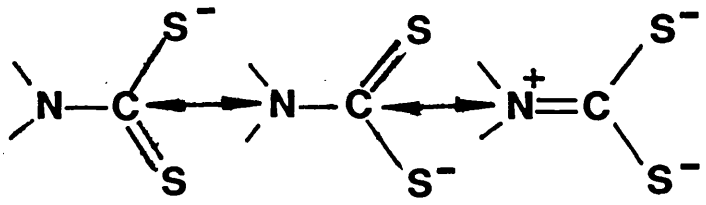

Fig. 4.2. I II III

This band, found at 1461cm^{-1} in the free ligand, is difficult to assign in some derivatives due to the presence of other bands in this region such as ν(C···C) for phenyltins, which occur at around 1475cm^{-1} (178). Octyl and butyltins also have bands in this region. In $(Me_3Sn)_2$pipdtc and Me_2Snpipdtc the vibration can be more confidently assigned to the bands at 1470cm^{-1} and 1480cm^{-1}. O'Connor et al (179) found that if a dithiocarbamate chelates a metal atom then the ν(C=N) band

moves to a higher frequency (greater than 1480cm^{-1}). If it remains monodentate then the band is found at a lower frequency. $Zn(S_2CNEt_2)_2$ exhibits ν(C=N) at 1501cm^{-1} (176) and is considered bidentate as are $RSn(S_2CNEt_2)_3$ and $RClSn(S_2CNEt_2)_2$ (R = Me, Bu, Ph) in which the vibration is usually found above 1500cm^{-1} (180). In the derivatives studied here, where other bands interfere in the ν(C=N) region, the fact that this vibration has not shifted to any great extent favours a monodentate or very anisobidentate chelating arrangement.

The region around 1000cm^{-1} also gives information on whether the $-NCS_2$ unit is behaving in a mono- or bidentate fashion. Bonati and Ugo (176) found that bidentate $Zn(S_2CNEt_2)_2$ exhibits only one band in this region at 995cm^{-1} whereas the unequivocally monodentate Et_2NCS_2Et shows a doublet (1005cm^{-1} and 983cm^{-1}). One of the bands in this doublet is assigned to uncomplexed ν(C=S) (176). Interference in this region from other bands again makes assignments difficult. Phenyltins exhibit in-plane C-H deformation modes in this region (178), whilst some of the alkyltins show a band due to $-CH_2-$ twisting (176). Methyltins are relatively free from interference in this region and both the di- and trimethyltin derivatives show a doublet in this region, in agreement with Bonati and Ugo's criterion for monodentate bonding. The cyclohexyl and phenyltin derivatives show three bands in this region two of which may correspond to the expected doublet.

Table 4.4 I.R. and Raman data for triorganotin derivatives of pipdtc (cm^{-1})

Assignment	Na_2pipdtc.$2H_2O$	$(Me_3Sn)_2$pipdtc	$(Bu_3Sn)_2$pipdtc	$(Cy_3Sn)_2$pipdtc	$(Ph_3Sn)_2$pipdtc
ν(C···N)	1461m	1470m	1465m	1460m	1460m
$-CH_2-$ scissors	1420s	1425s	1418s	1412s	1415s
ligand bands	1265s	1270s	1280s	1270s	1272s
"	1211s	1218s	1215s	1200s	1218s
"	1150m	1160m	1160m	1148m	1153m
ν(C=S)		1032m	1020m	1000m	1020m
"	1002vs br	998s	990s	990s, 980s	998s, 9985m
-C(S)=S	900s	910s	910s	915s	912s
Sn-Me rock		775s			
ν_{asym}(Sn-C)		548s (540m)*			
ν_{sym}(Sn-C)		514m(516vs)*			
ν(Sn-S)		382m	380w	377w	380w

vs = very strong
s = strong
m = medium
w = weak
br = broad
* values in brackets obtained from Raman spectroscopy

Table 4.5. I.R. data for diorganotin derivatives of pipdtc (cm^{-1})

Assignment	Na_2pipdtc.$2H_2O$	$(ClBu_2Sn)_2$pipdtc	Me_2Snpipdtc*	Bu_2Snpipdtc*	Ph_2Snpipdtc*	Octyl$_2$Snpipdtc*
ν(C⋯N)	1461m	1470m	1480m	1465m	1475m	1465m
$-CH_2-$ scissors	1420s	1430s	1420vs	1415s	1425s	1420s
ligand bands	1265s	1270s	1270s	1275s	1274s	1270s
"	1211s	1225s	1215s	1211s	1215s	1210s
"	1150m	1166m	1150m	1155m	1150m	1155m
ν(C=S)		1025m	1020m	1025m	1035m	1025m
"	1002vs.br	1000s	995s	999s	1008m, 995m	995s
-C(S)=S	900s	912s	912s	912s	912s	912s
Sn-Me rock			780vs			
ν_{asym}(Sn-C)			550s (556m)$^+$			
ν_{sym}(Sn-C)			515m (519s)$^+$			
ν(Sn-S)		390m	360m	368m	385w	360m

vs = very strong
s = strong
m = medium
br = broad

* Some bands in R_2Snpipdtc derivatives are exceptionally broad

Raman$^+$.

Both symmetric and asymmetric ν(Sn-C) stretches are observed in the i.r. and Raman of the methyltin derivatives, though ν_{asym} is much stronger in the i.r. This indicates that the Sn atom and methyl groups are not co-planar and therefore rules out the possibility of a bridged structure with a trans-R_3SnS_2 geometry. A tetrahedral or cis-R_3SnS_2 (or an intermediate) geometry could both explain the observed i.r. results. $Me_3SnS_2CNMe_2$ for example was found to exhibit both ν_{asym}(Sn-C) (546cm^{-1}) and ν_{sym}(Sn-C) (526cm^{-1}) in the i.r. (181) and was shown by X-ray diffraction studies to have a tetrahedral geometry distorted slightly towards cis-R_3SnS_2 by a long secondary Sn.....S bond (3.16Å) (167).

Sn-S vibrations were found in the range 360-390cm^{-1} which is in good agreement with values obtained for other organotin dithiocarbamates such as $R_2Sn(S_2CNEt_2)_2$ and $R_2XSn(S_2CNEt_2)$ (R = Me, i-Pr, n-Bu, Ph, X = halogen) which exhibit ν(Sn-S) in the 364-392cm^{-1} region (182).

4.3.4. N.m.r. spectroscopy

N.m.r. data for these compounds is given in Table 4.6. No n.m.r. results were obtained for the R_2Snpipdtc derivatives because of their insolubility in all solvents.

In the n.m.r. spectra of a series of Me_2NCS_2- complexes of ruthenium (179) which contained monodentate dithiocarbamate ligands δ-CH_2-N was found at 2.76 - 2.78ppm, whereas bidentate ligands exhibited δ-CH_2-N at 3.25 - 3.50ppm. The more downfield chemical shift for the methylene protons in the bidentate ligand is

explained by a greater contribution of canonical form III. The quaternary nitrogen present in this structure leads to a deshielding of the adjacent methylene protons.

Results for the compounds reported here show a shift upfield with respect to the free ligand on coordination indicating a lesser role for canonical form III though not necessarily an absence of chelation. Other organotin derivatives of dithiocarbamates show quite similar values of δ-CH_2-N whether the ligand behaves in a mono- or bidentate fashion. $Me_3SnS_2CNMe_2$ which has distinct C-S(1.80Å) and C=S (1.70Å) bonds (167) for example exhibits δ CH_2-N at a similar position [3.48ppm (180)] to $Ph_2Sn(S_2CNEt_2)_2$ [3.45ppm (183)] which has four almost equivalent C-S bonds (1.72 - 1.76Å) (33).

More definite proof of a tetrahedral configuration in solution comes from the $^2J(^{119}Sn\text{-}C\text{-}^1H)$ value of 58Hz for $(Me_3Sn)_2$pipdtc, which is in good agreement with the value of 57Hz found for $Me_3SnS_2CNMe_2$ (180). May et al. (180) consider this to represent 27% s-character in the bonds from tin to carbon which is consistent with the sp^3 hybrid orbitals used in a tetrahedral structure. This does not, however, necessarily mean that the compound adopts the same geometry in the solid state.

Table 4.6

N.m.r. data for organotin derivatives of pipdtc

Compound	Solvent	δ $-CH_2-N$ (ppm)	δ CH_3Sn (ppm)	$^2J(^{119}Sn-C-'H)$ (Hz)
$Na_2pipdtc.2H_2O$	D_2O	4.52s		
$(Bu_2ClSn)_2pipdtc$	$CDCl_3$	4.08s		
$(Bu_3Sn)_2pipdtc$	$CDCl_3$	4.25s		
$(Me_3Sn)_2pipdtc$	$CDCl_3$	4.29s	0.64	58
$(Cy_3Sn)_2pipdtc$	$CDCl_3$	4.39s		

4.3.5. Mössbauer spectroscopy

Isomer shift and quadrupole splitting values are given in Table 4.7, while variable temperature Mössbauer data is presented in Tables 4.8 and 4.9, and depicted in Fig. 4.3.

Quadrupole splitting values (1.81 - 2.32mms^{-1}) for the triorganotin derivatives are typical of either tetrahedral or cis-R_3SnS_2 geometries about tin (1), and are quite similar to those obtained for the derivatives of mbt, mbo and mbi (Table 3.8, Chapter 3). $(Me_3Sn)_2$pipdtc and $(Ph_3Sn)_2$pipdtc show ΔEq's in good agreement with their dithiocarbamate analogues $Me_3SnS_2CNMe_2$ [2.33mms^{-1} (180)] and $Ph_3SnS_2CNEt_2$ [1.77mms^{-1} (182)] and it is quite probable that they adopt a similar structure i.e. a tetrahedral geometry distorted towards cis-R_3SnS_2 by a long secondary Sn----S approach [3.16Å for $Me_3SnS_2CNMe_2$ (167) and 3.11Å for Ph_3SnS_2CNEt (33)] . The bonding in both the mono- and bis-dithiocarbamates is anisobidentate with one long and one short C-S bond e.g. for $Ph_3SnS_2CNEt_2$ C-S = 1.76Å, and 1.68Å (33).

The ΔEq value for $(Bu_2ClSn)_2$pipdtc (3.13mms^{-1}) indicates a more definite expansion in coordination number above four, and is similar to values found for other $R_2SnClSn(S_2CNR'_2)$ compounds (R = Me, Bu, R' = Me, Et) [2.72 - 3.14mms^{-1} (184)]. The exchange of a Bu group by a Cl atom when compared with $(Bu_3Sn)_2$pipdtc increases the Lewis acidity of the tin atom and chelation by the ligand is more likely as found in $Me_2ClSn(S_2CNMe_2)$ (185), where the two Sn-S bond distances are

closer in length (2.48Å and 2.79Å) and the structure better approximates cis-R_2ClSnS_2 with equatorial R groups.

The other diorganotins with the exception of $Ph_2Snpipdtc$ exhibit ΔEq values of around 3.00mms^{-1}, representing a considerable departure for what would be expected for a tetrahedral R_2SnS_2 system [1.91 - 2.02mms^{-1} (158)]. In these cases the secondary Sn---S interactions must be significant enough to distort the geometry towards octahedral. Analogous dithiocarbamates such as $Me_2Sn(S_2CNMe_2)_2$ (186) and $Me_2Sn[S_2CN(CH_2)_4]$ (33) exhibit such structures with <C-Sn-C opened to 136° and 129.7° respectively and ΔEq's of 3.14mms^{-1} (1) and 2.85mms^{-1} (183). A relationship is known to exist between ΔEq and <C-Sn-C for diorganotins with ΔEq increasing as the angle opens reaching a maximum at 180°C (58). This relationship (see Table 4.7) has been used to calculate possible <C-Sn-C angles for the compounds studied here. For all, except $Ph_2Snpipdtc$ the calculated angles were found to open to 126-129°.

$Ph_2Sn(pipdtc)$ exhibits a much lower ΔEq (2.34mms^{-1}) and this could mean that the geometry about tin in this compound deviates very little from tetrahedral (i.e. long Sn----S bonds), or that it adopts a cis-octahedral geometry. The latter is quite possible as phenyltins, because of their greater electronegativity, have a tendency to adopt cis-configurations. $Ph_2Sn(S_2CNEt_2)_2$ for example has been found by crystallographic studies to adopt a cis-R_2SnS_4 geometry with a Ph-Sn-Ph angle of 101.4° (33), and a

Δ Eq of 1.76mms^{-1} (183). Using the relationship mentioned earlier (58) the <C-Sn-C calculated for Ph_2Snpipdtc is 114° favouring a tetrahedral structure.

The variable temperature plots in Fig. 4.3 highlight the difference in lattice structure between the $(R_3Sn)_2$pipdtc and R_2Snpipdtc systems. The a-value obtained for $(Me_3Sn)_2$pipdtc ($2.12 \times 10^{-2}K^{-1}$) represents a very rapid fall in resonance absorption as the temperature increases, and clearly represents a monomeric lattice as found in $Ph_3SnSnPh_3$ ($a = 2.09 \times 10^{-2}K^{-1}$) (22). Me_2Snpipdtc shows a much shallower slope ($a = 1.58 \times 10^{-2}K^{-1}$) indicating stronger lattice interactions. This is easily explained by the fact that the diorganotin derivatives of this ligand are capable of forming covalently bonded polymers as shown in Fig. 4.5. Compared with other dimethyltin polymers such as Me_2SnO [$a = 0.87 \times 10^{-2}K^{-1}$ (137)] and $Me_2Sn(ONH.CO.Me)_2$ [H - bonded (32), $a = 0.92 \times 10^{-2}K^{-1}$ (137)] data for Me_2Snpipdtc show a relatively steep slope. This can be explained by three factors, firstly the bridging ligand must be quite flexible as the piperazine ring contains sp^3 carbons giving rise to a chair-configuration. Secondly because of the weak secondary Sn---S bonds the tin is held in the polymer by only two long (relative to Sn-O) Sn-S bonds, and finally considering the size of the ligand, propagation of the polymer in a helical fashion [class 3 or 4 (22)] is quite likely, as in $Ph_2Sn(OC_6H_4O)$ which exhibits an a-value of $1.73 \times 10^{-2}K^{-1}$ (22).

Table 4.7.

Mössbauer data (78K) for organotin derivatives of pipdtc (mms^{-1})

Compound	δ	ΔEq	Γ_1	Γ_2	<C-Sn-C[a]
$(Ph_3Sn)_2$pipdtc	1.29	1.81	0.920	0.913	
$(Cy_3Sn)_2$pipdtc	1.54	2.32	1.070	1.050	
$(Me_3Sn)_2$pipdtc	1.31	2.07	0.964	0.937	
$(Bu_2ClSn)_2$pipdtc	1.57	3.13	1.001	1.030	
$(Bu_3Sn)_2$pipdtc	1.46	2.28	1.03	0.98	
Me_2Snpipdtc	1.45	2.94	0.964	0.937	126°
Ph_2Snpipdtc	1.29	2.34	1.040	1.050	114°
Bu_2Snpipdtc	1.57	3.05	1.270	1.230	129°
$Octyl_2$Snpipdtc	1.61	2.99	0.891	0.844	127°

[a] calculated using $|QS| = 4\{R\}[1-3\cos^2\theta\sin^2\theta]^{\frac{1}{2}}$

where $\{Alkyl\} = -1.03 mms^{-1}$, $\{Ph\} = -0.95 mms^{-1}$

and θ = <C-Sn-C (58).

Table 4.8.

Variable temperature Mössbauer Data

for $(M_3Sn)_2$pipdtc

Temperature (K)	A	ln A_T / A_{78}	$\underline{a}(K^{-1})$
78	1.70	0	2.12×10^{-2}
85	1.54	-0.099	correlation factor = -0.997
90	1.37	-0.218	
95	1.27	-0.291	
100	1.10	-0.430	
110	0.89	-0.646	
120	0.71	-0.870	

Table 4.9. Variable temperature Mössbauer Data for $Me_2Sn(pipdtc)$

Temperature (K)	A	$\ln A_T/A_{78}$	a (K^{-1})
78	1.540	0	1.5×10^{-2}
85	1.390	-0.097	correlation factor = -0.999
90	1.300	-0.169	
95	1.170	-0.272	
100	1.110	-0.327	
110	0.950	-0.479	
120	0.790	-0.667	
130	0.685	-0.809	

Figure 4.3. Ln A_T/A_{78} v temperature plots for $(Me_3Sn)_2$pipdtc(○) and Me_2Snpipdtc (●).

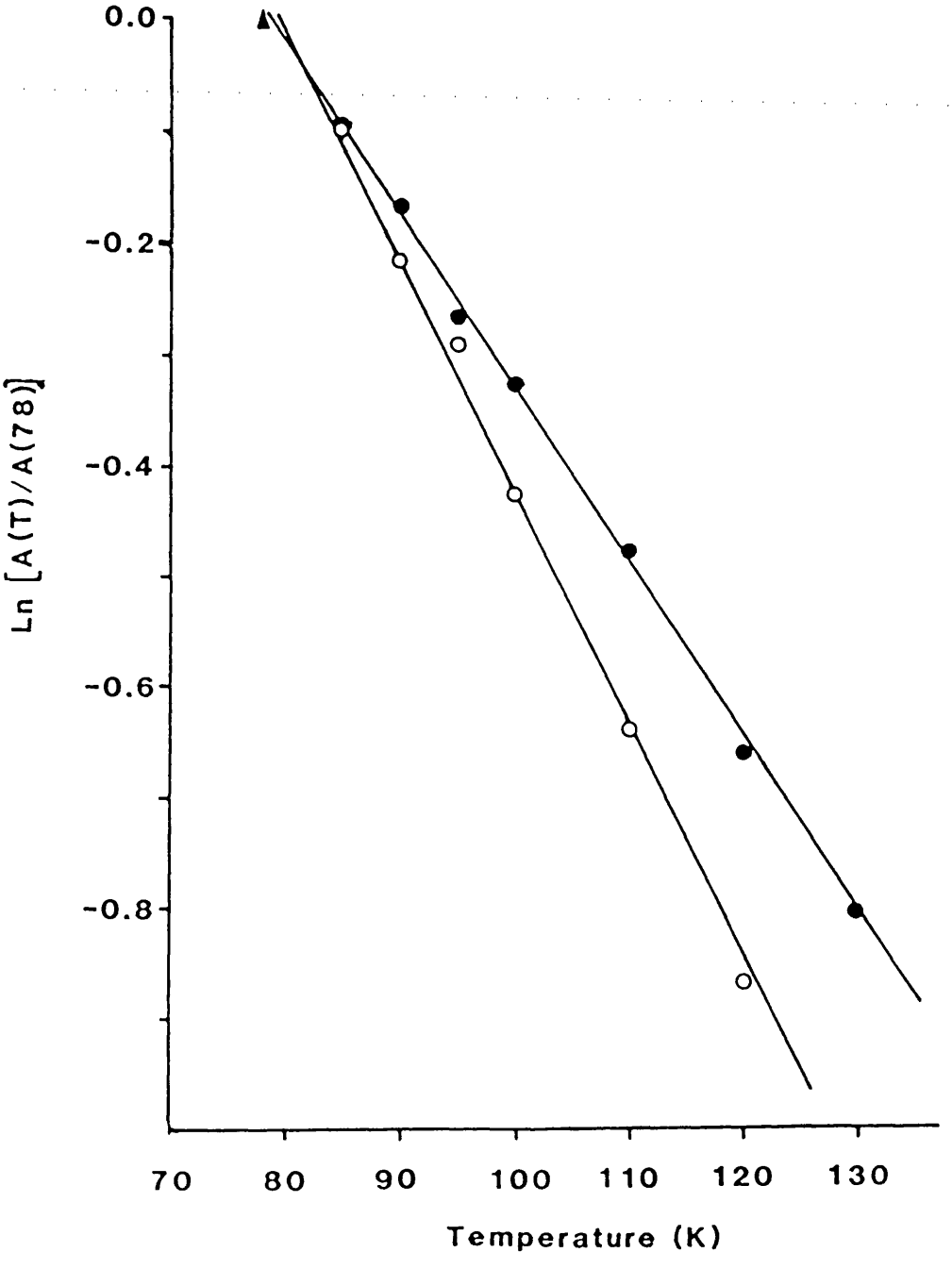

4.4. Conclusions

As no suitable crystals were obtained for diffraction studies, assigning structures for these compounds with certainty is quite difficult, especially as information from i.r. and n.m.r. spectroscopies is limited. N.m.r. data for $(Me_3Sn)_2$pipdtc quite clearly indicates four coordination, but this may only occur in solution. Mössbauer results agree quite well with those obtained for analogous mono-dithiocarbamate compounds, and structural assignments are based on comparisons with known organotin dithiocarbamate structures (167, 33, 185, 186).

The triorganotin derivatives should form ditin species (supported by mass spectrometry) and spectroscopy indicates structures in which the tin atom is in a tetrahedral geometry distorted towards *cis*-R_3SnS_2 by a long secondary Sn---S interaction (Fig. 4.4). $(Bu_2ClSn)_2$pipdtc should have a similar structure but with greater distortions towards five coordination due to the increased Lewis acidity of the tin atom.

The R_2Snpipdtc derivatives (Fig. 4.5) appear to all form covalently linked polymeric chains. This is supported by their physical properties, not melting below 200°C and being insoluble in all common solvents. It is also the structure adopted by transition metal complexes of this ligand (175, 187). The arrangement of R groups about tin is distorted-*trans* ($<C-Sn-C<< 180^o$) as shown in Fig. 4.5, except in the case of Ph_2Snpipdtc which should have a near tetrahedral geometry.

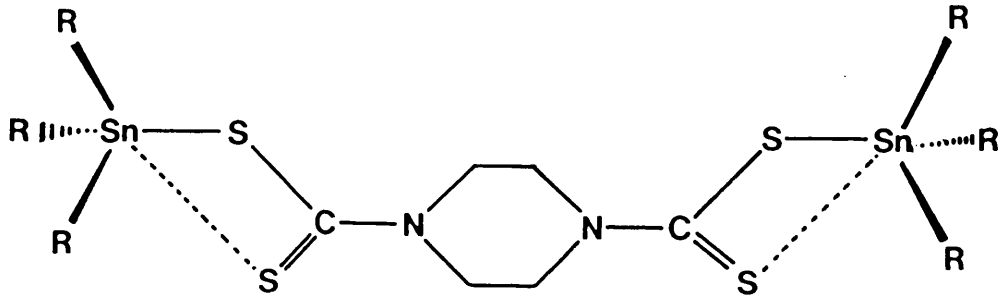

Figure 4.4. Proposed structure for $(R_3Sn)_2$pipdtc compounds

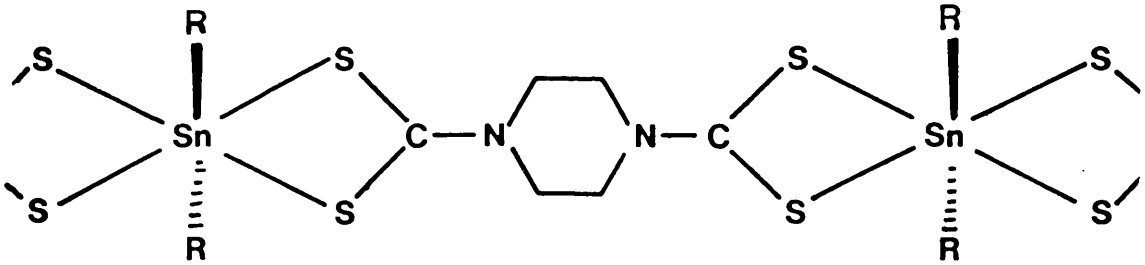

Figure 4.5. Proposed structure for R_2Snpipdtc compounds (R≠Ph).

Chapter Five

Organotin Derivatives of Two Phosphorodiamidic acid analogues

5.1. Introduction

Organophosphorus compounds are the single most important group of insecticides accounting for almost 20% of the insecticides in use in 1972 (116). As a result there has been much interest in organotin derivatives of organophosphorus ligands and several such compounds have been patented (188) [e.g. $Cy_3SnS_2P(OPr)_2$].

The ligands studied in this chapter N,N,N',N' tetraethyl-phosphorodiamidic acid (TEPA) and NN' diphenylphosphorodiamidic acid (DPPA) are shown in Figure 5.1. The triphenyltin derivative of both these ligands and the tributyltin derivative of TEPA have been reported before in the literature by Kubo (189) who tested them for biocidal activity and found them to be active against fungi, slightly phytotoxic, but posessing no pesticidal activity. No structural or spectroscopic work was carried out on these compounds however.

The biocidal effect of organophosphorus insecticides is due to their bonding to Acetylcholinesterase an enzyme important in the transmission of nerve impulses. They form a relatively long-lived substrate-enzyme complex which disrupts the normal functions of the enzyme i.e. the deacetylation of acetylcholine.

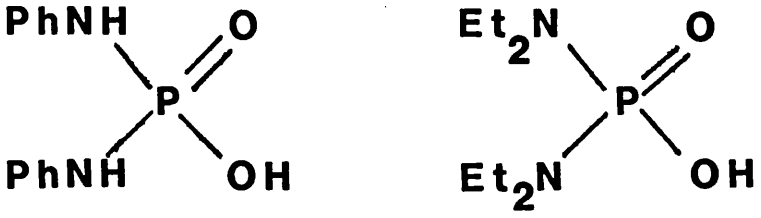

Figure 5.1. (a) TEPA (b) DPPA

5.2. Synthesis

Organotin starting materials were obtained as described in Appendix I. N,N' diphenylphosphorodiamidic chloride was prepared by the method of Cook et al. (190), using aniline and phosphorus oxychloride as starting materials. The product was hydrolysed using potassium hydroxide in ethyl methyl ketone (189). N,N,N',N' tetraethylphosphorodiamidic chloride was prepared by the method of Kubo (189) from diethylamine and phosphorus oxychloride and was purified by distillation.

Ph_3Sn(TEPA) and Bu_3Sn(TEPA) were prepared by the method of Kubo (189), except that in the synthesis of the latter Bu_3SnCl was added to the reaction mixture as an ethanolic solution and an oil was initially obtained which gave a solid on recrystallisation from ethanol. Ph_3Sn(DPPA) and Cy_3Sn(DPPA) were synthesised by a reaction of the type described in method (a), while Me_3Sn(DPPA) and Me_3Sn(TEPA) were synthesised by a reaction analogous to that used by Kubo (189) to synthesise Bu_3Sn(TEPA) and described in method (b).

Method (a): Ph_3SnOH (2.0g, 5.4mmol) was dissolved in hot toluene (80mls) and to this was added $(PhNH)_2P(O)OH$ (1.35g, 5.4mmol). The reaction mixture was refluxed for two hours and water formed removed using a Dean and Stark apparatus. On cooling a white solid rapidly precipitated which was collected and dried to yield 2.20g (60%) of product.

Method (b): To a suspension of $(PhNH)_2P(O)Cl$ (1.74g, 6.5mmol) in water (30mls) was added a solution of KOH (0.80g, 14.5mmol) in water (5mls). The mixture was heated gently with stirring for 10 mins and then left stirring overnight. To the aqueous solution of $K^{+-}O_2P(NHPh)_2$ thus generated was added trimethyltin chloride (1.30g, 5.4mmol) in water (40mls) with vigorous stirring. A white solid immediately precipitated which was filtered off after 30 mins, to yield 2.14g, (83%) of product which was recrystallised from ethanol.

The conditions for individual reactions are described in Table 5.1 while physical data for the compounds synthesised are contained in Table 5.2.

5.3. Results and Discussion

5.3.1. Synthesis

The phosphorodiamidic chlorides were both synthesised by an nucleophilic substitution of R_2N^- for Cl in $POCl_3$ (eqn [1] and [2])

Table 5.1. Reaction conditions for the synthesis of organotin derivatives of TEPA and DEPA

Starting Materials	Solvent	Reaction time	Recrystallisation solvent	Yield %	Product
Ph_3SnOH(5.4mmol) $(PhNH)_2P(O)OH$ (5.4mmol)	toluene	2hrs	*	60	Ph_3Sn(DPPA)
Me_3SnCl(6.5mmol) $(PhNH)_2P(O)Cl$ (6.5mmol) KOH (14.5mmol)	H_2O	30 mins	EtOH	83	Me_3Sn(DPPA)
Cy_3SnOH(4mmols) $(PhNH_2)_2P(O)OH$ (4mmols)	toluene	1½ hrs	EtOH	57	Cy_3Sn(DPPA)
Ph_3SnCl(3.4mmol) $(Et_2N)_2P(O)Cl$ (3.4mmol) KOH(7mmol)	H_2O/acetone	30 mins	*	65	Ph_3Sn(TEPA)
Me_3SnCl(5.1mmol) $(Et_2N)_2P(O)Cl$ (5.2mmol) KOH (11mmol)	H_2O	30 mins	EtOH/Et_2O	55	Me_3Sn(TEPA)
Bu_3SnCl(5.1mmol) $(Et_2N)_2P(O)Cl$ (5.2mmol) KOH(10.5mmol)	H_2O/EtOH	15 mins	EtOH	56	Bu_3Sn(TEPA)

* unable to recrystallise due to insolubility in all common solvents.

Table 5.2.

Physical Data for Organotin derivatives of phosphoradiamidic acid analogues

Compound	m.p. (°C)	Calculated(%)			Found(%)		
		C	H	N	C	H	N
Ph_3Sn(TEPA)	235d[a]	56.04	6.33	5.03	55.1	6.40	4.90
Bu_3Sn(TEPA)	154-155[b]	48.31	9.51	5.63	48.23	9.51	5.50
Me_3Sn(TEPA)	d > 230	35.61	7.88	7.55	35.52	7.75	7.51
Ph_3Sn(DPPA)	228-230[c]	60.33	4.56	4.69	59.30	4.70	4.69
Cy_3Sn(DPPA)	204-208d	58.56	7.37	4.55	59.30	7.50	4.54
Me_3Sn(DPPA)	180-182	43.83	5.15	6.81	43.91	5.28	6.88

(a) lit. m.p. >250°C Kubo(1)

(b) lit. m.p. 151 - 153°C Kubo (1)

(c) lit. m.p. 187 - 189°C Kubo (1)

$$4\ Et_2NH + POCl_3 \rightarrow (Et_2N)_2P(O)Cl + 2\ Et_2NH_2Cl \qquad [1]$$

$$4\ PhNH_2 + POCl_3 \rightarrow (PhNH)_2P(O)Cl + 2\ PhNH_3Cl \qquad [2]$$

Excess $PhNH_2$ is used to act as an acceptor for the hydrogen chloride produced and the reaction proceeds in two steps (191) as supported by the detection of some phosphoroamidate dichloride in the synthesis of $(Et_2N)_2P(O)Cl$. This was easily removed by exposure to more Et_2NH and further distillation. The first (eqn. [3]) step should be faster as the Lewis acidity at phosphorus is reduced for the second step (eqn. [4]).

$$2\ R_2NH + POCl_3 \rightarrow R_2NP(O)Cl_2 + R_2NH_2Cl \qquad [3]$$

$$2\ R_2NH + R_2NP(O)Cl_2 \rightarrow (R_2N)_2P(O)Cl + R_2NH_2Cl \qquad [4]$$

In the case of derivatives of DPPA where the free acid form of the ligand was synthesised by hydrolysis of the P-Cl bond a dehydration reaction with an organotin hydroxide (eqn. [5]) was sufficient to yield a product.

For Me_3Sn(DPPA) and all derivatives of TE A it was necessary to generate the potassium salt of the ligand in situ and then react it with an organotin halide (eqn. [6]).

$$R_3SnOH + (PhNH)_2P(O)OH \rightarrow R_3SnO_2P(NHPh)_2 + H_2O \qquad [5]$$

$$R_3SnCl + (R'R''N)_2P\ O_2K \rightarrow R_3SnO_2P(NR'R'')_2 + KCl \qquad [6]$$

R' = Ph, R'' = H

R' = R'' = Et

5.3.2. Mass spectrometry

Fragments found in the EI (70ev) mass spectra of these compounds, along with suggested structural assignments are given in Table 5.3. Parent ($P^{+\cdot}$) ions are found for both trimethyltin derivatives and for Ph_3Sn(TEPA) and furthermore a ditin species is indicated in the spectrum of Me_3Sn(DPPA) which has an m/e value fitting a structure containing the ligand bridging two tin units. Such a structure suggests that a polymeric lattice may exist in the solid state for this compound and which retains some of its integrity in the gas phase. The fragmentation pattern for this compound is illustrated in Scheme 5.1. Loss of ligand or $Me^{\cdot}$ is the initial step and fragmentation proceeds by further loss of $Me^{\cdot}$ (or C_2H_6) from the tin atom or loss of $PhNH_2$ or biphenyl (Ph_2) from the ligand moiety.

The fragmentation pattern is less obvious for the DPPA derivatives of Ph_3Sn- and Cy_3Sn- as less peaks are found in the mass spectra. Common R_3Sn^+ and R_2Sn^+ fragments are observed however, for both compounds, but contrary to expectations (78) the odd electron ion $Cy_2Sn^{+\cdot}$ is more abundant than the even electron ions Cy_3Sn^+ and $CySn^+$ in the spectrum of Cy_3Sn(DPPA).

In the spectra of the TEPA derivatives, $P^{+\cdot}$ ions are observed for both Me_3Sn- and Ph_3Sn- derivatives whilst for Bu_3Sn(TEPA) $P^{+\cdot}$-Bu is the peak with both the highest m/e and greatest abundancy. Fragmentation yields R_3Sn^+ and RSn^+ ions in high abundance.

Scheme 5.1. Fragmentation pattern for $Me_3Sn(DPPA)$

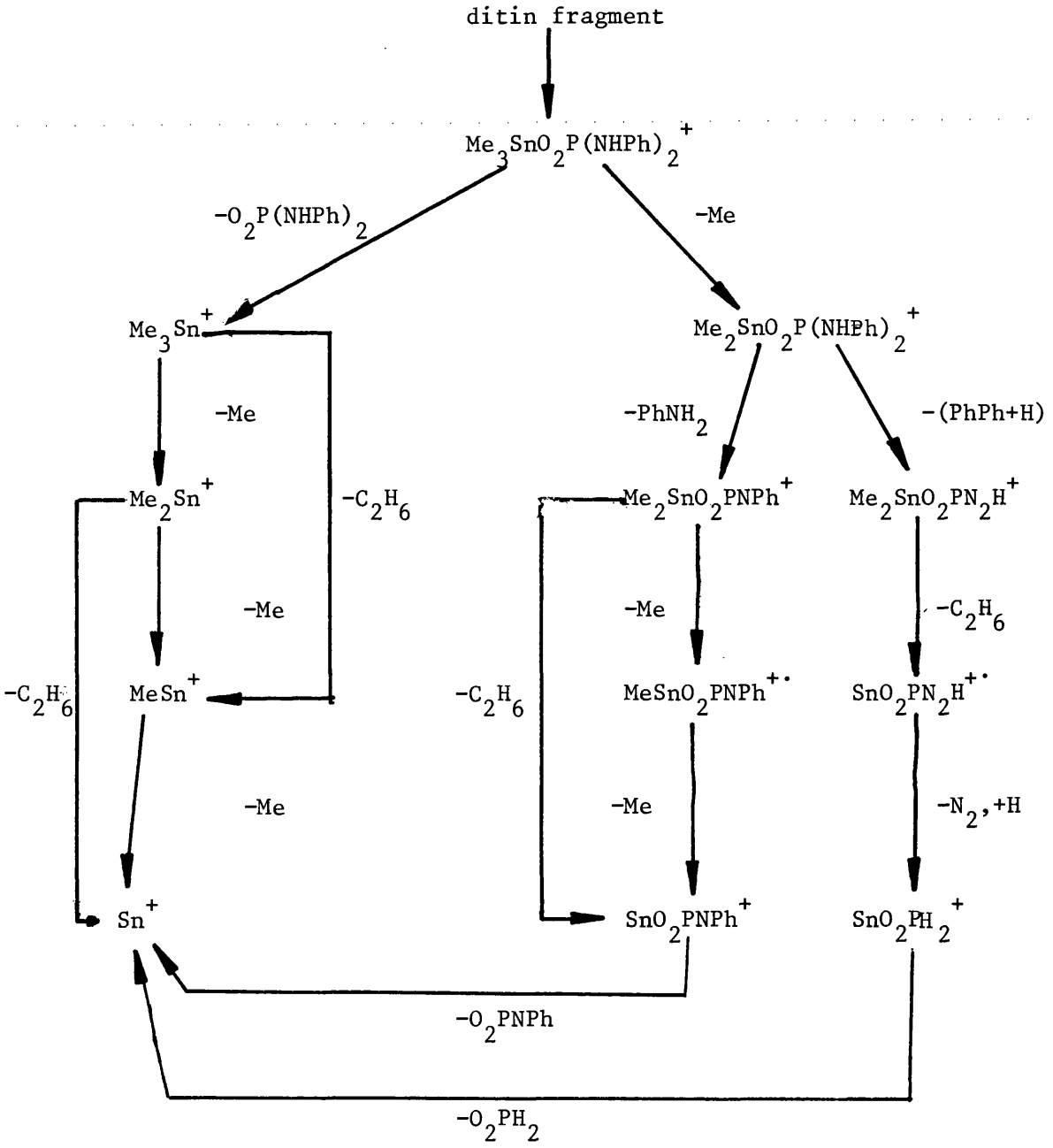

Table 5.3. Mass spectral (EI, 70eV) for organotin derivatives of DPPA and TEPA

Compound	m/e	abundance(%)	assignment
$Me_3Sn(DPPA)$	561	0.8	$[Me_3SnOP(NHPh)_2OSnMe-H]^+$
	412	28.0	$P^{+\cdot}$
	397	100.0	$Me_2SnO_2P(NHPh)_2^+$
	304	42.5	$Me_2SnO_2PNPh^+$
	289	6.3	$MeSnO_2PNPh^{+\cdot}$
	274	7.5	SnO_2PNPh^+
	242	17.4	$Me_2SnO_2PN_2H^+$
	212	24.0	$SnO_2PN_2H^+$
	185	29.9	$SnO_2PH_2^+$
	165	72.8	Me_3Sn^+
	150	15.3	$Me_2Sn^{+\cdot}$
	135	22.2	$MeSn^+$
	120	11.6	Sn^+
$Ph_3Sn(DPPA)$	386	1.0	? monotin
	351	25.0	Ph_3Sn^+
	309	34.0	? monotin
	197	7.5	$PhSn^+$
	154	47.0	Ph_2^+
	120	3.8	Sn^+

Table 5.3. (contd)

Compound	m/e	abundance (%)	assignment
$Cy_3Sn(DPPA)$	452	81.2	$H_2CySnO_2P(NHPh)_2^+$
	369	2.0	Cy_3Sn^+
	367	4.5	$SnO_2P(NHPh)_2^+$
	365	6.9	$Cy_2SnO_2PNH_2^+$
	345	4.5	? monotin
	331	3.2	$[Cy_2SnOP-2H]^+$
	321	3.9	? monotin
	286	79.9	$Cy_2Sn^{+\cdot}$
	228	2.6	? monotin
	222	4.8	? monotin
	203	16.0	$CySn^+$
	121	9.9	SnH^+
	120	6.2	Sn^+
$Me_3Sn(TEPA)$	372	7.7	$P^{+\cdot}$
	357	27.5	$Me_2Sn[O_2P(NEt_2)_2]^{+(a)}$
	343	1.5	$Me_3Sn[O_2P(NEt_2)(NEt)]^+$
	300	28.0	$Me_3SnO_2PNEt_2^+$
	286	23.0	$Me_3SnO_2PNEtCH_3^+$
	165	41.7	Me_3Sn^+
	150	8.4	Me_2Sn^+
	135	7.9	$MeSn^+$
	120	1.7	Sn^+

Table 5.3 (contd)

Compound	m/e	abundance (%)	assignment
$Ph_3Sn(TEPA)$	558	7.4	$P^{+\cdot}$
	543	4.6	$Ph_3SnO_2P(NEt_2)(NEtCH_2)^+$
	527	1.5	$Ph_3SnO_2P(NEt_2)(NEt)^+$
	481	67.6	$Ph_2Sn[O_2P(NEt_2)_2]^+$
	408	8.0	$[Ph_2SnO_2PNEt_2-H]^+$
	351	31.0	Ph_3Sn^+
	332	22.4	$PhSnO_2PNEt_2$
	309	19.7	? monotin
	275	10.8	Ph_2SnH^+
	197	28.2	$PhSn^+$
	120	10.0	Sn^+
$Bu_3Sn(TEPA)$	441	100.0	$Bu_2Sn[O_2P(NEt_2)_2]^+$
	370	38.0	$Bu_2Sn(O_2PNHEt_2)^+$
	327	11.9	$Sn[O_2P(NEt_2)_2]^+$
	291	3.8	Bu_3Sn^+
	256	15.8	$SnO_2PNHEt_2^+$
	235	6.0	Bu_2SnH^+
	177	16.9	$BuSn^+$
	121	5.6	SnH^+

(a) This peak could also be assigned to $Me_3Sn[O_2P(NEt)(NEtCH_2)]^+$

Unlike in the spectrum of $Cy_3Sn(DPPA)$ $R_2Sn^{+\cdot}$ ions are absent or are in low abundance and in the case of the Ph_3Sn- and Bu_3Sn- derivatives of TEPA are replaced by the more stable even-electron ions R_2SnH^+. As well as loss of R groups from the tin atom these compounds fragment by loss of methyl, ethyl and diethylamine groups from the ligand. The peak at m/e = 357 (27.5%) in the spectrum of $Me_3Sn(TEPA)$ can arise from either loss of Me$^\cdot$ from tin or the ligand and probably receives contributions from both. The pattern of losing R groups from the ligand whilst maintaining one or more Sn-C bonds, observed in the mass spectra of the compounds studied here has also been found to occur for the analogous organotins $Me_3SnS_2P(OR_2)$, R = Et, i-Pr (173).

5.3.3. Infra-red spectroscopy

I.r. data for selected bands in the derivatives of DPPA and TEPA are given in Tables 5.4 and 5.5.

The low frequency of ν(N-H) in the uncoordinated form of DPPA has been considered indicative of a zwitterionic form ($RN^+H_2PO_2^-$) for many phosphoroamidates (192). However, a sharp ν(O-H) band at 3365cm^{-1}m is found in the spectrum of this ligand discounting such a structure and instead the low frequency of ν(N-H) can be accounted for by hydrogen-bonding in the lattice involving N-H---O=P. This structure is disrupted, on coordination to an organotin moiety as shown by the shift of ν(N-H) to a higher frequency (ca. 3400cm^{-1}) for all derivatives which is typical of a free N-H group. The disappearance of ν(O-H) and ν(P-OH) bands is consistant with the expected bonding to tin via oxygen.

In DPPA derivatives a drop in the frequency of the $\nu_{asym}(PO_2)$ band with respect to the free acid is observed on coordination, and this is considered to be evidence for the ligand bonding to tin in a bidentate fashion. In TEPA derivatives $\nu_{asym}(PO_2)$ is exhibited at even lower frequencies (1110 - 1145cm^{-1}) than that found for DPPA derivatives (1150 - 1145cm^{-1}), suggesting that in these compounds a strong secondary P=O → Sn bond is also to be expected. Previous work on organotin derivatives of analogous organophosphorus ligands $R_2PO_2^-$ (R = H, Me, C_6H_{13}) have similar values of $\nu_{asym}(PO_2)$ (1134 - 1173cm^{-1}) and $\nu_{sym}(PO_2)$ (1046 - 1067cm^{-1}) and in all cases the authors considered this to be evidence for the ligand behaving in a bidentate, bridging fashion (193 - 195).

As a cis-bidentate structure would lead to a similar drop in the frequency of $\nu_{asym}(PO_2)$, information from the Sn-C stretching region was crucial to determining whether a planar SnC_3 unit had been formed. Chivers et al (194, 195) and Ridenour and Flagg (193) report that the ν_{sym}(Sn-C) bond is absent in the i.r. spectra of methyltin derivatives of $R_2PO_2^-$ (R = H, Me, C_6H_{13}). This band was found in the Raman spectra of $Me_3SnO_2PH_2$ at 519cm^{-1} (195) and at 500cm^{-1} for $Me_3SnO_2PMe_2$ (193). This was considered further evidence for a bridged polymeric structure. In the compounds studied here a band assignable to ν_{asym}(Sn-C) is found at 550cm^{-1} for Me_3Sn(TEPA) and 552cm^{-1} for Me_3Sn(DPPA). For Me_3Sn(DPPA) two medium bands are found at 530 and 505cm^{-1} assignable to ν_{sym}(Sn-C) but as these occur in all derivatives they may be due to ligand vibrations. For Me_3Sn(TEPA), however,

the Raman spectra shows a shift in the 505w (i.r.) band to 514cm^{-1} accompanied by a considerable increase in intensity. This band is assigned to ν_{sym}(Sn-C) while the band found at 550cm^{-1}m in the Raman is assigned to the asymmetric stretch. The reversal of intensities on going from i.r. to Raman is considered to be an indication of a SnC_3 unit approaching planarity, which is consistent with a bridging mode for the ligand.

Strong bands at around 1170cm^{-1} and 1025cm^{-1} in TEPA derivatives have been assigned in the literature (192) to be related to the Et_2N-P group and in the case of the triphenyltin derivative one of these bands appears to coincide with $\nu_{sym}(PO_2)$.

Solution i.r. studies on the soluble derivatives of these ligands (see Table 5.4 and 5.5) show very little change in the position of (PO_2) related bands with respect to the solid state indicating that the same structure exists in both phases. The low frequency of these bands in both solid and solution phase studies rules out a tetrahedral geometry about tin with a monodentate ligand, leaving <u>cis</u>-R_3SnO_2 and <u>trans</u>-R_3SnO_2 as the most viable structural options. The later structure would have to be polymeric as the ligand is unable to span both axial sites but an associated lattice would also be expected to dissociate into monomers upon dissolution and therefore show a shift in $\nu_{asym}(PO_2)$ to higher frequencies in solution. This strengthens the case for a <u>cis</u>-R_3SnO_2 configuration but the possibility of a cyclic oligiomeric structure as found for the related compound $Ph_3SnO_2P(OPh)_2$ (196) cannot be ruled out.

Table 5.4. I.R. data for organotin derivatives of N'N' diphenylphosphorodiamidic acid

Assignment	$(PhNH)_2P(O)OH$ (cm^{-1})	$Ph_3Sn(DPPA)$ (cm^{-1})	$Cy_3Sn(DPPA)$ (cm^{-1})	$Me_3Sn(DPPA)$ (cm^{-1})
ν(O-H)	3365m;n	absent	absent	absent
ν(N-H)	3320,3150m,br	3360m	3430,3440m	3410,3390m
			(3420m)	(3400m)
$\nu_{asym}(PO_2)$	1215s	1150s	1175s	1160s
			(1170s)	(1160s)
$\nu_{sym}(PO_2)$	980s	1070s	1060s	1070s
			(1065m)	(1060s)
νP-OH	960s	absent	absent	absent
ν_2P-N-C	920s	930s	930s	930s
			(920s)	(920s)
ν_{asym}Sn-C				552m
		530m	530m	530m
		505m	505m	505m
(PO_2) bend	460m	455m	420vw	450vw

Values in brackets are from solution studies ($CHCl_3$).

asym: asymmetric

sym: symmetric

s: strong

m: medium

n: narrow

br: broad

v.w.: very weak

Table 5.5. I.R. data for organotin derivatives of N,N,N',N' tetraethylphosphorodiamidic acid

Assignment	$(Et_2N)_2P(O)Cl$ (cm^{-1})	Ph_3Sn(TEPA) (cm^{-1})	Bu_3Sn(TEPA) (cm^{-1})	Me_3Sn(TEPA) (cm^{-1})
ν(P=O)	1250s	absent	absent	absent
	1170s	1185m	1190s	1175s
$\nu_{asym}(PO_2)$		1110s	1135s	1145s
			(1155,1140s)	(1150s)
$\nu_{sym}(PO_2)$		1025s	1050s	1050s
			(1050s)	(1050s)
	1025s	1025s	1020s	1025s
ν_{asym}Sn-C				550s(550m)[a]
		520m	510m	510w(514s)[a]
(PO_2) bend		460m	460sh	470sh

asym: asymmetric

sym: symmetric

s: strong

m: medium

sh: shoulder

w: weak

Values in brackets are for solution ($CHCl_3$) studies except, [a] Raman (solid state).

5.3.4. N.m.r. spectroscopy

H^1 n.m.r. data for some of the compounds under investigation are given in Table 5.6. The $^2J(^{119}Sn\text{-}C\text{-}^1H)$ coupling constants are quite large for both trimethyltin derivatives showing a significant increase over those found for $Me_3Sn(mbt)$ (58.8Hz) and $(Me_3Sn)_2pipdtc$ (58Hz) (Chapters 3 and 4 respectively) which were considered to be tetrahedral. The increase in $^2J(^{119}Sn\text{-}C\text{-}^1H)$ represents an expansion in coordination from four to five, with the SnC_3 unit moving towards a planar configuration. A similar coupling constant was found for the analogous compound, $Me_3SnO_2P(OPh)_2$ (73Hz) which was claimed to be five coordinate in solution (196). $Me_3Sn(DPPA)$ shows an identical coupling constant in d^6 acetone and $CDCl_3$ indicating that the acetone molecule does not coordinate the tin atom though a shift in $\delta(\underline{NH})$ may indicate H-bonding of the solvent molecule with this portion of the complex.

A cis-R_3SnO_2 structure could maintain five coordination in solution but could not however, explain the significant increase in percentage s-character over a tetrahedral geometry reflected in the $^2J(^{119}Sn\text{-}C\text{-}^1H)$ values obtained. A typical $^2J(^{119}Sn\text{-}C\text{-}^1H)$ coupling constant for a cis-Me_3SnO_2 system is 54Hz as found for $Me_3Sn(ON.Ph.CO.Ph)$ (197) a compound known to adopt such a configuration in the solid state (135). An extended polymer chain would not be expected to be significantly soluble in the solvents used for n.m.r. experiments so a cyclic oligiomeric conformation becomes an even more plausible (in the light of

Table 5.6. ^{1}H n.m.r. data for organotin derivatives of DEPA and TEPA

Compound	Solvent	Chemical shifts (ppm)	$^{2}J(^{31}P\text{-}NH)$ (Hz)	$^{3}J(^{31}P\text{-}N\text{-}CH)$ (Hz)	$^{2}J(^{119}Sn\text{-}C^{1}\text{-}H)$ (Hz)
$Me_3Sn(DPPA)$	$CDCl_3$	CH_3-Sn; 0.50s	8		72
		NH; 4.62d			
		Ph; 6.80m			
	d^6 acetone	CH_3Sn; 0.52s	8		72
		NH; 6.10d			(72)[a]
		Ph; 6.77m			
$Cy_3Sn(DPPA)$	$CDCl_3$	$-CH_2-$; 1.80m	8		
		NH; 5.18d			
		Ph; 6.98m			
$Me_3Sn(TEPA)$	$CDCl_3$	CH_3Sn; 0.43s		10.5	74
		CH_3; 0.98t			
		$-CH_2-$; 2.78m			
$(Et_2N)_2P(O)Cl$		CH_3; 1.11t		14	
		CH_2; 3.05m			

m; multiplet; d: doublet; s: singlet; t: triplet.

[a] same sample diluted by half.

i.r. data) structural assignment for solid and solution phases of these compounds. The insolubility of Ph_3Sn- derivatives may indicate that these compounds adopt extended linear polymeric structures.

The methylene protons of the TEPA derivative are split into a complex multiplet consisting of two quartets arising from coupling (6.5Hz) with the methyl protons to give a quartet which is further split by long range coupling to ^{31}P (10.5Hz). An explanation as to why the $^3J(^{31}P\text{-}N\text{-}C\text{-}^1H)$ coupling should be so significant has been offered by Cowley et al (198) who suggested that there may be some π-bonding between nitrogen and phosphorus via contributions of the type $R_2N^+{=}P^-(O)O$. Similar three atom couplings were found for organotin derivatives of $(RO)_2PS_2^-$ (R = Me, Et, Pr, i-Pr, Bu, Ph) (173, 61) where $^3J(^{31}P\text{-}O\text{-}C\text{-}^1H)$ values were found in the range 9.0-15Hz. These coupling constants, however, yield no structural information with regard to the configuration of ligands about tin as shown for $Me_3SnS_2P(Oi\text{-}Pr)_2$ which exhibits the same value (13Hz) in $CDCl_3$ and pyridine whilst the $^2J(^{119}Sn\text{-}C\text{-}^1H)$ coupling increases from 57.5Hz ($CDCl_3$) to 70Hz(pyridine)(173).

5.3.5. Mössbauer spectroscopy

Mössbauer data for derivatives of DPPA and TEPA are given in Tables 5.7 - 5.10 ΔEq values in all cases are indicative of five coordination at tin with ligand donor atoms in a trans- position (1). The possibility of a cis-R_3SnO_2 geometry can now be ruled out, and it seems that all the compounds studied here

adopt some type of polymeric lattice. ΔEq values (3.53 - 4.15mms^{-1}) for triorganotin derivatives of analogous organophosphorus ligands [$H_2PO_2^-$ (195), $Me_2PO_2^-$, $(C_6H_{13})_2PO_2^-$ (193), $(PhO)_2PO_2$ (196), $Ph(PhO)PO_2^-$ (199)] are in good agreement with those reported here (3.35 - 3.91mms^{-1})

Variable temperature Mössbauer data is given in Tables 5.8 - 5.10 and depicted in Figs. 5.2 and 5.3. The $\underline{a}$ value obtained for $Me_3Sn(DPPA)$ ($2.11 \times 10^{-2}K^{-1}$) is quite high for a would be polymer and is quite similar to that obtained for the analogous triphenyltin phosphinate $Ph_3SnO_2PPh_2$ ($\underline{a} = 2.09 \times 10^{-2}K^{-1}$) whose structure was considered to consist of "S"-shaped polymer chains (22). A cyclic oligiomeric structure consisting of only a few monomer units should also lead to enhanced vibrational motion of the tin atom and cause the unit to behave as a monomer. $Ph_3SnO_2P(OPh)_2$ which has been found to adopt a cyclic structure exhibits an $\underline{a}$-value of $1.37 \times 10^{-2}K^{-1}$ (200). This lower value should not rule out a cyclic structure for $Me_3Sn(DPPA)$ however, as different packing factors will exist for triphenyltin compounds.

The $\underline{a}$-value obtained for $Ph_3Sn(DPPA)$ is also quite high ($1.84 \times 10^{-2}K^{-1}$) and is again quite typical of "S"-shaped polymers such as Ph_3SnOAc ($\underline{a} = 1.91 \times 10^{-2}K^{-1}$) (26). We are more reluctant to propose cyclic structures for the triphenyltin derivatives because of their insolubility in common solvents, and the $\underline{a}$-value of $Ph_3Sn(TEPA)$ ($1.33 \times 10^{-2}K^{-1}$) is also considered to represent a long chain polymer structure though in this case due to the lower value of $\underline{a}$, a chain less helical in shape is expected. The structural differences between these two triphenyltins, as

Table 5.7.

Mössbauer data for organotin derivatives of phosphorodiamidic acid analogues

Compounds	δ (mms^{-1})	Δ Eq (mms^{-1})	Γ_1 (mms^{-1})	Γ (mms^{-1})
Ph_3Sn(DPPA)	1.27	3.38	0.904	0.863
Cy_3Sn(DPPA)	1.58	3.91	0.909	0.897
Me_3Sn(DPPA)	1.30	3.73	0.860	0.814
Ph_3Sn(TEPA)	1.23	3.35	0.914	0.884
Bu_3Sn(TEPA)	1.41	3.68	0.862	0.849
Me_3Sn(TEPA)	1.30	3.43	0.924	0.835

Γ = Full-width at half-height of absorption peak

Table 5.8.

Variable Temperature Mössbauer

Spectroscopic data for $Me_3Sn(DPPA)$

Temperature (K)	Area	$\ln A_T/A_{78}$	a (K^{-1})
78	1.881	0	2.11×10^{-2}
85	1.675	-0.116	correlation factor =
90	1.497	-0.228	0.999
95	1.349	-0.332	
100	1.211	-0.440	
110	0.977	-0.655	
120	0.800	-0.855	
130	0.633	-1.081	

Table 5.9.

Variable Temperature Mössbauer

Spectroscopic data for $Ph_3Sn(TEPA)$

Temperature (K)	Area	$\ln A_T/A_{78}$	a (K^{-1})
78	1.531	0	1.33×10^{-2}
85	1.133[a]	-0.075	correlation factor = -0.998
90	1.329	-0.141	
95	0.979[a]	-0.222	
100	1.123	-0.310	
110	0.995[a]	-0.431	
120	0.868	-0.567	
130	0.625	-0.671	

[a] second sample, normalised using $A_{78} = 1.222$

Table 5.10

Variable Temperature Mössbauer data for $Ph_3Sn(DPPA)$

Temperature (K)	Area	ln A_T/A_{78}	a (K^{-1})
78	1.239	0	1.84×10^{-2}
90	1.017	-0.198	correlation factor: -0.998
95	0.674[a]	-0.294	
100	0.871	-0.353	
105	0.574[a]	-0.456	
110	0.703	-0.567	
120	0.597	-0.731	
130	0.472	-0.965	

[a] second sample, normalized using $A_{78} = 0.905$

Figure 5.2. Plots of $\ln A_T/A_{78}$ versus Temperature for $Ph_3Sn(TEPA)$ (○) and $Ph_3Sn(DPPA)$ (●).

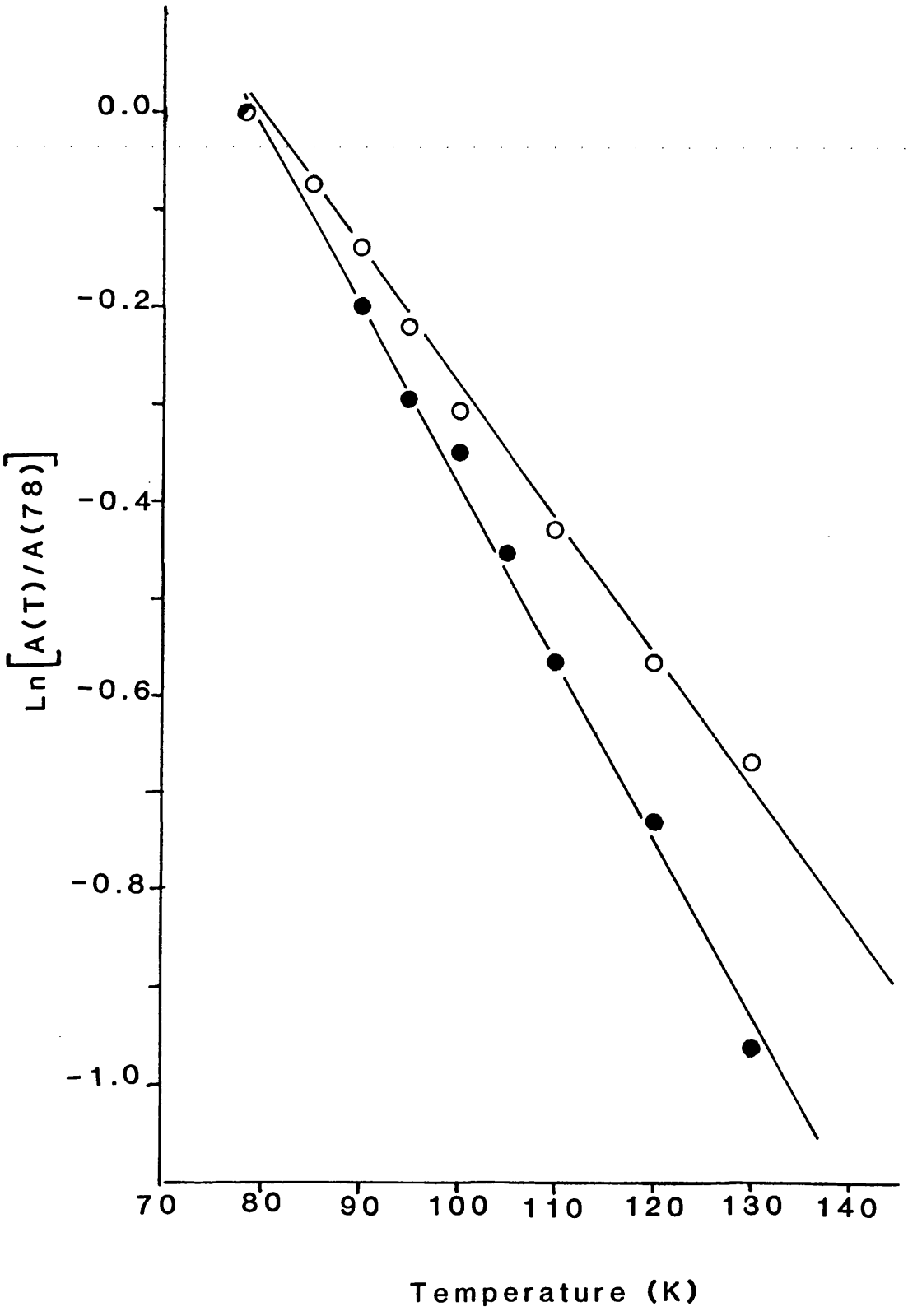

Figure 5.3. Plot of $\ln A_T/A_{78}$ versus temperature for $Me_3Sn(DPPA)$.

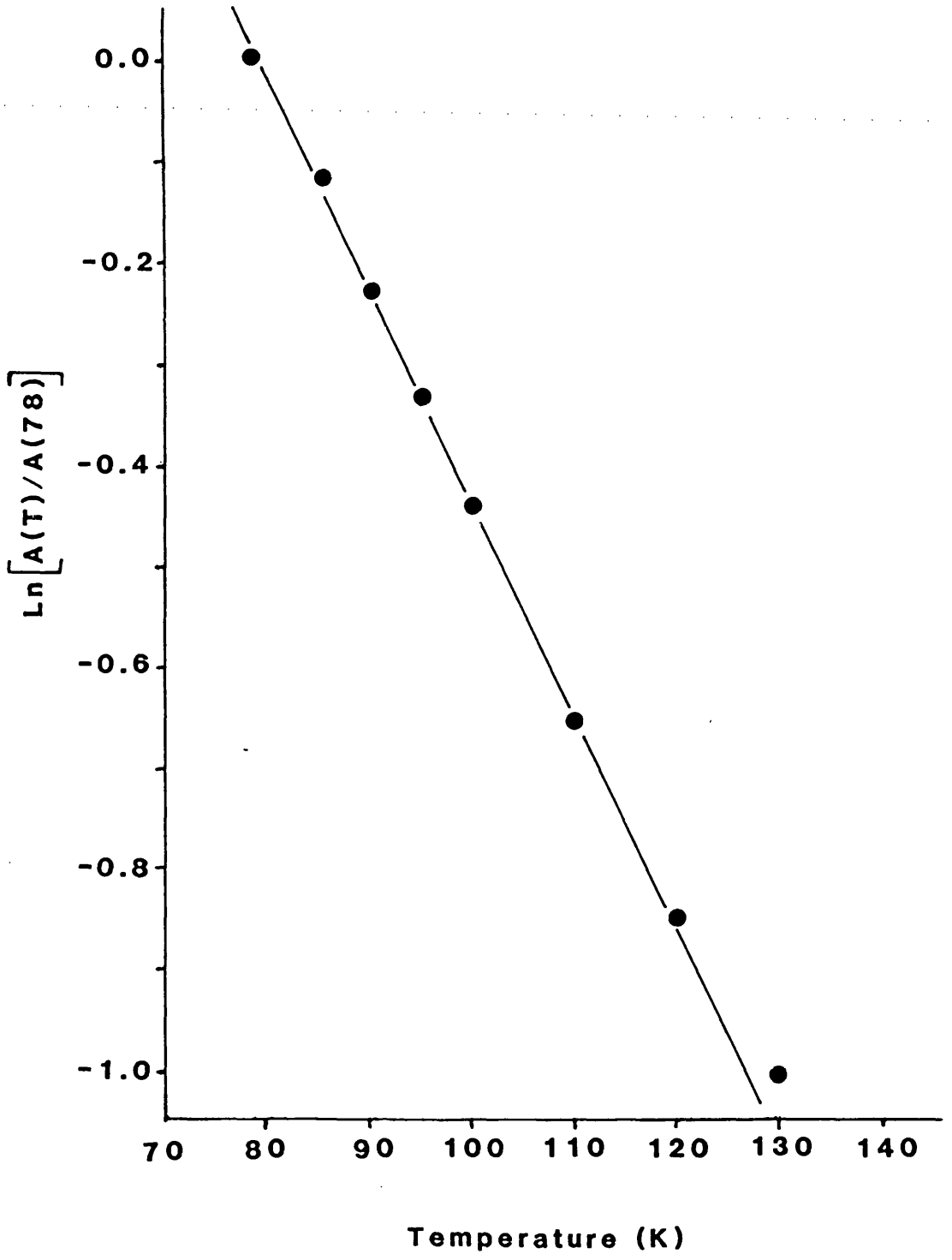

highlighted by variable temperature Mössbauer spectroscopy, may be similar to that found between Ph_3SnOAc and Ph_3SnO_2CH . The former adopts a highly helical structure and exhibits an a-value of $1.91 \times 10^{-2}K^{-1}$ (26) while the latter which exhibits an a-value of $1.15 \times 10^{-2}K^{-1}$ (22) has been found to form polymer chains considerably less coiled in nature (201).

5.4. Structural conclusions

Evidence from i.r. and ^1H n.m.r. for the Me_3Sn derivatives clearly indicates them to be five coordinate polymers in both solution and the solid state. This is corroborated for the solid state by Mössbauer data. The problem is, however, whether the lattice consists of short chain linear polymers or cyclic oligiomers as both would lead to similar spectroscopic behaviour. Ridenour and Flagg (193) propose a linear structure for $Me_3SnO_2PMe_2$ and have determined its molecularity in benzene to be 4.6 and claim to find terminal phosphinato moieties in the ^{31}P n.m.r. Blunden et al (202) also find terminal phosphosphorus atoms in the ^{31}P n.m.r. spectrum of $Bu_3SnO_2PPh_2$ and on the basis of the ratio of this signal to the main ^{31}P resonance estimate a molecularity of 40. Evidence also exists in the literature for cyclic structures, however, such as $Ph_3SnO_2P(OPh)_2$ (196) which forms a hexamer, and since no dissociation occurred on dilution as monitored by ^1H n.m.r. for $Me_3Sn(DPPA)$ (Table 5.6) such a cyclic structure is proposed for this compound. A pentameric structure is most likely as it is the smallest size which would facilitate efficient packing by forming a planar ring (203).

Short chain polymers in the solid state i.e. where n in the generalised formula $[^{-}R_3SnOPO^{-}]_n$ is <20 can be ruled out for all derivatives on the basis that such structures would have >10% terminal tin sites which would exhibit an additional doublet in the Mössbauer spectrum and this is not observed. The structures of all but the triphenyltins are best explained in terms of either cyclic structures or long chain polymers which dissociate into short chain polymers in solution with little change in spectroscopic behaviour. The triphenyltins however, as indicated by their insolubility in all common solvents, most likely adopt a lattice structure consisting of long chain polymers in which the $-PO_2-$ forms strong bridges between tin sites and O-P-O, and O-Sn-O bonding should be close to isobidentate [e.g. in $Ph_3SnO_2P(OPh)_2$ (193) Sn-O = 2.234(15)Å; P-O = 1.487(12)Å]. From variable temperature Mössbauer work it is apparent that some coiling of the polymer must exist for both compounds but less so in the case of $Ph_3Sn(TEPA)$.

Chapter Six

Organotin Derivatives of Bipyridylium Herbicides

6.1. Introduction

Bipyridylium cations are well known and powerful herbicides with compounds such as 1,1' dimethyl-4,4'-bipyridylium dichloride (Fig. 6.1a) and 6,7-dihydrodipyrido [1,2-a:2,1-c] pyrazinediium dibromide (Fig. 6.1b) marketed as paraquat ($pq^{2+}[2Cl^-]$) and diquat ($dq^{2+}[2Br^-]$) respectively. These compounds owe their herbicidal activity to their ability to undergo a one electron reduction process by accepting an electron from redox systems involved in plant photosynthesis (204, 116). The stable radical monocation thus formed (Fig. 6.2) generates toxic hydrogen peroxide by its reversible oxidation with O_2. The system is cyclic and therefore leads to a build up of H_2O_2 in the host organism eventually causing death.

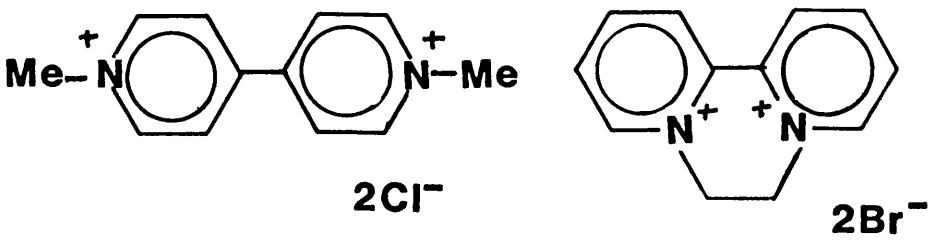

Fig. 6.1 a b

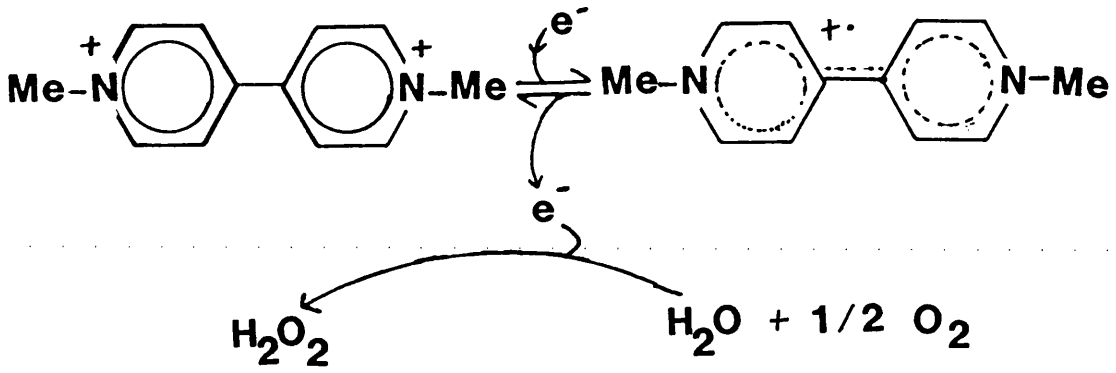

Fig. 6.2

In this chapter the synthesis of novel organotin derivatives of paraquat and diquat and investigations into the voltammetric behaviour of these cations both on their own and in the presence of anionic tin counterions is reported. Voltammetric studies are important to see if complex formation affects the ability to accept electrons and hence the biological activity of the bipyridylium cations. Also reported for comparison are data for new inorganic Sn(IV), Sn(II), Zn(II), Co(II), Cd(II) and Hg(II) derivatives of these dications. Previous work has reported paraquat derivatives of inorganic Cu(I), Hg(II), Pb(II), Cd(II), (205,206) Mn(II), Fe(II), Pd(II), Pt(II), Zn(II), Cu(II), Sn(II), Ag(I), Fe(III) (206), In(I) and In(III) (207). The crystal structures of $pq^{2+}[CoCl_4]^{2-}$, $pq^{2+}[CuCl_2]_n^{n-}$ and $pq^{2+}[PdCl_4]^{2-}$ have also been reported (208).

6.2. Synthesis

Paraquat dichloride and diquat dibromide were obtained as gifts from ICI, and used without further purification. Paraquat dibromide was prepared by halide exchange of $pq^{2+}[2Cl^-]$ with KBr as described elsewhere (206). Organotin starting materials were obtained as described in Appendix I. The preparation of organotin and inorganic salts of the bipyridylium cations is typified by the following examples:

(a) $Pq^{2+}[SnCl_6]^{2-}.H_2O$: Paraquat dichloride (0.50g, 1.95mmol) in methanol (25ml) was added to a stirred solution of tin(IV) chloride pentahydrate (0.70g, 2.00mmol) in the same solvent (10ml). A white precipitate formed immediately. The product (0.94g, 90%) was isolated by filtration after a further 15mins of stirring. Recrystallisation was from a $MeOH/H_2O$ (ca. 1:1) mixture.

(b) $Dq^{2+}[BuSnCl_3Br_2]^{2-}$: A solution of butyltin trichloride (0.41g, 1.45mmol) in methanol (10ml) was added dropwise to a stirred solution of diquat dibromide (0.50g, 1.45mmol) in methanol (20ml) at room temperature. After a few minutes a floccular pale yellow precipitate began to form. Stirring was continued for 20mins, the product was (0.24g) isolated by filtration, washed with methanol and dried in air. Concentration of the filtrate and cooling to -5^oC yielded a further 0.41g of product (total yield 71%). An analytically pure sample was obtained by recrystallisation from hot methanol.

(c) $Pq^{2+}[Me_2SnCl_4]^{2-}$: Following the method of Buttenshaw et al (209), equimolar (3.89mmol) quantities of dimethyltin dichloride and paraquat dichloride were dissolved in methanol (40ml) and concentrated HCl (5ml) added. The resulting solution was allowed to evaporate in a dessicator (over Drierite). After two days, pale yellow needle crystals (0.42g) had formed which were isolated by filtration and dried. The filtrate was allowed to evaporate further until crystallisation recommenced and then cooled to $0^{o}C$ to obtain a second crop (0.58g), total yield 54%) of product. Microscopic examination of the compound revealed at least some of the crystals containing entrapped solution, and the material was found to be analytically impure (Table 6.1). The identity of the product is assigned on the basis of spectroscopic data.

(d) $Pq^{2+}[SnCl_3]_2^-$: A solution of stannous chloride (1.00g, 5.27mmol) in degassed MeOH/HCl (50/5ml) was made up and maintained under an inert atmosphere. Against a counter flow of dinitrogen gas solid paraquat dichloride (0.66g, 2.64mmol) was added, and a yellow precipitate formed immediately. After stirring for 30 mins the precipitate was isolated by filtration (under N_2) and dried in vacuo (Yield: 0.95g, 82%).

Physical data for all compounds prepared are given in Table 6.1.

Table 6.1. Physical Data for Inorganic and Organometallic Salts of Paraquat and Diquat.

Compound	Colour	m.p.	%C[a]	%H	%N	Yield %
$pq^{2+}[Me_2SnCl_4]^{2-}$	pale yellow	259-bld	33.80 (35.27)	3.97 (4.23)	5.90 (5.87)	54
$pq^{2+}[BuSnCl_5]^{2-}.2H_2O$[b]	white	159d	33.31 (33.40)	4.66 (4.74)	4.86 (4.87)	62
$pq^{2+}[BuSnCl_3Br_2]^{2-}.2H_2O$[c]	white	176d	28.95 (28.93)	3.79 (4.11)	3.60 (4.21)	80
$dq^{2+}[BuSnCl_3Br_2]^{2-}$	pale yellow	160d	30.61 (30.69)	3.54 (3.38)	4.32 (4.47)	71
$pq^{2+}[SnCl_6]^{2-}.H_2O$[d]	white	> 300	26.91 (26.90)	2.98 (3.02)	5.06 (5.23)	90
$dq^{2+}[SnCl_4Br_2]^{2-}$	white	> 300	23.73 (23.84)	2.28 (2.00)	4.71 (4.63)	100
$pq^{2+}[SnBr_4Cl_2]^{2-}$	yellow	> 300	19.56 (20.72)	2.02 (2.03)	3.55 (4.03)	76
$dq^{2+}[SnBr_6]^{2-}$	yellow	> 300	18.52 (18.38)	2.04 (1.78)	3.38 (3.57)	85
$pq^{2+}[SnCl_3]_2^-$	yellow	175d	22.63 (22.65)	2.16 (2.22)	4.32 (4.40)	82
$dq^{2+}[ZnBr_2Cl_2]^{2-}$	cream	> 300	30.08 (30.12)	2.75 (2.52)	6.02 (5.85)	4
$dq^{2+}[CoBr_2Cl_2]^{2-}$	green	> 300	30.65 (30.41)	2.59 (2.62)	6.11 (6.07)	73
$pq^{2+}[CdBr_2Cl_2]^{2-}$	white	275d	26.95 (27.23)	2.93 (2.67)	4.93 (5.29)	95
$dq^{2+}[CdBr_4]^{2-}$	white	> 300	23.03 (23.39)	2.02 (1.96)	4.32 (4.55)	81
$dq^{2+}[HgCl_2Br_2]^{2-}$	cream	290d	23.63 (23.42)	1.76 (1.97)	4.44 (4.55)	73

[a] calculated values in brackets

[b] ca. 3% weight loss up to 185°C, by tga; ν(O-H): 3620; 3500br cm^{-1}, absent after heating for 3 hr at 110°C

[c] ν(O-H) 3620; 3450 br cm^{-1}

[d] ca. 0.6% weight loss up to 160°C by tga.

6.3. Results and discussion

6.3.1. Synthesis

The compounds were prepared as specified in equations [1] to [2]. With strong Lewis acids such as Sn(IV) halides and other metal(II) halides in general the reaction is immediate, and yields are always in excess of 70%.

$$SnX_4 + pq^{2+}[2Cl^-] \rightarrow pq^{2+}[SnX_4Cl_2]^{2-} \quad [1]$$

X = Br, Cl

$$SnX_4 + dq^{2+}[2Br^-] \rightarrow dq^{2+}[SnX_4Br_2] \quad [2]$$

X = Br, Cl

$$MX_2 + pq^{2+}[2Cl^-] \rightarrow pq^{2+}[MX_2Cl_2]^{2-} \quad [3]$$

M = Cd, X = Br

$$MX_2 + dq^{2+}[2Br^-] \rightarrow dq^{2+}[MX_2Br_2]^{2-} \quad [4]$$

X = Cl, M = Zn, Co, Hg; X = Br, M = Cd

$$2\ SnCl_2 + pq^{2+}[2Cl^-] \rightarrow pq^{2+}[SnCl_3]_2^- \quad [5]$$

As the Lewis acidity of the metal is reduced by sequentially replacing halide by hydrocarbon moieties, the reaction becomes less facile. For butyltin trichloride the reaction is apparent after ca. 5 mins, and the ultimate yields are reduced (Table 6.1).

$$BuSnCl_3 + Bip^{2+}[2Y^-] \rightarrow Bip^{2+}[Bu\ SnCl_3Y_2]^{2-} \quad [6]$$

$Bip^{2+} = pq^{2+}$, Y = Cl; $Bip^{2+} = dq^{2+}$, Y = Br

With diorganotin dihalides the reaction only proceeds in the presence of a high Cl^- concentration which drives the reaction forward.

$$Me_2SnCl_2 + pq^{2+}[2Cl^-] \rightarrow pq^{2+}[Me_2SnCl_4]^{2-} \quad [7]$$

No reaction was observed according to eqn. [7] for $octyl_2SnCl_2$ or Bu_2SnCl_2, nor for the analogous reaction involving Me_3SnCl, Bu_3SnCl and Ph_3SnCl (stoichiometry 2:1) to yield anions of type $R_3SnX_2^-$. This latter observation was discouraging, in as much as it is triorganotin derivatives which are known to exhibit the maximum biocidal activity (10).

6.3.2. Spectroscopy

Mössbauer data for the tin containing products are shown in Table 6.2. The magnitude of the ΔEq value for $pq^{2+}[Me_2SnCl_4]^{2-}$ ($4.12 mms^{-1}$) established the ubiquitous trans-octahedral R_2SnX_4 geometry (1). Support for this molecular configuration comes from an enhanced $^2J(^{117,119}Sn\text{-}C\text{-}^1H)$ coupling in the ^1H n.m.r. spectrum (83, 88Hz respectively) and the observation of one Sn-C and one Sn-Cl active mode in the i.r., corresponding to ν_{asym}(Sn-C) ($575 cm^{-1}$) and ν_{asym}(Sn-Cl) ($228 cm^{-1}$). Previous work (210) has assigned these to the E_u and A_{2u} modes (assuming ideal D_{4h} geometry) and were found to occur at 580 and $227 cm^{-1}$ (211). Mössbauer data for the mono-organotins are in good agreement with previously reported values for $[BuSnCl_5]^{2-}$ and $[BuSnCl_3Br]^{2-}$

[1.86 and 1.85mms^{-1} respectively (212)]. In principle three isomers of the $[RSnCl_3X_2]^{2-}$ anion are possible, but these are indistinguishable on the basis of ΔEq data, given the essential equality of the partial quadrupole splittings attributable to $[Cl^-]$ and $[Br^-]$. In the case of the mixed halogen anions $[SnX_4Y_2]^{2-}$ (X, Y = halogen) both cis and trans-Y_2 arrangements are possible, with ΔEq(trans) ≃ 2 ΔEq(cis) (55). While the ΔEq values will in any case be small due to the similarity in ligands X and Y, the narrowness of the spectral envelope suggests a preference for the cis-$[Y_2SnX_4]^{2-}$ configuration in both cases. In the series $[SnCl_nBr_{6-n}]^{2-}$ where Cl is sequentially replaced by Br there is an increase in δ reflecting a drop in the sum of the electronegativities of the atoms coordinating tin (53).

The δ value for $pq^{2+}[SnCl_3]_2^-$ (3.42mms^{-1}) is clearly in the range associated with Sn(II) compounds although a small (<5%) shoulder occurs at 0.15mms^{-1} reflecting some oxidation to a Sn(IV) species. Formation of two equivalents of the trichlorostannate anion is supported by microanalytical data, and a quadrupole split Mössbauer spectrum (1.16mms^{-1}) in good agreement with literature values [0.77 - 1.37mms^{-1} (50)]. The large line-widths in this spectrum possibly result from non-equivalent $SnCl_3^-$ geometries. A previous report (206) claiming the formation of $pq^{2+}[SnBr_4]^{2-}$ from the reaction between paraquat dibromide and stannous dibromide is almost certainly in error, since little precedent exists for the formation of SnX_4^{2-} anions, and the microanalytical data upon

Table 6.2. Mössbauer Data for Inorganic and Organotin Derivatives of Paraquat and Diquat.

Compound	δ (mms^{-1})	Δ Eq (mms^{-1})	Γ^a (mms^{-1})
$pq^{2+}[Me_2SnCl_4]^{2-}$	1.52	4.12	1.06[b]
$pq^{2+}[BuSnCl_5]^{2-}.H_2O$	1.04	1.86	0.93, 0.92
$pq^{2+}[BuSnCl_3Br_2]^{2-}.H_2O$	1.20	1.96	0.92, 0.92
$dq^{2+}[BuSnCl_3Br_2]^{2-}$	1.18	1.98	0.95, 0.94
$pq^{2+}[SnCl_6]^{2-}.H_2O$	0.44	0	1.25
$dq^{2+}[SnCl_4Br_2]^{2-}$	0.60	0	1.08
$pq^{2+}[SnCl_2Br_4]^{2-}$	0.83	0	1.08
$dq^{2+}[SnBr_6]^{2-}$	0.82	0	1.17
$pq^{2+}[SnCl_3]_2^{-}$	3.42	1.16	1.30, 1.30

[a] Full-width at half-height

[b] Constrained to be equal for the two wings of the doublet.

which the formulation is based are also valid for $pq^{2+}[SnBr_3]_2^-$, particularly if the presence of small amounts of oxidation product are assumed.

In three instances $pq^{2+}[BuSnCl_5]^{2-}$, $pq^{2+}[BuSnCl_3Br_2]^{2-}$ and $pq^{2+}[SnCl_6]^{2-}$, the products are best formulated as hydrated species. The extent of hydration is suggested on the basis of microanalytical data, (Table 6.1), but the structural role of water is uncertain. Thermal gravimetric analysis indicates that in each case only about half the theoretical amount of water is lost up to 170°C at normal heating rates, implying that the water is quite tightly bound within the lattice. The structure of $[2\text{-}H_3NC_6H_4C(O)NH_2]_2^+$ $[Me_2SnCl_4]^{2-}.2H_2O$ (213) shows water molecules hydrogen-bonded to both the anion (OH------Cl; 3.119Å) and the anilium nitrogen (NH---O; 2.721Å) to form part of a 3D network of bonds. At least the former possibility could arise in the compounds described here.

6.3.3. Voltammetric behaviour

The voltammetric behaviour of both paraquat and diquat has been shown previously (204) to involve two distinct one-electron reduction processes. The first process for both compounds has been shown to be reversible and is pH-independent across the entire pH range. This reduction process leads to the formation of the respective radical monocations which then undergo a further irreversible one electron reduction

at a more negative potential. For paraquat the potential of the second reduction is pH-independent, whereas for diquat it is pH-dependent.

When the DC polarographic behaviour of paraquat and diquat was investigated at the 5×10^{-4}M level in the presence of increasing amounts of $SnCl_4$ the potential of the first reduction process became about 20 - 30mV more negative with increasing Sn(IV) concentration in Britton-Robinson (BR) buffer solutions of pH 2-4. This shift became less noticeable at higher pH and was absent in solutions of pH 6.0. In the case of the second process, the potential was found to become less negative with increasing Sn(IV) concentration in solutions of pH 2-10. This is illustrated for the case of paraquat in BR buffer pH 4.0 in Fig. 6.2. In the case of both processes there was a tendency for the waves exhibited using both DC polarography and cyclic voltammetry to become more irreversible in nature.

When similar experiments were carried out using Me_2SnCl_2, no shifts were seen in the potential of reduction of the waves even at pH 2, reflecting the difficulty of forming the complex $[Me_2SnCl_4]^{2-}$ anion. However, all waves were again shown to become increasingly more irreversible in nature with increasing Me_2SnCl_2 concentration.

The shift of the potential of the first reduction process of paraquat in the presence of $SnCl_4$ to more negative values indicates that the formation of the radical cation becomes more

difficult as formation of the $SnCl_6^{2-}$ anion takes place. The radical cation is probably generated in vivo by coupling with a redox system involved in photosynthesis (116) and should the reduction potential of the bipyridylium dication deviate from the range of the redox system it is apparent from the Nernst equation that the concentration of the radical cation present would be reduced (214). The ease with which the radical cation is formed depends on factors which stabilise its structure, notably a delocalisation across both pyridine rings. This delocalisation depends on the rings being co-planar and studies have shown that substituents on paraquat and diquat which sterically hinder co-planarity increase the potential of the first reduction wave (215) and therefore reduce the biocidal activity. It is apparent from the results obtained here that $SnCl_6^{2-}$ present in solution causes the two heterocyclic rings to twist with respect to one another, and as a result inhibits stabilisation of the radical cation. This twisting may have to be quite significant to exert a real effect on the reduction potential as diquat dibromide which is very active has been shown by X-ray crystallographic studies to have a dihedral angle of 20.4^{o} and INDO calculations using the atomic coordinates indicated the energy barrier to adopting a planar configuration for the radical cation is quite low (216). Crystallographic analysis of $pq^{2+}[CoCl_4]^{2-}$ showed a much greater dihedral angle of 50^{o} while in $pq^{2+}[CoCl_4]^{2-}$ and $pq^{2+}[CuCl]_n^{n+}$ the dication is planar (208). It seems more likely that ion-pair between octahedral $[SnCl_6]^{2-}$ and paraquat would more closely mimic that of $[PdCl_4]^{2-}$ than either of the tetrahedral anions.

Two other important factors determining the biocidal activity of bipyridylium herbicides is the reversibility of the first reduction step and the potential and reversibility of the second reduction process. The irreversibility of the first reduction process of pq^{2+} in the presence of both $SnCl_4$ and Me_2SnCl_2 suggests that the biocidal properties will be lost in these. The shift of the second reduction potential to a less negative position indicates greater ease of formation of the neutral species shown in Fig. 6.4. In the 1,1' dibenzyl 4,4'-bipyriylium dication for example although it exhibited a first reduction potential similar to that of diquat it was found to be inactive as a herbicide because the half-wave potential for the second reduction process occurred at a potential just above that of the first, therefore reducing the lifetime of the radical cation (217). Changes in the position and reversibility of the second reduction for the compounds studied here further suggest a loss of herbicidal activity.

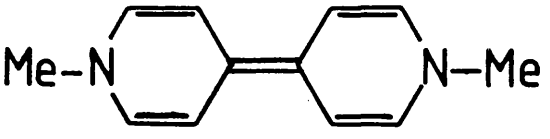

Fig. 6.4.

Figure 6.2. The first (●) and second (■) half-wave reduction potentials for paraquat dichloride in the presence of $SnCl_4$.

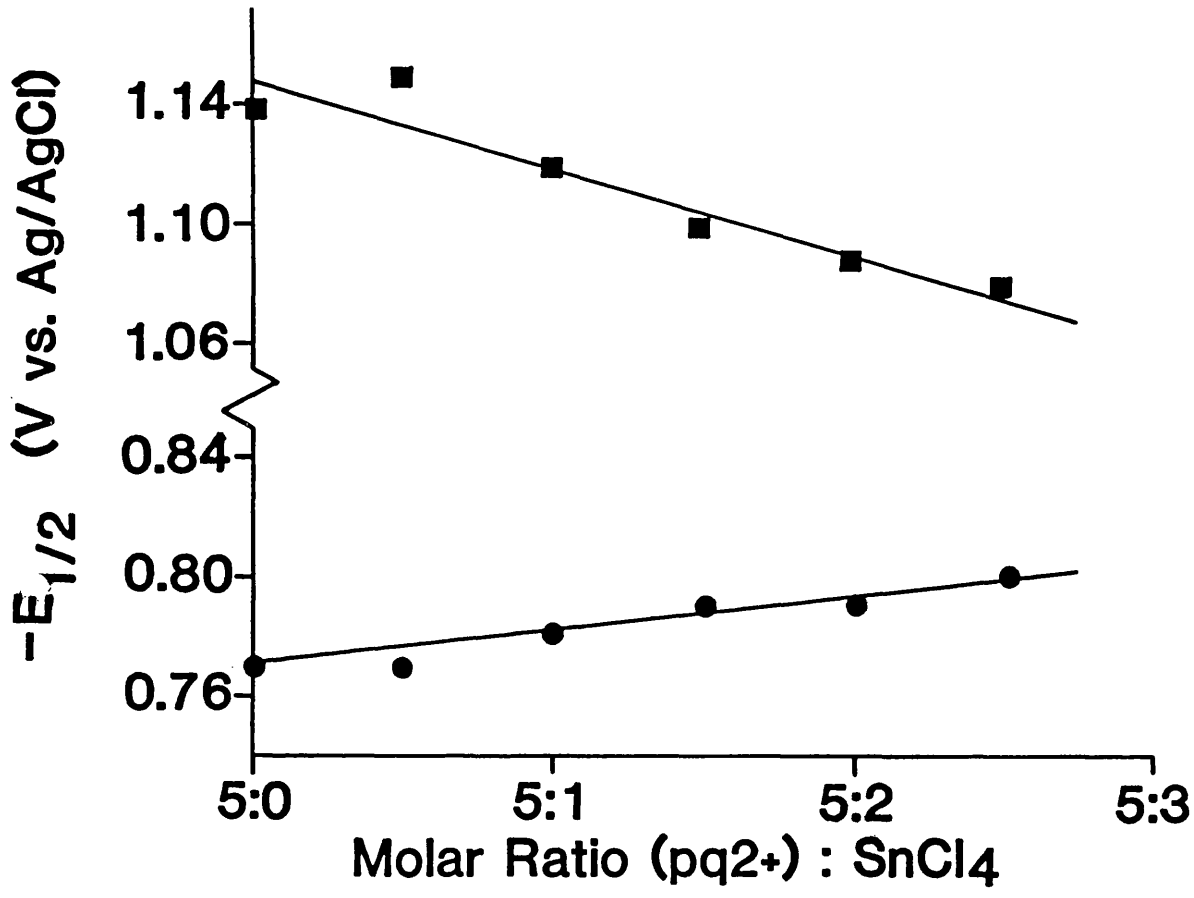

Appendix I

Synthesis of Organotin Starting Materials

Cy_3SnOH, Ph_3SnOH, $(Bu_3Sn)_2O$, Me_2SnCl_2 and $Octyl_2SnCl_2$ were obtained as gifts from the International Tin Research Institute (Greenford, London). Ph_3SnCl, Bu_3SnCl, Bu_2SnCl_2, and Bu_2SnO were purchased from Merck while Ph_2SnCl_2 was purchased from Aldrich. All were used without further purification. The following organotins were synthesised in our own laboratories:

(a) Me_3SnCl; Trimethyltin chloride was obtained from the disproportionation reaction of tetramethyltin (Riedel de Haen) with anhydrous stannic chloride in the ratios indicated by eqn. [1] (1). The reagents were refluxed together at approximately 150°C for two hours, and the product isolated and purified by sublimation under static vacuum at 25 - 30°C.

$$3\ Me_4Sn + SnCl_4 \rightarrow 4\ Me_3SnCl \qquad [1]$$

(b) Me_3SnOH; Trimethyltin chloride and potassium hydroxide were refluxed in MeOH for 30 mins. The solution was cooled before filtering off KCl formed, (eqn [2]), evaporated to dryness (by standing in fume hood for several days) and purified by sublimation under static vacuum at 50 - 60°C.

$$Me_3SnCl + KOH \rightarrow Me_3SnOH + KCl \qquad [2]$$

(c) $\underline{Me_2SnO}$; An ether solution of Me_2SnCl_2 was shaken with an aqueous solution of potassium hydroxide and the resulting precipitate (Me_2SnO) removed by filtration. The insoluble product was washed repeatedly with Et_2O and H_2O (218)

$$Me_2SnCl_2 + 2\ KOH \rightarrow Me_2SnO + 2\ KCl \qquad [3]$$

(d) $\underline{Cy_3SnCl}$: A solution of Cy_3SnOH in toluene was stirred vigorously with $cHCl/H_2O$ for 30 mins. The toluene layer was separated, dried with anhydrous $MgSO_4$ and evaporated to dryness, to yield the product which was recrystallised from toluene m.p. = 127 - 128°C [lit. 129 - 130 (218)].

$$Cy_3SnOH + HCl \rightarrow Cy_3SnCl + H_2O \qquad [4]$$

(e) $\underline{Bz_3SnCl}$; Benzyl chloride was added to a suspension of tin powder in boiling water and refluxed for 1½ hrs. The precipitate formed was filtered after cooling and Soxhlet extracted with acetone. Evaporation of the acetone solution yielded product which was recrystallised from ethyl acetate (219).

$$3\ BzCl + 2\ Sn \rightarrow Bz_3SnCl + SnCl_2 \qquad [5]$$

(f) $\underline{BzSnOH}$; Synthesised according to method (c) above using NaOH instead of KOH. The product was recrystallised from ethanol m.p. 120 - 122°C [lit. 124° (2)].

$$Bz_3SnCl + NaOH \rightarrow Bz_3SnOH + NaCl \qquad [6]$$

Appendix II

Crystallographic Analysis and Structure Refinement of Tricyclohexyltin(3-Indolylacetate)

(a) Crystal data

$C_{28}H_{41}NO_2Sn$ = 542.30, orthorhombic, $\underline{a}$ = 16.487(6)Å $\underline{b}$ = 10.674(4)Å, $\underline{c}$ = 14.804(5)Å, $\underline{V}$ = 2605.2Å^3, ρcalc = 1.382gmcm^{-3}, Z = 4, F(000) = 1128, μ(Mo-K_α) = 9.10cm^{-1}, space group $P2_12_12_1$. For 2091 observed reflections R = 0.0351 and R_W = 0.0248

(b) Crystallographic analysis

A crystal with the dimensions 0.32 x 0.40 x 0.20mm was glued to the top of a glass fibre and placed in the nitrogen stream of the diffractometer. It was used for preliminary crystal analysis and final data collection performed at 150(3)K on a Syntex $P2_1$ automatic four circle counter diffractometer controlled by a Nova 1200 computer. Final cell dimensions were obtained for least square refinement of the angular settings of 15 accurately centred reflections. The intensities of all reflections with $2\theta<50^\circ$ were measured. Two reflections were used as standard and their intensities were monitored after each 50 observations. No significant changes in the intensities of the monitor reflections were noted.

F_O values were calculated from the raw data. Corrections for Lorentz and polarisation effects were applied, but no absorption correction was made (μ = 9.10cm^{-1})

(c) Structure solution and refinement

From the systematically absent reflections the space group was determined to be $P2_12_12_1$. The position of the tin atom was calculated from a three dimensional Patterson map. A difference Fourier map based on the heavy atom phases revealed the positions of all other non-hydrogen atoms. These atoms were refined by first using isotropic and then anisotropic thermal parameters. All hydrogen positions were calculated [d(C-H) = 1.08Å] but only the positional parameters of H(1) (bonded to N) were refined in the least square procedure. The isotropic temperature factor for all hydrogens was held at U = 0.05Å^2.

The maximum parameter shifts in the final cycle of refinement were 0.001 of their estimated standard deviations. A difference Fourier map calculated from the final structure factors showed no features greater than 0.44e^-/Å^3. The strongest peaks in this map were located in the vicinity of the tin atom. The final R value is 0.0351 for 2091 reflections [$I>2\sigma(I)$] included in the least-squares sums (R_W = 0.0248).

All calculations were performed using the program SHELX (220). Atomic scattering factors for C, N, and O were obtained from ref. (221) and those for Sn from ref. (222). The $\Delta f'$ and $\Delta f''$ components of anomalous dispersions are from ref. (223).

Appendix III

Crystallographic Analysis of Tricyclohexyltin (2-mercaptobenzothiazole)

(a) Crystal data

$C_{25}H_{37}NS_2Sn$ = 535.43, triclinic, space group $P\bar{1}$, a = 13.0336Å, b = 11.1264Å, c = 10.1878Å, α = 62.49°, β = 94.79°, γ = 95.51°, V = 1302.02Å^3, ρcalc = 1.362g cm^{-3}, Z = 2, F(000) = 522, μ(Mo-K_α) = 10.52cm^{-1}. For 2377 observed reflections R = 0.0542 and R_W = 0.0600.

(b) Analysis and structure refinement

Data collection was performed at room temperature using Mo-K_α radiation (λ = 0.71069Å). The unit cell parameters were obtained by a least squares fit of θ values for twelve reflections (with θ values in the range 12 - 2θ°). The angles used in this calculation were measured on the diffractometer.

The structure was solved by direct methods using MULTAN (224) and refinement calculations were performed using the SHELX program (220). Atomic scattering factors for the non-hydrogen atoms were obtained from ref. (221) and those for hydrogen atoms from Ref. (225), while anomalous dispersion corrections for non-hydrogen atoms were from Ref. (223).

Appendix IV

Instrumental Details

(a) Vibrational spectroscopy

Infra-red spectra were recorded as KBr discs, or nujol mulls on KBr or CsI plates on Perkin Elmer 1330, 599B, and 597 spectrometers in the region 4000-250cm^{-1}. Calibration was with polystyrene film.

The Raman spectra were obtained from powdered samples in Pyrex capillary tubes using a Lexel 85 Ar^{+} laser. The scattered radiation was resolved on a double monochromator (Spex 1401).

(b) N.m.r. spectroscopy

H^{1} n.m.r. spectra were recorded on Perkin Elmer R12B and R24B 60MHz spectrometers using TMS as an internal standard. ^{119}Sn n.m.r. spectra (^{1}H decoupled) were recorded by Dr. S. Blunden at the International Tin Research Institute (London) on a JEOL FX60Q spectrometer. Chemical shifts [$\delta(^{119}Sn)$] are relative to Me_4Sn.

(c) Mass spectrometry

Mass spectra were collected on a V.G. 70-70E instrument with a DS2025 data system under electron ionisation (70eV) or chemical ionisation (iso-butene) conditions.

(d) Microanalysis

Carbon, hydrogen and nitrogen were analysed for at the microanalytical services of University College Dublin, the University of Bath and Butterworth Laboratories Ltd.

(e) Mössbauer spectroscopy

Mössbauer spectra were recorded on a constant acceleration Mössbauer spectrometer (Cryophysics) fitted with a 5mCi calcium stannate-119m source (Amersham Int.) and operated in a sawtooth wave mode. The sample temperature was controlled using a continuous flow liquid nitrogen cryostat linked to a DTC-2 digital variable temperature controller (Oxford Instruments). Temperature stability was ± 0.1K of the set temperature. The source was at ambient temperature. Samples were prepared as finely ground powders. Calibration was based on the spectrum of natural iron with ^{119}Sn chemical shifts quoted relative to SnO_2 (zero velocity). Spectra were fitted to Standard Lorentzian line shapes, with a correction for parabolic background curvature using a conventional least squares technique.

CONCLUSIONS

With the exception of the studies on organotin derivatives of paraquat and diquat, two general types of ligand were used in this investigation, those containing two oxygen donor atoms (3-indolylacetates and phosphorodiamidates) and those with either two sulphur donor atoms (dithiocarbamates) or one sulphur with one nitrogen or oxygen donor atom (2-mercaptobenzothiazole and analogues). The different types of structures adopted by organotin derivatives of these ligands were found to be segregated along similar lines. The ligands containing two oxygen donor atoms tended to chelate in a bridging fashion (spectroscopic evidence) while the other ligand types coordinate the tin atom in either a monodentate or very anisobidentate fashion giving rise to a tetrahedral geometry at tin with varying degrees of distortion towards cis-R_3SnX_2. The principle exceptions to this pattern were tricyclohexyltin derivatives of IAA and N-Me,IAA where the steric bulk of the C_6H_{11}- groups and the reduced Lewis acidity at tin has prevented bidentate bonding of the ligand.

The nature of the donor atom is obviously crucial in determining the extent to which any coordination expansion at tin occurs. As sulphur has an electronegativity similar to that of carbon it does not demand the two more electronegative axial sites that would arise from the bridging structures (trans-R_3SnS_2), which are seemingly generally preferred by the more electronegative oxygen ligands. As a result any coordination expansion by a bidentate XS_2 ligand would be towards a cis-R_3SnX_2 configuration with sulphur atoms in axial and equatorial positions. As tin-sulphur

bonds are somewhat longer than tin-oxygen bonds any four membered ring, SnX_2Y- arising from chelation would involve more strain for X = S than for X = O (203), hence the propensity for the dithiocarbamate systems to bond in an anisobidentate fashion, with one long and one short tin-sulphur contact. The lone pair of the second donor atom for mbt(N), mbo(O) and mbi(N) may contribute to the aromatic ring system in these ligands leading to a reduction in Lewis basicity and therefore a reduced tendency to cordinate the metal atom. However, the greater electronegativity of oxygen is again highlighted by Bu_3Sn(mbo) forming a trans-tbp configuration in the solid state (Mössbauer evidence).

With regard to biocidal activity the geometry least likely to be active appears to be the cis-R_3SnX_2 configuration in which coordination saturation at tin is considered to occur (84). Although evidence for minor distortions from tetrahedral towards this geometry has been found for derivatives of pipdtc and mbt (and analogues) no structures with isobidentate chelation have been observed and so all the novel triorganotin derivatives synthesised might be expected to show some biocidal activity. The polymeric trans-R_3SnO_2 geometries such as some of the 3-indolyl acetates and the phosphorodiamidates can exhibit biological activity by eventual dissolution to four coordination in solution as found for Ph_3SnOAc (92). The possible formation of cyclic systems in solution by some phosphorodiamidates may lead to a loss of activity for these compounds.

References

(1) A.G. Davies and P.J. Smith in "Comprehensive Organometallic Chemistry" ed. G. Wilkinson, F.G.A. Stone and E.W. Abel, Pergamon Press, New York, (1982), p519.

(2) A.G. Davies and P.J. Smith, Adv. Inorg. Chem. Radiochem., 23, 1, (1980).

(3) J.A. Zubieta and J.J. Zuckerman, Prog. Inorg. Chem.,24, 251, (1978).

(4) R.C. Poller, "The Chemistry of Organotin Compounds" Logos, London, 1970.

(5) W.P. Neumann "The Organic Chemistry of Tin",Wiley, London, 1970.

(6) "Organotin Compounds",ed. A.K. Sawyer, Dekker, New York, 1971, Vols. 1, 2, 3.

(7) "Organotin Chemistry", Adv. Chem. Ser. 157, (1976), ed. J.J. Zuckerman.

(8) A. Bokranz and H. Plum, "Fortschritte der Chemischem Forschung", 16, 365, (1971), Springer Verlag, Berlin.

(9) P.A. Cusack, P.J. Smith, J.D. Donaldson, S.M. Grimes, "A Bibliography of X-Ray Structures of Tin Compounds", International Tin Research Institute, London 1981 (Publication 588).

(10) R. Hulme, J. Chem. Soc.,1524, (1964).

(11)(a) P. Chieh and J. Trotter, J. Chem. Soc. (A), 911,(1970);

(b) N.A. Akhmed and G.G. Aleksandrov, J. Struct. Chem, 11, 824, (1970).

(12) F.A. Boer, G.A. Doorkian, H.H. Freeman and S.U. McKinley, J. Am. Chem. Soc., 92, 1225, (1970).

(13) F.A. Boer, F.P. Van Remoortere, P.P. North and G.N. Reeke, Inorg. Chem. 10, 529, (1971).

(14) H. Puff, W. Schuh, R. Sievers, W. Wald, and R. Zimmer, J. Organomet. Chem. 260, 271, (1984).

(15) N.G. Boki, Yu.T. Struchnov, D.N. Krausov, and E.M. Rokhlina, J. Struct. Chem. 14, 258, (1973).
J. Struct. Chem. 15, 424, (1974).

(16) M.J.S. Gynane, M.F. Lappert, S.J. Miles, A.J. Carty and N.J. Taylor, J. Chem. Soc., Dalton Trans., 2009, (1977).

(17) P.J. Vergamini, H. Vahrenkamp, and L.F. Dahl,J. Am. Chem. Soc., 93, 6327, (1971).

(18) P.G. Harrison, K.C. Molloy, R.C. Phillips, P.J. Smith and A.J. Crowe, J. Organomet. Chem. 160, 421, (1980).

(19) A.G. Davies, J.P. Goddard, M.B. Hursthouse, and N.P.C. Walker, J. Chem. Soc., Chem. Commun., 597,(1983).

(20) G. Van Noten, J.G. Noltes, and A.L. Spek, J. Organomet. Chem., 118, 183, (1978).

(21) G.M. Bancroft, B.W. Davies, N.C. Payne and T.K. Shaw, J. Chem. Soc., Dalton Trans., 973, (1975).

(22) K.C. Molloy and K. Quill, J. Chem. Soc., Dalton Trans., 1417, (1985).

(23) E.O. Schlemper and D. Britton, Inorg. Chem., 5, 507, (1966).

(24) C. Glidewell and D.C. Liles, Acta. Cryst., B34, 129, (1978).

(25) N.W. Alcock and R.E. Timms, J. Chem. Soc.(A), 1873, (1968).

(26) K.C. Molloy, T.G. Purcell, K. Quill and I.W. Nowell, J. Organomet. Chem., 267, 237, (1984).

(27) R. Hengel, U. Kunze and J. Strahle, Z. Anorg. Chem., 35, 423, (1976).

(28) F.W.B. Einstein and B.R. Penfold, J. Chem. Soc.(A), 3019, (1968).

(29) D.L. Evans and B.R. Penfold, J. Cryst. Mol. Struct., 5, 93, (1975).

(30) M. Webster, K.R. Mudd and D.J. Taylor, Inorg. Chim. Acta., 20, 231, (1976).

(31) G.A. Miller and E.O. Schlemper, Inorg. Chem., 12, 677, (1973).

(32) P.G. Harrison, T.J. King and R.C. Philips, J. Chem. Soc., Dalton Trans., 2317, (1976).

(33) P.F. Lindley and P. Carr, J. Cryst. Mol. Struct., 4, 173, (1974).

(34) T. Kimura, N. Yasuaka, N. Kasai and M. Kakuda, Bull. Chem. Soc. Japan., 45, 1649, (1972).

(35) J.S. Morris and E.O. Schlemper, J. Cryst. Mol. Struct., 9, 13, (1980).

(36) P.G. Harrison, T.J. King and J.A. Richards, J. Chem. Soc., Dalton Trans., 1722, (1974).

(37) G. Valle, G. Plazzogna and R. Ettorre, J. Chem. Soc., Dalton Trans., 1271 (1985).

(38) E.O. Schlemper and W.C. Hamilton, Inorg. Chem., 5, 995, (1966).

(39) P.T. Greene and R.F. Bryan, J. Chem. Soc. (A), 2549, (1971).

(40) A.G. Davies, H. Judith Milledge, D.C. Puxley, P.J. Smith, J. Chem. Soc.(A), 2862, (1970).

(41) N.W. Alcock and J.F. Sawyer, J. Chem. Soc., Dalton Trans., 1090, (1977).

(42) N.G. Boki, Yu.T. Struchrov and A.K. Prokot'ev, J. Struct. Chem., 13, 619, (1972).

(43) B.K. Nicholson, J. Organomet. Chem., 265, 153, (1984).

(44) C. Lecomote, J. Protas and M. Devaud, Acta. Cryst. B32, 923, (1976).

(45) J.S. Morris and E.O. Schlemper, J. Cryst. Mol. Struct., 8, 295, (1978).

(46) C. Pelizzi, G. Pelizzi, and G. Predieri, J. Organomet. Chem., 263. 9. (1984).

(47) N.N. Greenwood and T.C. Gibb, "Mössbauer Spectroscopy", Chapman and Hall, London, (1971).

(48) G.M. Bancroft, "Mössbauer Spectroscopy, An Introduction for Inorganic Chemists and Geochemists", McGraw-Hill, London (1973)

(49) G.M. Bancroft and R.H. Platt, Adv. Inorg. Radiochem. 15, 59, (1976).

(50) J.N.R. Ruddick, Rev. Silicon, Germanium, Tin, Lead, Compd., 15, 59, (1976).

(51) J.J. Zuckerman in "Chemical Mössbauer Spectroscopy", ed. R.H. Herber, Plenum New York, 267 - 293, (1984).

(52) R.V. Parish and R.H. Platt, J. Chem. Soc.(A), 2145, (1969).

(53) L.A. Hobbs and P.J. Smith, J. Organomet. Chem., 206, 59, (1981).

(54) R.V. Parish, Prog. Inorg. Chem., 15, 101, (1972).

(55) B.W. Fitzsimmons, N.J. Seely and A.W. Smith, J. Chem. Soc.(A), 143, (1969).

(56) B.M. Bancroft, V.G. Kumar Das, T.K. Sham and M.G. Clark, J. Chem. Soc., Chem. Commun., 236, (1974).

(57) M.G. Clark, A.G. Maddock and R.H. Platt, J. Chem. Soc., Dalton Trans., 281, (1972).

(58) T.K. Sham and B.M. Bancroft, Inorg. Chem., 14, 228, (1975).

(59) E.O. Schlemper, Inorg. Chem., 5, 995, (1966).

(60) K.C. Molloy, M.B. Hossain, O. Van der Helm, J.J. Zuckerman, and I. Haiduc, Inorg. Chem., 19, 2041, (1980).

(61) J.L. Lefferts, K.C. Molloy, J.J. Zuckerman, I. Haiduc, M. Curtui, C. Guta and D. Ruse, Inorg. Chem., 19, 2861, (1980).

(62) T. Tanaka, Organomet. Chem. Rev.(A), 5, 1, (1970).

(63) L.E. Levchuk, J.R. Sams and F. Abuke, Inorg. Chem., 11, 43, (1972).

(64) R. Okawara, D.E. Webster and E.G. Rochow, J. Am. Chem. Soc., 82, 3287, (1960).

(65) N. Kasai, K. Yasuda and R. Okawara, J. Organomet. Chem., 3, 172, (1965).

(66) R. Okawara and K. Yasuda, J. Organomet. Chem., 1, 356, (1965).

(67) M.M. McGrady and R.S. Tobias, Inorg. Chem., 8, 1157, (1964).

(68) M.C. Henry and J.G. Noltes, J. Am. Chem. Soc., 82, 1271, (1960).

(69) R.C. Poller, Spectrochim. Acta., 22, 935, (1966).

(70) V.S. Petrosyan and O.A. Reutov, Pure Appl. Chem., 37, 147, (1974).

(71) J.R. Holmes and H.D. Kuez, J. Am. Chem. Soc., 83, 3903, (1961).

(72) V.S. Petrosyan, Prog. Nucl. Magn. Reson. Spectrosc. 11, 115, (1977).

(73) K. Kawakami, M. Miya-Uchi, and T. Tanaka, J. Inorg. Nucl. Chem., 33, 3773, (1971).

(74) A.G. Davies, P.G. Harrison, J.D. Kennedy, T.N. Mitchell, R.J. Puddephatt and W. McFarlane, J. Chem. Soc.(C)., 1136, (1969).

(75) D.C. Giles and D. Shaw, Annu. Rev. N.M.R. Spectrosc., 5, 557, (1972).

(76) W. McFarlane and R.J. Wood, J. Organomet. Chem., 40, C17, (1972).

(77) A. Carrick and F. Glocking, J. Chem. Soc.(A), 40, (1966).

(78) D.B. Chambers, F. Glocking and M. Weston, J. Chem. Soc.(A), 1759, (1967).

(79) P.J. Smith, "Toxicological Data on Organotin Compounds", International Tin Research Institute, London, publication No. 538, (1978).

(80) P.J. Smith, International Tin Research Institute, London, publication No. 569, (1978).

(81) A.K. Sijpesteijn, J.G.A. Luijten and G.J.M. Van der Kerk in "Fungicides an Advanced Treatise" Vol. II, ed. D.C. Torgeson, Acad. Press, New York, 331, (1969).

(82) C.J. Evans, Tin Its Uses, 86, 7, (1970).

(83) C.J. Evans, Tin Its Uses, 110, 6, (1976).

(84) S.J. Blunden, P.J. Smith and B. Sugavanam, Pestic. Sci., 15, 253, (1984).

(85) J.M. Brown, A.C. Chapman, D. Harper, D.J. Mowthorpe, A.G. Davies and P.J. Smith, J. Chem. Soc., Dalton Trans., 338, (1972).

(86) A.G. Maddock and R.H. Platt, J. Chem. Soc.(A), 1191, (1971).

(87) A. Tzschnach, E. Reuss, P. Held and W. Bollman, E. German Patent 63490, (1980).

(88) B.G. Farrow and A.P. Dawson, Eur. J. Biochem., 86, 85, (1978).

(89) G. Van Koten, J.T.B.H. Jastrzebski, Jan G. Noltes, A.L. Spek and J.C. Schoone, J. Organomet. Chem., 148, 233, (1978).

(90) P.J. Smith and A.P. Tupciauskas, Annu. Rev. N.M.R. Spectrosc., 8, 291, (1978).

(91) S.J. Blunden, P.J. Smith and D.G. Gillies, Inorg. Chem. Acta., 60, 105, (1982).

(92) K.R.S. Ascher and N.E. Nemny, Experienta, 32, 902, (1976).

(93) W.N. Aldridge and J.E. Cremer, Biochem. J., 61, 406, (1955).

(94) W.N. Aldridge and B.W. Street, Biochem. J., 91, 287, (1964).

(95) M.J. Selwyn, A.P. Dawson, M. Stockdale and N. Gains, Eur. J. Biochem., 14, 120 (1970).

(96) M.J. Selwyn in ref. (7), p. 204.

(97) M. Stockdale, A.P. Dawson and M.J. Selwyn, Eur. J. Biochem., 15, 342, (1970).

(98) R.G. Wulf and K.H. Byington, Arch. Biochem. Biophys., 167, 176, (1975).

(99) M.S. Rose and W.N. Aldridge, Biochem. J. 106, 821, (1968).

(100) W.N. Aldridge and B.W. Street, Biochem. J, 120, 171, (1970).

(101) M.S. Rose and E.A. Lock, Biochem. J., 120, 151, (1970).

(102) B.M. Elliot, W.N. Aldridge and J.W. Bridges, Biochem. J., 177, 461, (1979).

(103) B.G. Farrow, A.P. Dawson and M.J. Selwyn, Biochem. J., 202, 163, (1982).

(104) W.N. Aldridge and J.E. Cremer, Biochem. J., 61, 406, (1955).

(105) W.N. Aldridge in ref. (7), 186.

(106) E.C. Kimmel, E.H. Fish and J.E. Casida, J. Agric. Food Chem.,

(107) S.J. Blunden, L.A. Hobbs and P.J. Smith, "Environmental Chemistry", ed. H.J.M. Brown (Specialist Periodical Reports), R.S.C., London, (1984).

(108) R.D. Barnes, A.T. Bull and R.C. Poller, Pestic. Sci., 4, 49, (1973).

(109) New Scientist No. 1469, 20, (1985).
The Guardian, p. 28, 20.5.85.
The Guardian, p. 7, 27.7.85.

(110) K.D. Freitag and R. Bock, Pestic. Sci., 5, 731, (1974).

(111) P.J. Smith, A.J. Crowe, D.W. Allen, J. Brooks and R. Formstone, Chem. Ind. (London), 874, (1977).

(112) A.W. Sheldon, J. Paint Technol., 47, 54, (1975).

(113) L.D. Dizikes, W.P. Ridely and J.M. Wood, J. Am. Chem. Soc., 100, 1012, (1978).

(114) P.J. Craig and S. Rapsomankis, Inorg. Chim. Acta, 107, 39 (1985).

(115) P.J. Smith and L. Smith, Chem. Brit.

(116) J.R. Corbett, "Biochemical Mode of Action of Pestcides" Acad. Press, New York, (1974).

(117) P. Rosemund, G. Meyer and I. Hansel, Chem. Ber., 108, 3528, (1975).

(118) D.B. Chambers, F. Glocking and M. Weston, J. Chem. Soc.(A), 1759, (1967).

(119) F.W. McCleverty, "Interpretation of Mass Spectra", B.A. Benjamin, (1973).

(120) H. Chih and B.R. Penfold, J. Cryst. Mol. Struct., 3, 285, (1973).

(121) C. Poder and J.R. Sams, J. Organomet. Chem., 19, 67, (1969).

(122) N.W. Alcock and R.E. Timms, J. Chem. Soc.(A), 1876, (1968).

(123) J.F. Vollano, R.O. Day, D.N. Rau, V. Chandrasekhar and R.R. Holmes, Inorg. Chem., 23, 3153, (1984).

(124) J.F. Vollano, V. Chandrasekhar, R.O. Day and R.R. Holmes, Inorg. Chem., 23,3147, (1984).

(125) S. Calogero, D.A. Clemente, V. Peruzzo and G. Ta, J. Chem. Soc., Dalton Trans., 1172, (1979).

(126) P.B. Simons and W.A.G. Graham, J. Organomet. Chem., 8, 479, (1967).

(127) T.P. Poeth, P.G. Harrison, T.U. Long, B.R. Willeford and J.J. Zuckerman, Inorg. Chem., 10, 522, (1971).

(128) S.B. Nagelberg, C.E. Reinhold, B.R. Willeford, M.P. Bigwood, K.C. Molloy and J.J. Zuckerman, Organometallics, 1, 855, (1982).

(129) N.W.G. Debeye, D.E. Fenton, S.E. Urlich and J.J. Zuckerman, J. Organomet. Chem., 28, 339, (1971).

(130) S.J. Blunden and R. Hill, Inorg. Chim. Acta, 98, L7, (1985).

(131) P.G. Harrison in "Comprehensive Organometallic Chemistry", ed. G. Wilkinson, F.G.A. Stone and E.W. Abel, Pergamon Press, New York, (1982), p. 633.

(132) B.Y.K. Ho and J.J. Zuckerman, Inorg. Nucl. Chem. Letts. 7, 849, (1971).

(133) S. Calogero, P. Ganis, V. Peruzzo and G. Tagliavani, J. Organomet. Chem., 191, 381, (1980).

(134) P.G. Harrison, K. Lambert, T.J. King and B. Magee,. J. Chem. Soc., Dalton Trans., 363, (1983).

(135) P.G. Harrison, T.J. King and K.C. Molloy, J. Organomet. Chem., 185, 199, (1980).

(136) S. Calogero, P. Ganis, V. Peruzzo, G. Tagliavani and G. Valle, J. Organomet. Chem., 220, 11, (1981).

(137) P.G. Harrison, R.C. Phillips and E.W. Thornton, J. Chem. Soc., Chem. Commun., 603, (1977).

(138) I.L. Karle, K. Britts and P. Grim, Acta. Cryst., 17, 496, (1964).

(139) B.Y.K. Ho, K.C. Molloy and J.J. Zuckerman, J. Organomet. Chem., 187, 213, (1980).

(140) P.G. Harrison and R.C. Phillips, J. Organomet. Chem., 182, 37, (1979).

(141) G.A. Jeffery and L. Lewis, Carbohydrate Res. 60, 179, (1978).

(142)(a) R. Taylor, O. Kennard and V. Werner, J. Am. Chem. Soc., 105, 5761, (1983).

(b) R. Taylor, O. Kennard and V. Werner, J. Am. Chem. Soc., 106, 244, (1984).

(143) R.G. Owens in "Fungicides an Advanced Treatise", Vol. II, ed. D.C. Torgeson, Acad. Press, New York, 147, (1969).

(144) E. Czerwinska, Z. Eckstein, Z. Ejmocki and R. Kowalik, Bull. Acad. Pol. Sci. Ser. Sci. Chim., 15, 335, (1967).

(145) R.R. Ison, G.T. Newbold and D.T. Saggers, J. Pestic. Sci, 2, 152, (1971).

(146) G. Domazetis, R.J. Magee and B.D. James, J. Organomet. Chem., 148, 339, (1978).

(147) G. Domazetis, R.J. Magee, B.D. James and J.D. Cashion, J. Inorg. Nucl. Chem., 43, 1351, (1981).

(148) J.P. Cheswick and J. Donohue, Acta. Cryst. B27, 1441, (1971).

(149) G.R. Form, E.S. Raper and T.C. Downie, Acta. Cryst., B.32, 345, (1976).

(150) R.H. Fish, R.L. Holmstead and J.E. Casida, Tetrahedron Letts., 14, 1303, (1974).

(151) M. Üher, S. Kovac, A. Martvon and M. Jezek, Chem. Zvesti., 32(4), 486, (1978).

(152) F.A. Devillanova and G. Verani, Aust. J. Chem., 33, 279, (1980).

(153) S. Banerji, R.E. Byrne and S.E. Livingstone, Trans. Met. Chem., 7, 5, (1982).

(154) J. Dehand and J. Jordanov, Inorg. Chim. Acta., 17, 37, (1976).

(155) S. Jeannin, Y. Jeannin and G. Lavigne, Trans. Met. Chem., 1, 192, (1976).

(156) M.F. El-Shazly, T. Salem, M.A. El-Sayed and S. Hedowy, Inorg. Chim. Acta., 29, 155, (1978).

(157) I.P. Khullar and U. Agurwada, Can. J. Chem., 53, 1165, (1975).

(158) C.I. Balcombe, E.C. McMullin and M.E. Peach, J. Inorg. Nucl. Chem., 36, 2449, (1974).

(160) S.J. Blunden and R.S. Hill, Inorg. Chim. Acta., 98, L7, (1985).

(161) G. Domazetis, B.D. James, F. Mackay and R.J. Magee, J. Inorg. Nucl. Chem., 41, 1955, (1980).

(162) R.C. Poller and J.N.R. Ruddick, J. Chem. Soc., Dalton Trans., 555, (1972).

(163) P.L. Clarke, M.E. Cardick and J.L. Wardell, J. Organomet. Chem., 63, 279, (1973).

(164) R. Barbieri, E. Rivarola, F. Di Bianca and F. Huber, Inorg. Chim. Acta., 57, 37, (1982).

(165) S. Calogero, P. Ganis, V. Peruzzo and G. Tagliavani, J. Organomet. Chem., 179, 148, (1979).

(166) N.G. Boki, Yu. T. Strucknov, T.N. Kravstow and E.M. Rokhlina, J. Struct. Chem., 14, 458, (1973).

(167) G.M. Sheldrick and W.S. Sheldrick, (a) J. Chem. Soc.(A), 490, (1969), (b) ibid, 493, (1969).

(168) G.D. Andretti, G. Bocelli, G. Colestra and P. Sgaraboto, J. Organomet. Chem., 273, 31, (1984).

(169) I.G. Dance and D. Issac, Aust. J. Chem., 30, 2425, (1977).

(170) J.A. McCleverty, S. Gill, R.S.Z. Kowalski, N.A. Bailey, H. Adams, K.W. Lumbard and M.A. Murphy, J. Chem. Soc., Dalton Trans., 493, (1982).

(171) S. Jeannin, Y. Jeannin and G. Lavigne, Trans. Met. Chem., 1, 186, (1976).

(172) J.A. McCleverty, N.J. Morrison, N. Spencer, C.A. Ashworth, N.A. Bailey, M.R. Johnson, J.M.A. Smith, B.A. Tobbiner, and C.R. Taylor, J. Chem. Soc., Dalton Trans., 1945, (1980).

(173) J.L. Lefferts, K.C. Molloy, J.J. Zuckerman, I. Haiduc, C. Guta and D. Ruse, Inorg. Chem., 19, 1662, (1980).

(174) K.S. Siddiqi, F.R. Zaidi and S.A.A. Zaidi, Synth. React. Inorg. Met-Org. Chem., 10(6), 569, (1980).

(175) J. Tombeux, L.C. Van Poucke and Spectrochim. Acta., 28A, 1943, (1972).

(176) F. Bonati and R. Ugo, J. Organomet. Chem., 10, 257, (1967).

(177) A.G. Davies and J.D. Kennedy, J. Chem. Soc. (C), 759, (1970).

(178) R.C. Poller, J. Inorg. Nucl. Chem., 24, 593, (1962).

(179) C. O'Connor, J.D. Gilbert and G. Wilkinson, J. Chem. Soc.(A), 84, (1969).

(180) J.C. May, D. Petridis and C. Curran, Inorg. Chim. Acta, 5, 511, (1971).

(181) T.A. George, K. Jones and M.F. Lappert, J. Chem. Soc., 2157, (1965).

(182) J.L.K.F. de Vries and R.H. Herber, Inorg. Chem., 11, 1678, (1972).

(183) B.W.Fitzsimmons, A.A. Owusu, N.J. Seely and A.W. Smith, J. Chem. Soc.(A), 935, (1970).

(184) B.W. Fitzsimmons and A.C. Sawbridge, J. Chem. Soc., Dalton Trans., 1678, (1972).

(185) K. Farue, T. Kimura, N. Yasuoka, N. Kasai and M. Kakudo, Bull. Chem. Soc. Japan, 43, 1661, (1970).

(186) T. Kimura, N. Yasuoka, N. Kasai and M. Kakudo, Bull. Chem. Soc. Japan, 45, 649, (1972).

(187) Y.K. Bhoon and R.P. Singh, Acta Sienca Indica, VIIC, 111, (1981).

(188) U.S. Patent, 3,917,827, (1975), Chem. Abs., 84, 85684, (1976).
U.S. Patent, 3,919,418, (1975), Chem. Abs., 84, 5644, (1976).
U.S. Patent, 3,947,481, (1976), Chem. Abs., 85, 46858, (1976).
U.S. Patent, 3,992,425, (1976), Chem. Abs., 86, 90031, (1977).
U.S. Patent, 4,012,412, (1977), Chem. Abs., 87, 6201, (1977).

(189) H. Kubo, Agr. Biol. Chem., 29(1), 43, (1965).

(190) H.G. Cook, J.D. Ilett, B.C. Saunders, G.J. Stacey, H.G. Watson, I.G.E. Wilding and S.J. Woodcock, J. Chem. Soc., 2921, (1949).

(191) A. Michaelis, Ann. 326, 129, (1903).

(192) Interpretation of the Infrared Spectra of Organophosphorus Compounds", L.C. Thomas, Heyden and Son, (1974).

(193) R.E. Ridenour and E.E. Flagg, J. Organomet. Chem., 16, 393, (1969).

(194) T. Chivers, J.H.G. Van Roode, J.N.R. Ruddick and J.R. Sams, Can. J. Chem., 51, 3702, (1973).

(195) T. Chivers, J.H.G. Van Roode, J.N.R. Ruddick and J.R. Sams, Can. J. Chem., 54, 2184, (1976).

(196) K.C. Molloy, F.A.K. Nasser, C.L. Barnes, D. Van der Helm and J.J. Zuckerman, Inorg. Chem., 21, 960, (1982).

(197) P.G. Harrison, Inorg. Chem., 12, 1545, (1973).

(198) A.H. Cowley and R.P. Pinnell, J. Am. Chem. Soc., 82, 4454, (1965).

(199) D. Cunningham, L.A. Kelly, K.C. Molloy and J.J. Zuckerman, Inorg. Chem., 21, 1416, (1982).

(200) F.A.K. Nasser and J.J. Zuckerman, J. Organomet. Chem., 244 17, (1983).

(201) K.C. Molloy, K. Quill and I.W. Nowell, Unpublished Results.

(202) S.J. Blunden, R. Hill and D.G. Giles, J. Organomet. Chem., 270, 39, (1984).

(203) K.C. Molloy and J.J. Zuckerman, Acc. Chem. Res., 16, 386, (1983).

(204) A. Calderbank, Adv. Pest. Control Res., 8,217, (1968).

(205) B. Emmert and H. Lauritzen, Ber., 71, 240, (1938).

(206) A.J. MacFarlane and R.J.P. Williams, J. Chem. Soc., (A), 1517, (1969).

(207) J. Guillermo Contreas, J.S. Poland and D.G. Tuck, J. Chem. Soc., Dalton Trans.,

(208) C.K. Prout and P. Murray-Rust, J. Chem. Soc.(A), 1520, (1969).

(209) A.J. Buttenshaw, M. Duchene and M. Webster, J. Chem. Soc., Dalton Trans., 2230, (1975).

(210) M.K. Das, J. Buckle and P.G. Harrison, Inorg. Chim. Acta., 6, 17, (1972).

(211) J.P. Clarke and C.J. Wilkins, J. Chem. Soc.,(A), 871, (1966).

(212) A.G. Davies, L. Smith and P.J. Smith, J. Organomet. Chem., 23, 135, (1970).

(213) F.A.K. Nasser, M.B. Hossain, D. Van der Helm, and J.J. Zuckerman, Inorg. Chem., 23, 606, (1984).

(214) R.F. Homer, G.C. Mees and T.E. Tomlinson, J. Sci. Food Agric., 309, (1960).

(215) L.A. Summers, Adv. Pest. Sci., Plenary Lect. Symp. Pap. Int. Congr. Pestic. Chem. 4th, 1978, 2, 244, (1979), ed. H. Geissbuehlar, Pergamon.

(216) P.D. Sullivan and M.C. Williams, J. Am. Chem. Soc., 98, 1711, (1976).

(217) J. Volke, Collection Czechoslov, Commun., 33, 3044, (1968).

(218) R.K. Ingham, S.D. Rosenberg and H. Gilman, Chem. Rev., 60, 459, (1960).

(219) K. Sisido, Y. Takeda and Z. Kinagawa, J. Am. Chem. Soc., 83, 538, (1961).

(220) G.M. Sheldrick, "SHELX 76 Systems of Programs", (1976).

(221) D.T. Cromer and J.B. Mann, Acta. Cryst., A24, 321, (1968).

(222) D.T. Cromer and J.B. Mann, Acta. Cryst., A24, 390, (1968).

(223) D.T. Cromer and D. Liberman, J. Chem. Phys., 53, 1891, (1970).

(224) P. Multan Main, S.E. Fiske, S.L. Hull, G. Germain, J.P. Declerq and M.M. Woolfson, "Multan, a System of Computer Programs for Crystal Structure Determination from X-Ray Diffraction Data", Universities of York (England) and Louvain (Belgium), (1980).

(225) R.F. Stewart, E.R. Davidson and W.T. Simpson, J. Chem. Phys., 42, 3175, (1965).